INTERACTION OF FREE AND FORCED CONVECTIVE MASS TRANSFER FROM OBLATE SPHEROIDS.

A thesis submitted for the degree of

Doctor of Philosophy

in the

Faculty of Engineering

of the

University of London

by

JAMES CHARLES INGRAM, B.Sc.(Eng.), A.C.G.I.

Department of Chemical Engineering
and Chemical Technology,
Imperial College of Science and Technology,
London, S.W.7.

August, 1966.

ABSTRACT.

The effect of the interaction between free and forced convection upon mass transfer rates from spheres and oblate spheroidal bodies has been investigated experimentally.

Many correlations exist for the prediction of mass transfer rates from single spheres by either free or forced convection alone. Little work has been published, however, concerning the interaction of these effects. Furthermore, there is much evidence to suggest that drops passing through a second liquid are often oblate spheroidal in shape.

To investigate the effect of both shape and the interaction of free and forced convection upon mass transfer rates, benzoic acid bodies of five different oblate spheroidal shapes were dissolved in water in a low speed water tunnel; mass transfer rates were obtained by direct weighing. A schlieren technique was employed to photograph the flow patterns around the dissolving bodies.

Eight characteristic dimensions were considered in an attempt to produce a single correlation for all five shapes. The data for Reynolds numbers greater than 45 were correlated with mean and maximum deviations

of 2.4% and 7.1% by the expression :

$$Sh_3 = 23.7 + 0.196\ Re_3^{0.78}\ Sc^{1/3} \qquad 45 \leqslant Re_3 \leqslant 195$$

where the dimensionless groups are based upon the characteristic dimension proposed by Pasternak and Gauvin. The increase of the Reynolds number exponent from the theoretical value of 0.50 for forced convection may be an effect of free convection. This conclusion is supported by the photographic evidence which shows the existence of four distinct flow regimes in the range $0 \leqslant Re_3 \leqslant 195$ with an influence of free convection upon the flow patterns around the dissolving bodies even at the highest Reynolds numbers employed.

At Reynolds numbers in the range $0 \leqslant Re_3 \leqslant 45$ none of the characteristic dimensions employed successfully unified the data for all shapes.

The dimensionless group (Gr/Re^2) has been shown to be an important criterion in deciding whether either free or forced convection may be neglected in the calculation of mass transfer rates.

ACKNOWLEDGEMENTS.

The author wishes to express his sincere thanks to Dr. A.R.H.Cornish for his help and guidance during this investigation.

Financial assistance from the Esso Petroleum Company is gratefully acknowledged.

Thanks are also due to Mr.J.S.Oakley and his staff, particularly Messrs Lewis and Simmonds, for help in the construction of the apparatus.

TABLE OF CONTENTS.

LIST OF ILLUSTRATIONS.

LIST OF TABLES.

LIST OF TABLES (continued).

LIST OF SYMBOLS.

A	Surface area.	L^2
A	Constant in equation (5.3)	-
A	Defined in equations (2.38) to (2.42)	-
B	Constant in equation (5.3)	-
B	Defined in equations (2.38) to (2.42)	-
c_s	Saturation concentration of benzoic acid in water	ML^{-3}
c_o	Concentration of benzoic acid in recirculating water	ML^{-3}
c_p	Specific heat at constant pressure	$HM^{-1}\theta^{-1}$
C_1 to C_{17}	Constants	-
C_{1_3} and C_{2_3}	Constants in equation (5.1)	-
C_{1_5} and C_{2_5}	Constants in equation (5.2)	-
C_{1_9} and C_{2_9}	Constants in Table 11	-
C_A	Concentration of component A	ML^{-3}
C_{Ao}	Concentration of component A remote from surface	ML^{-3}
C_{As}	Saturation concentration of component A	ML^{-3}
C_A^*	Dimensionless concentration defined in Chapter 3	-
d	Diameter of a sphere	L
d_1	Diameter of a sphere with the same volume as a body	L
d_2	Length of the minor axis of a spheroid	L
d_3	Surface area of a body divided by the perimeter normal to flow	L

d_4	Diameter of the sphere with the same surface area as a body.	L
d_5	Arithmetic mean of the major and minor axes of a spheroid.	L
d_6	Diameter of the sphere with the same volume as a body multiplied by the sphericity of the body.	L
d_7	Length of the major axis of a spheroid	L
d_8	Geometric mean of the major and minor axes of a spheroid	L
d_9	Characteristic dimension defined in equation (5.125)	L
d_{Ch}	Characteristic dimension of a body	L
d_M	Length of the major axis of a spheroid	L
D	Substantial differential operator	-
D_v	Diffusion ~~constant~~ coefficient	L^2T^{-1}
e	Eccentricity (ratio of minor to major axis) of a spheroid	-
f	Frossling "wind factor" Defined in equations (2.6) to (2.9)	-
f	Semi-minor axis of a spheroid	L
f	Degrees of freedom	-
f( )	Function symbol	-
F	Water tunnel throughput (lb./min.)	
$F_{\alpha, f, inf.}$ and $F_{\alpha, inf., f}$	Values of the F-distribution at a probability level of $(1-2\alpha)$ with degrees of freedom f and inf.	-
g	acceleration due to gravity	LT^{-2}
$\bar{g}$	gravitational acceleration vector	LT^{-2}
g	Semi-major axis of a spheroid	L

Gr	Grashof number $\frac{\rho_s - \rho}{\rho} \cdot \frac{d^3 g \rho^2}{\mu^2}$	-
Gr_1 to Gr_8	Grashof number based on d_1 to d_8	-
Gr_H	Grashof number for heat transfer $\frac{g d_{Ch}^3 \beta \Delta T}{\nu^2}$	-
h	Heat transfer coefficient	$HL^{-2}T^{-1}\theta^{-1}$
ΔH	Manometer reading (cm.water)	
k	Defined equations (2.8) to (2.10)	-
k	Thermal conductivity	$HL^{-1}T^{-1}\theta^{-1}$
k_c	Continuous phase mass transfer coefficient	LT^{-1}
k_d	Disperse phase mass transfer coefficient	LT^{-1}
k_{loc}	Local mass transfer coefficient at a point on a surface	LT^{-1}
K	Bulk viscosity	$ML^{-1}T^{-1}$
K_{oc}	Overall mass transfer coefficient Defined equation (2.2)	LT^{-1}
K_{od}	Overall mass transfer coefficient Defined in equation (2.3)	LT^{-1}
L	Lewis "film thickness"	L
m	Slope of the equilibrium curve in equations (2.2) and (2.3)	-
m	Mass	M
m	Exponent of the Schmidt number	-
M	Molecular weight	M
n	Exponent of the Reynolds number	-
$n_3, n_{3_1}, n_{3_2}, n_{3_3}$	Exponents of Re_3	-

n_5	Exponent of Re_5	-
n_9	Exponent of Re_9	-
N	Distance in the direction normal to a surface	L
N*	Dimensionless distance normal to a surface defined in Chapter 3.	-
N_R	Defined in Chapter 2 equation (2.53)	-
N_G	Defined in Chapter 2 equation (2.54)	-
N_K	Defined in Chapter 2 equation (2.55)	-
Nu	Nusselt number $(\frac{hd}{k})$	-
Nu_{free}	Nusselt number in free convection	-
Nu_{forced}	Nusselt number in forced convection	-
$Nu_{resultant}$	Nusselt number in combined free and forced convection. Defined in equation (2.47)	-
P	Pressure	$ML^{-1}T^{-2}$
P_i	Vapour pressure at an interface	mm. Hg
P_b	Partial pressure of diffusing species remote from the interface.	mm. Hg
P_o	Pressure at a point in a stagnant fluid.	$ML^{-1}T^{-2}$
P'	Defined in Chapter 3	$ML^{-1}T^{-2}$
P'*	Dimensionless pressure. Defined in Chapter 3	-
Pr	Prandtl number $\frac{c_p \mu}{k}$	-
q_A	Mass flux of component A	$ML^{-2}T^{-1}$
R	Universal gas constant 62.368×10^{-3} $cm^3(mm.Hg)/^oK$ (gr.mole)	
Re	Reynolds number $\frac{\rho v d}{\mu}$	-

Re_1 to Re_9	Reynolds number based upon d_1 to d_9	-
Re_s	Reynolds number for a sphere	-
Re_{Ch}	Reynolds number based upon d_{Ch}	-
$Re_{free_{max}}$	Equivalent maximum Reynolds number for free convection. Defined in equation (2.35)	-
Re_E	Equivalent Reynolds number for combined free and forced convection. Defined in equation (2.37)	-
Re_{TR}	"Transition" Reynolds number. Defined in Chapter 5.	-
Sc	Schmidt number $\frac{\mu}{\rho D_v}$	-
Sh	Sherwood number $\frac{k_c d}{D_v}$	-
Sh_1 to Sh_9	Sherwood numbers based upon d_1 to d_9	-
Sh_{1f}	Sherwood number based upon the surface area of the sphere of the same volume as a drop or oblate spheroid and d_1	-
Sh_{Ch}	Sherwood number based upon d_{Ch}	-
Sh_s	Sherwood number for a sphere	-
Sh_{mol}	Sherwood number for molecular diffusion	-
Sh_{free}	Sherwood number for free convection	-
$Sh_{3_{free}}$	Sherwood number for free convection based upon d_3	-
Sh_{loc}	Local value of the Sherwood number at a point on a surface	-
S^2	Estimate of the variance based on the deviation of data points from their predicted values.	-
t	Time	T
t*	Dimensionless time. Defined in Chapter 3	-

T	Temperature ^{o}K.	
T	Total number of data points in a correlation	-
ΔT	Temperature difference between the surface and the bulk fluid remote from the surface	θ
U_{inf}	Undisturbed bulk velocity	LT^{-1}
v	Velocity	LT^{-1}
$\bar{v}$	Velocity vector	LT^{-1}
$\bar{v}^*$	Dimensionless velocity vector. Defined in Chapter 3	-
V_m	Equivalent $\overset{\text{maximum}}{\backslash}$velocity of free convective motion	LT^{-1}
V	Volume	L^3
V_m	Molal volume cm^3/grm.mole	
W	Weight loss g./hr.	
X	An independent variable	-
X_P	Wilke-Pin Chang parameter. Defined in Section (4.7)	-
X_m	Particular observed value of X	-
Y	A dependent variable	-
Y_m	Particular observed value of Y	-
$\bar{Y}_m$	Value of Y_m predicted by equation(5.3)	-
α	Probability level in the f-ratio	-
β	Temperature coefficient of volumetric expansion in the Grashof number for heat transfer	θ^{-1}
θ_s	Separation angle measured from the front stagnation point (degrees)	-

μ	Viscosity	$ML^{-1}T^{-1}$
μ_{H_2O}	Viscosity of pure water	$ML^{-1}T^{-1}$
υ	Kinematic viscosity	L^2T^{-1}
ρ	Density	ML^{-3}
ρ_s	Density of a saturated solution	ML^{-3}
ρ_o	Constant density of bulk fluid remote from the surface	ML^{-3}
ρ_{H_2O}	Density of pure water	ML^{-3}
ρ^*	Dimensionless density. Defined in Chapter 3	-
σ^2	True variance calculated at infinite degrees of freedom	-
$\emptyset$	Sphericity. Defined as the surface area of the sphere with the same volume as a particle divided by the true surface area of the particle	-
$\psi(\ )$	Function symbol	-
∇	Vector operator "del" or "nabla"	L^{-1}
∇^*	Dimensionless vector operator. Defined in Chapter 3	-
$\Big\vert_{surface}$	Denotes evaluated at the surface	-

CHAPTER 1.

INTRODUCTION.

Many chemical engineering processes involve the transfer of mass between phases. In order to enhance this mass transfer it is desirable to increase the contact area between the phases and this is often accomplished by dispersing one phase, in the form of particles, drops, or bubbles, in the second phase. The phases are then known as the disperse and continuous phases, respectively. Systems frequently encountered are solid particles in a liquid or gas, liquid drops in a gas or liquid, and bubbles in a liquid.

In recent years research workers have shown an increasing interest in the more fundamental aspects of the mass transfer processes involved in such systems. In particular, the precise nature of the mechanism of mass transfer from a single particle, bubble, or drop has been the subject of much theoretical and experimental study.

The passage of drops through a second liquid may be complicated by such factors as internal circulation, oscillations, deformations, and interactions with neighbouring drops. In order to study this situation experimentally, with a view to gaining some insight into the mechanisms of the mass transfer process, as well as to obtaining empirical correlations, it is necessary to

introduce certain simplifications and to concentrate on particular aspects of the general problem. For example, in order to investigate the relationship between drop Reynolds number and continuous phase mass transfer coefficient, many recent researchers have considered a drop to behave as a solid body. They have then measured mass transfer rates experimentally by suspending a solid body representing a drop in a liquid stream moving at a controlled velocity. Such experiments eliminate the effects of internal circulation, oscillation and deformation. By considering a single body the effects of interactions with neighbouring drops are also eliminated.

A further complication, not eliminated by the above model, may be present when drop Reynolds number, relative to the continuous phase, is low. In such circumstances free convective forces may have a considerable effect upon the fluid motion around a drop or solid particle, and hence upon the mass transfer from it. These forces are caused by density differences between the bulk fluid of the continuous phase and the solution formed by transfer of a component from the drop or particle. When drop Reynolds number is high, these free convective forces become negligible compared with forces set up by the relative motion of the continuous phase itself.

Previous workers who have used the solid, rigidly-supported model, have concentrated upon the situation in which free convective forces may be neglected and have paid little attention to ranges of Reynolds number in which free and forced convection might be expected to interact. Furthermore most of these workers have simplified the model one stage further by taking the sphere as the idealised drop shape. Although research has shown drops in liquid-liquid systems to be spherical under certain circumstances, there is much evidence to show that the model would be more general if the drops were represented by oblate spheroids [1-8]. Use of this idealized shape would still include the sphere as a limiting case. The only workers [9,10] who have used oblate spheroids, have worked in ranges of Reynolds number where free convection is negligible and, in one particular instance [11], where there is free convection only. These investigations are of value as limiting cases when considering the interaction of free and forced convection. Workers with oblate spheroids have considered at some length the effect of eccentricity on mass transfer. They have attempted to produce a single correlation for all oblate spheroidal shapes by choice of a suitable characteristic dimension for use in dimensionless groups.

With these considerations in mind it was decided to study experimentally mass transfer from oblate spheroidal bodies under conditions such that free and forced convection interact. The feasibility of correlating the data thus obtained, if possible by use of a suitable characteristic dimension in a manner similar to that successfully employed in forced convection, was to be investigated. An attempt was also made to discover criteria for deciding when free convection or forced convection may be considered negligible. Photographic techniques were employed to study the mechanisms involved in the mass transfer process.

CHAPTER 2.

LITERATURE SURVEY.

2.1. MASS TRANSFER THEORY.

In September 1916 W.K.Lewis [12] presented the first clear statement of the so-called film theory of mass transfer. Lewis considered the extraction of a component from a solid particle by a countercurrently flowing liquid. He proposed that in this situation the liquid could be regarded as forming a thin, almost stationary film on the solid particle, whilst outside this film turbulence kept the liquid concentration uniform. Mass transfer was assumed to be controlled by diffusion through the stagnant film. As a consequence, the continuous phase mass transfer coefficient, k_c, could be related to the diffusion coefficient of the transferred component in the continuous phase, D_v, by :

$$k_c = \frac{D_v}{L} \qquad (2.1)$$

The quantity L in this equation is the thickness of the supposedly stagnant film.

Lewis and Whitman [13] extended the film theory by consideration of gas absorption. For this process they postulated the existence of two films, one on either side of the interface, each of which is thin and relatively

undisturbed by bulk motion. These authors showed that the overall mass transfer coefficients based on the continuous and disperse phases, K_{oc} and K_{od}, could be related to the film mass transfer coefficients, k_c and k_d, by :

$$\frac{1}{K_{oc}} = \frac{1}{k_c} + \frac{m}{k_d} \qquad (2.2)$$

$$\frac{1}{K_{od}} = \frac{1}{k_d} + \frac{1}{m\,k_c} \qquad (2.3)$$

where m is the slope of the equilibrium line, assumed straight in the region of interest. The modern interpretation of equations (2.2) and (2.3) is that $1/k_c$ and $1/k_d$ represent resistances to mass transfer in the continuous and disperse phases respectively, whilst $1/K_{oc}$ and $1/K_{od}$ represent total resistances to mass transfer across the interface.

The prediction of the individual film coefficients has been a subject of great interest since the presentation of equations (2.2) and (2.3) by Lewis and Whitman. Prediction of k_c by equation (2.1) is unsatisfactory since this equation is based upon the physically unrealistic concept of a stagnant film. Much research has been carried out to obtain more satisfactory models and the penetration theory of Higbie [14], the surface-renewal theory of Dankwerts [15], and the film-penetration theory

of Toor and Marchello [16] are the results of such work.

Since a large number of mass transfer operations are based upon the passage of bubbles, drops, or solid particles through a continuous phase, other workers have attempted to predict the continuous phase mass transfer coefficient in terms of the relative velocity of the disperse and continuous phases. As it is to this end that the present work is directed, the results of these predictions will now be considered in some detail.

2.2. CORRELATIONS BASED ON RELATIVE VELOCITY.

Frossling [17] considered the rate of evaporation of a falling drop to be the result of two effects: the rate of evaporation which would occur by molecular diffusion if the drop were at rest, and an additional rate of evaporation due to drop motion. Mass transfer from a spherical drop by molecular diffusion into an infinite stagnant medium had already been analysed mathematically by Langmuir [18]. Langmuir showed that under these conditions the rate of mass transfer is given by :

$$\frac{dm}{dt} = \frac{2\pi D_v M(P_i - P_b)d}{RT} \qquad (2.4)$$

In this equation d is the drop diameter, P_i the vapour pressure at the interface, P_b the partial pressure of the diffusing species far from the drop, T the absolute

temperature, M the molecular weight of the diffusing component, and R the universal gas constant. Equation (2.4) may be written in dimensionless form as :

$$Sh_{mol.} = 2 \qquad (2.5)$$

where Sh is the Sherwood number and the subscript mol. indicates transfer by molecular diffusion alone.

Frossling assumed that the effect of drop motion was to increase mass transfer by a factor f, which he called a wind factor. In the presence of drop motion equation (2.4) therefore becomes :

$$\frac{dm}{dt} = \frac{2\pi D_v M(P_i - P_b)d}{RT} \cdot f \qquad (2.6)$$

or in dimensionless form :

$$Sh = 2f \qquad (2.7)$$

From consideration of the boundary layer equations for fluid motion around a sphere, Frossling concluded that f is related to drop Reynolds number by :

$$f = kRe^{1/2} \qquad (2.8)$$

where k is a function of the Schmidt number. So that equation (2.7) reduced to equation (2.5) when drop Reynolds number is zero, Frossling modified equation (2.8) such that :

$$f = 1 + kRe^{1/2} \qquad (2.9)$$

Frossling further assumed, on the basis of heat transfer studies by Pohlhausen [19] and Kroujiline [20] that :

$$k = C_1(Sc)^m \qquad (2.10)$$

where m was probably close to 1/3.

This semi-theoretical approach led Frossling to use a correlation for mass transfer data from falling drops of the form :

$$Sh = 2 + C_2 \, Re^{1/2} \, Sc^{1/3} \qquad (2.11)$$

In order to verify equation (2.11), Frossling evaporated drops of nitrobenzene and water in an air stream. To test the assumption that the drops could be regarded as rigid spheres he also measured rates of sublimation of naphthalene spheres. His results, which covered the Reynolds number range 2 to 800 and the Schmidt number range 0.6 to 2.7 were correlated on the basis of equation (2.11) as :

$$Sh = 2 + 0.552 \, Re^{1/2} \, Sc^{1/3} \qquad (2.12)$$

This equation may be written explicity in terms of the continuous phase mass transfer coefficient as :

$$k_c = \frac{D_v}{d} (2 + 0.552 Sc^{1/3} \, Re^{1/2}) \qquad (2.13)$$

It is, however, more commonly written in the dimensionless form.

In a later paper Frossling [21] used the boundary layer equations derived by Boltze [22], to show that for a body of revolution with its axes parallel to flow, local values of the Sherwood number are proportional to the square root of the Reynolds number. This derivation was quite general for axisymmetric bodies with laminar boundary layers. Frossling also showed that, when the Schmidt number is large, local values of the Sherwood number are proportional to the cube root of the Schmidt number.

To obtain these results Frossling transformed the boundary layer equations of Boltze into an infinite set of non-linear ordinary differential equations which were solved numerically to give the velocity distribution in the boundary layer. The velocity distribution was then used in conjunction with the diffusion equation to obtain a further set of ordinary differential equations. Frossling solved the first few equations of this latter set numerically and obtained a solution in series form for the local mass transfer rates.

The solution for local Sherwood numbers obtained by Frossling cannot be used to predict local mass transfer rates beyond the boundary layer separation point. The local Sherwood numbers predicted by boundary layer theory cannot, therefore, be integrated to give overall values

of the Sherwood number for the sphere.

Frossling claims good agreement between the predicted local rates of mass transfer from naphthalene spheres and the experimental results of his earlier work.

Since this pioneer work by Frossling many workers have carried out similar theoretical and experimental research programmes. As a result, it has become evident that an equation of the form of (2.11) is not always successful in correlating mass transfer data. In particular free convection has been found to have a considerable effect upon mass transfer at low Reynolds numbers when the Grashof number is high [23-26]. However, before discussing the correlations which have been proposed for the more general situation in which free and forced convection interact, it is of interest to examine the expressions proposed for the limiting cases of free convection and forced convection alone. The expressions proposed for forced convection fall into two categories dependent upon whether the flow is within or outside the so-called "creeping flow" region. Although it is generally accepted that the creeping flow approximations are only valid at "very low" Reynolds numbers there is no universally accepted value for the upper limit of their applicability. These approximations are, however, frequently held to be valid for Reynolds numbers of less than one.

2.2.1. FORCED CONVECTION.

i). Outside Creeping Flow Region.

It is to this category that the work of Frossling belongs and subsequent workers have produced correlations similar in form to equation (2.11). Some workers have assumed the indices of Re and Sc of equation (2.11) i.e. 1/2 and 1/3, and simply used their experimental data to obtain values of C_2 for different systems and over different ranges of Reynolds number. Other workers have assumed a more general form of equation (2.11), i.e.

$$Sh = 2 + C_3 Re^n Sc^{1/3} \qquad (2.14)$$

and have obtained values of both C_3 and n by analysis of their experimental data. Still other workers have considered the contribution of the term for molecular diffusion into an infinite stagnant medium to be meaningless in the presence of forced convection. These workers have correlated their results on the assumption that :

$$Sh = C_4 Re^{1/2} Sc^{1/3} \qquad (2.15)$$

or

$$Sh = C_5 Re^n Sc^{1/3} \qquad (2.16)$$

It is convenient to compare these various correlations by means of the following table.

TABLE 1

FORCED CONVECTION CORRELATIONS (Outside Creeping Flow Region)

Author	Correlation	Range of Re Nos.	System Employed	Geometry of System
Vyrubov[27]	$Sh = 0.54Re^{1/2}$	200-3000	Ammonia from air stream transferred to ortho-phospheric acid spheres	Spheres
Linton and[28] Sherwood	$^{\ast}Sh = 0.33Re^{1/2}Sc^{1/3}$	1500-10000	Benzoic acid -water	Spheres
Maisel and[29] Sherwood	Logarithmic plot	2000-40000	Benzene saturated sand-air	Spheres, Discs, Cylinders
Ranz and[30] Marshall	$Sh=2+0.60Re^{1/2}Sc^{1/3}$	2-200	Aniline, Benzene, water-air	Suspended liquid drops
Axel'rud[31]	$Sh=0.82Sc^{1/3}Re^{1/2}$	200-4000	Potassium and Sodium nitrates -water	Spheres
Garner and[32] Suckling	$Sh=2+0.95Re^{1/2}Sc^{1/3}$	100-700	Benzoic acid -water	Spheres

*Obtained by Rowe, Claxton and Lewis,[38] from a logarithmic plot presented by the original authors.

TABLE 1 (continued)

Author	Correlation	Range of Re Nos.	System Employed	Geometry of System
Steele and[33] Geankoplis	Logarithmic plot	600-140000	Benzoic acid, Cinnamic acid, 2 naphthol-water	Spheres
Linton and[34] Sutherland	$Sh=0.582Re^{1/2}Sc^{1/3}$	500-8000	Benzoic acid -water	Spheres
Pasternak[35] and Gauvin	$Sh_3=0.692Re_3^{0.514}Sc^{1/3}$	3000-15000	Cellite saturated with acetone-air	Cylinders, Cubes, Spheres, Prisms
Evonchides[36] and Thodos	$Sh=0.33Re^{0.6}Sc^{1/3}$	1500-12000	Cellite saturated with water or nitro-benzene -air	Spheres
Skelland and[9] Cornish	$Sh_3=0.74Re_3^{0.50}Sc^{1/3}$	120-6000	Naphthalene-air	Oblate Spheroids
Yen and[37] Thodos	$Sh=0.358Re^{0.58}Sc^{1/3}$	1750-8922	Cellite saturated with water-air	Spheres
Rowe, Claxton[38] and Lewis	$Sh=2+0.68Re^{1/2}Sc^{1/3}$	96-1052	Naphthalene -air	Spheres
Rowe, Claxton[38] and Lewis	$Sh=2+0.73Re^{1/2}Sc^{1/3}$	27-1149	Benzoic acid -water	Spheres

In table I indices of Re and Sc which are given as fractions have been assumed by the authors, those given as decimals have been obtained from experimental data. Since many studies of mass transfer from drops and drop shaped bodies have been undertaken, no attempt has been made to include in table I the many correlations which exist for other geometries, such as flat plates, nor have the many analogous heat transfer correlations been included.

The subscript on the Sherwood and Reynolds numbers in the correlations presented by Skelland and Cornish [9], and Pasternak and Gauvin [35], refers to the characteristic dimension used in calculation of these dimensionless groups. These authors examined the feasibility of unifying mass transfer data for several shapes by choice of a suitable characteristic dimension for use in the dimensionless groups. Of several such dimensions tried, these authors found that the dimension defined as :

$$d_{Ch} = \frac{\text{Surface area}}{\text{Perimeter normal to flow}} \quad ,$$

d_3 in the present work, was the most satisfactory.

ii). Within Creeping Flow Region.

Friedlander [39] analysed theoretically mass transfer from a sphere at very low Reynolds numbers. At low

Reynolds numbers the equations of fluid motion may be linearised by the assumption that viscous forces are very much greater than inertia forces ~~and~~ which may therefore be neglected. A solution of these linearised equations of motion, due to Tomotika and Aoi [40], was used by Friedlander to obtain a velocity distribution round the sphere. This velocity distribution was then used to solve the diffusion equation. On the basis of comparison of his theoretical solution with experimental data, Friedlander claimed validity of his solution up to Reynolds numbers of approximately 5. Tomotika and Aoi, however, upon whose solution Friedlander's analysis was based, only claimed applicability of their solution for $Re \ll 1$.

Friedlander's solution may be summarised as :

$$Sh = 0.89\ Re^{1/3}\ Sc^{1/3} \qquad (Re.Sc) > 1000 \qquad (2.17)$$

$$Sh = \frac{4}{Re.Sc} \ln\left(\frac{1}{1-\frac{1}{2}Re.Sc}\right) 0.1 \qquad (Re.Sc) < 1 \qquad (2.18)$$

$$Sh = 2 \qquad (Re.Sc) < 10^{-1} \qquad (2.19)$$

In a further paper [41] Friedlander modified his earlier work in the light of numerical solutions of the diffusion equation obtained by Yuge [42]. Friedlander's solution at high values of (Re.Sc) was now presented as :

$$Sh = 0.991\ Re^{1/3} Sc^{1/3} \qquad (Re.Sc) > 100 \qquad (2.20)$$

Axel'rud [31] dissolved benzoic acid spheres in vegetable oil at a Schmidt number of 2.3×10^6. The spheres were moved along a circular path in the oil bath followed by a small stirrer to disperse the solution formed. The stirrer was assumed to have no effect upon the mass transfer from the sphere. The Reynolds number range covered was 0.1 to 2.5 and the data correlated by :

$$Sh = 1.1\ Re^{1/3}\ Sc^{1/3} \qquad (2.21)$$

Equation (2.21) is in good agreement with the theoretical prediction of Friedlander for $(Re.Sc) > 100$.

2.2.2. FREE CONVECTION.

Mathers, Madden and Piret [43] obtained approximate solutions to the differential equations describing free convection mass transfer from a vertical plate into an infinite fluid. The resultant solution was expressed in the form :

$$Sh_{free} = 0.670\ (Gr.Sc)^{1/4} \qquad (2.22)$$

To verify this theoretical solution, brass spheres coated with naphthalene and solid benzene were sublimed in air. The data were plotted on logarithmic co-ordinates as Sh_{free} vs. (Gr.Sc). A single curve could be drawn through the data for both systems. This curve was expressed analytically as :

$$Sh_{free} = 2 + 0.282(Gr.Sc)^{0.37} \quad (Gr.Sc) < 100 \tag{2.23}$$

$$Sh_{free} = 2 + 0.5(Gr.Sc)^{1/4} \quad 10^2 < (Gr.Sc) < 10^6 \tag{2.24}$$

Garner and Keey [44] dissolved spheres of benzoic and adipic acid in water. Schlieren photographs taken by these workers showed a thin layer of saturated solution on the sphere surface which thickened towards the rear pole causing minimum transfer there. At values of $(Gr.Sc) > 10^8$ however, the schlieren photographs indicated the onset of turbulence in this surface layer causing material to be convected away from the surface at a faster rate and hence increasing mass transfer. Their data, mostly obtained in the laminar regime, were correlated as :

$$Sh_{free} = 23 + 0.58(Gr.Sc)^{1/4} \quad 4 \times 10^6 < Gr.Sc < 1.5 \times 10^8 \tag{2.25}$$

Earlier experimental work of King [45] and Saunders [46], who investigated heat transfer from vertical flat plates, had suggested the existence of two regimes of free convective mass transfer, laminar and turbulent, and that :

$$Nu_{free} \propto (Gr_H Pr)^{1/4} \text{ for laminar free convection ;} \tag{2.26}$$

$$Nu_{free} \propto (Gr_H Pr)^{1/3} \text{ for turbulent free convection.} \tag{2.27}$$

On the evidence of their schlieren photographs and assuming the analogy between the heat and mass transfer processes, Garner and Keey concluded that, for mass transfer from spheres, transition from laminar to turbulent free convection occurred at $(Gr.Sc) \doteq 3.5 \times 10^8$.

Garner and Hoffman [47] continued the work of Garner and Keey by employing a wider range of sphere diameters and also other systems. Spheres of benzoic, salicylic and succinic acids were dissolved in water, benzene and n-butanol respectively. As with the work of Garner and Keey [44], the final correlation for overall mass transfer rates was subject to mean errors of about 14% largely attributable to the photographic technique employed. The onset of turbulence, as evidenced by the shift of the minimum local mass transfer rate from the rear pole, occurred at $(Gr.Sc) \doteq 6 \times 10^8$. The data for the laminar regime were correlated by :

$$Sh_{free} = 5.4 + 0.440(Gr.Sc)^{1/4} \qquad 2\times10^6 < Gr.Sc < 2\times10^8 \qquad (2.28)$$

Sandoval [11] studied the dissolution of oblate spheroids, of various eccentricities, cast from benzoic acid. The solvents used were water and 40%, 50% and 60% solutions of propylene glycol. The data for all systems could not be uniquely represented and were correlated by :

for water solvent,

$$Sh_{s_{free}} = 0.121(Gr_s Sc)^{1/3} \qquad 2.1\times10^{7} < Gr_s Sc < 2.1\times10^{8} \tag{2.29}$$

for 40% propylene glycol solvent,

$$Sh_{s_{free}} = 7.7+0.039(Gr_s Sc^{1.30})^{1/3} \qquad 6.0\times10^{7} < Gr_s Sc < 3.3\times10^{8} \tag{2.30}$$

for 50% and 60% propylene glycol solvent,

$$Sh_{s_{free}} = 5.9+0.025(Gr_s Sc^{1.30})^{1/3} \qquad 8.8\times10^{7} < Gr_s Sc < 8.5\times10^{8} \tag{2.31}$$

In these correlations the characteristic dimension employed was that suggested by Pasternak and Gauvin [35]. Sandoval found however, that any characteristic dimension which conserved true surface area was equally satisfactory in correlating his data.

Sandoval's correlation for the benzoic acid - water system is of the form suggested by earlier workers for turbulent free convection. This is in direct contradiction with the correlation of Garner and Hoffman, which, though covering the range of(Gr.Sc) employed by Sandoval, is in a form suggesting laminar free convection.

Sections 2.2.1 and 2.2.2 have been concerned with correlations presented for situations in which either free convection or forced convection could be neglected. Consideration will now be given to work specifically concerned with situations in which these effects interact.

2.2.3. INTERACTING FREE AND FORCED CONVECTION.

Garner and Grafton [23] dissolved 1/2 inch diameter benzoic acid spheres in water in a horizontal water tunnel. Mass transfer was measured by a photographic technique which, while allowing investigation of local mass transfer rates, resulted in large errors, $\pm$ 25%, when the local rates were integrated to give overall rates. Both laminar and turbulent flow were employed but no significant difference between the results in these two regimes was apparent. These workers correlated their data as :

$$Sh = 44 + 0.48\ Re^{1/2}Sc^{1/3} \qquad 20 < Re < 850 \qquad (2.32)$$

The large constant term was attributed to free convection. The authors claim that the value 44 is in agreement with a free convection mass transfer correlation due to Wagner [48]. The latter was obtained from experimental work on the dissolution of sodium chloride plates and is expressed as :

$$Sh_{free} = 0.545\ (Gr.Sc)^{1/4} \qquad (2.33)$$

On this basis Garner and Grafton claimed that, at low Reynolds numbers, the effect of free convection may be regarded as directly additive to forced convection mass transfer. They proposed a final correlation of the form :

$$Sh = 0.5(Gr.Sc)^{1/4} + 0.48\ Re^{1/2}Sc^{1/3} \qquad 20 < Re < 850 \qquad (2.34)$$

Garner and Keey [24] extended the work of Garner and Grafton by investigating the dissolution of benzoic acid spheres in a vertical water tunnel which allowed either up or down flow. Working in a range of Reynolds number 2.3 to 255 they concluded that the minimum rate of mass transfer did not occur at the lowest Reynolds number. It was suggested that the depression in the mass transfer rate, with a minimum at a Reynolds number of approximately fifty, was caused by an interaction of free convective and forced convective forces. Data, presented as a small scale logarithmic plot of Sherwood number versus Reynolds number, fall on separate curves, between Reynolds numbers of 20 and 250, for upflow and downflow. Extrapolation of these curves suggests that they would meet at a Reynolds number of approximately 750. At Reynolds numbers less than 20 a single curve represents the data for both upflow and downflow.

It is interesting to note that in downflow, where Garner and Keey expected that free and forced convective effects might be mutually assisted, the mass transfer rates were lower than in upflow where these effects might be expected to be mutually opposed.

The experimental results of Garner and Keey cast great doubt upon the concept of additivity of free and forced convection effects.

Krischer and Loos [25] investigated the evaporation of water from bodies covered with filter paper into an air stream. The filter paper was kept saturated with water from a reservoir by capillary attraction and mass transfer measured by determination of the volumetric loss from the reservoir. Various shapes were used including flat plates, cylinders, prisms and spheres. The data for spheres was more limited to five observations in the Reynolds number range 18 to 2400.

Krischer [49] had earlier proposed that in the Grashof number for heat transfer, $Gr_H = \frac{d_{Ch}^3 g \beta \Delta T}{\nu^2}$, the group $(d_{Ch} g \beta \Delta T)$ could be replaced by $\frac{1}{2}V_m^2$, where V_m is the maximum velocity of free convective motion. It followed that:

$$Gr_H = \frac{d_{Ch}^2 V_m^2}{2\nu^2} = 1/2\ Re^2_{free_{max}} \qquad (2.35)$$

where $Re_{free_{max}}$ is an equivalent Reynolds number for the free convective motion. Rearranging equation (2.35) gives :

$$Re_{free_{max}} = (2Gr_H)^{1/2} \qquad (2.36)$$

Krischer and Loos's experiments were conducted such that the air stream flowed vertically downwards over the test bodies. Assuming that, under these conditions, the free and forced convective velocities are directly additive and that the mean free convective velocity is $\frac{1}{2}V_m$, these authors correlated their data in terms of an equivalent Reynolds number, Re_E, where :

$$Re_E = Re + \frac{1}{2}\left[(2Gr)^{\frac{1}{2}}\right] \qquad (2.37)$$

Experimental data are presented as separate logarithmic plots of Sh versus Re_E for each shape investigated. Although no conclusion can be drawn from the five data points for spheres, this method of correlation appears to be quite successful for flat plates and cylinders.

Steinberger and Treybal [26] also investigated mass transfer from benzoic acid spheres under conditions where free and forced convection might be expected to interact. In analysing their experimental data these workers assumed a correlation of the form :

$$Sh = A + B\,Re^n \qquad (2.38)$$

In equation (2.38) A was expected to be a function of the Grashof and Schmidt numbers accounting for free convective mass transfer at zero Reynolds number, and B was expected to be of the form :

$$B = C_6\,Sc^m \qquad (2.39)$$

The contributions to mass transfer of free and forced convection were thus assumed to be additive.

The value of n giving the minimum pooled estimate of variance of the data was found to be 0.62. The corresponding values of A and B for the systems investigated, i.e. benzoic acid dissolving in water,

40% propylene glycol solution, and 60% propylene glycol solution, were then correlated together with the data of earlier workers [21,23,29,30,32,43,44,50,51,52] to give :

$$A = 2 + 0.569(Gr.Sc)^{1/4} \qquad (Gr.Sc) < 10^8 \qquad (2.40)$$

$$A = 2 + 0.0254(Gr.Sc)^{1/3}Sc^{0.244} \qquad (Gr.Sc) > 10^8 \qquad (2.41)$$

$$B = 0.347\ Sc^{0.312} \qquad (2.42)$$

The final correlations presented were :

$$Sh = 2 + 0.569(Gr.Sc)^{1/4} + 0.347Sc^{0.312}\ Re^{0.62}$$

$$10 < Re < 17x10^3 \text{ and } (Gr.Sc) < 10^8 \qquad (2.43)$$

$$Sh = 2 + 0.0254(Gr.Sc)^{1/3} + 0.347Sc^{0.312}\ Re^{0.62}$$

$$10 < Re < 17x10^3 \text{ and } (Gr.Sc) > 10^8 \qquad (2.44)$$

In obtaining these two correlations Steinberger and Treybal assumed a transition from laminar to turbulent free convective mass transfer at $(Gr.Sc) = 10^8$.

Rowe, Claxton and Lewis [38] carried out an experimental programme in which benzoic acid spheres were dissolved in water flowing in a horizontal open channel. Although these workers employed similar ranges of (Gr.Sc) and Re to those investigated by Garner and Grafton [23], Garner and Keey [24], and Steinberger and Treybal [26], they found that their data for the benzoic acid-water system

could be successfully correlated on the assumption that free convection was negligible. Their correlation, which has also been included in section 2.2.1, was of the form suggested by Frossling [17] and was presented as :

$$Sh = 2 + 0.73\ Re^{1/2}Sc^{1/3} \qquad 27 < Re < 1149$$
$$6\times10^{6} < (Gr.Sc) < 3.5\times10^{8} \qquad (2.45)$$

It is evident from the correlations presented in this section that some confusion exists concerning the effect of the interaction of free and forced convection upon mass transfer rates. Some workers have concluded that the effect of free convection is to produce additional mass transfer that is directly additive to that caused by forced convection while others have found its effect negligible. Still other workers have found that the interaction between free and forced convection causes a reduction in mass transfer compared with that due to free convection alone.

In view of the contradictory evidence of these mass transfer correlations it is of interest to consider investigations which have been carried out for the analogous heat transfer process.

Acrivos [53], Sparrow and Gregg [54], and Sparrow, Eichhorn and Gregg [55], have each obtained theoretical solutions to the equations of motion and energy for heat

transfer from a flat vertical plate where both free and forced convection are important.

By transforming the equations of motion and energy into dimensionless form, Acrivos [53] showed the importance of the dimensionless group (Gr_H/Re^2), for situations in which both free and forced convective heat transfer are important. Assuming velocity and temperature profiles which were functions of this dimensionless group, Acrivos obtained numerical solutions to the Pohlhausen - von Karmen momentum integral equations at Prandtl numbers of 0.73, 10, and 100. These solutions are presented in graphical form as plots of $\left[\left(\frac{Nu}{Re^{\frac{1}{2}}}\right) \cdot \left(\frac{Re^2}{Gr_H}\right)\right]^{\frac{1}{2}}$ v. $\left(Gr_H/Re^2\right)$ on logarithmic co-ordinates. Acrivos then compared these numerical solutions with the asymptotic solutions as $(Gr_H/Re^2) \longrightarrow 0$ and $(Gr_H/Re^2) \longrightarrow$ infinity, to obtain the values of this dimensionless group above and below which forced and free convection could be considered negligible. His results are summarized in the following table.

TABLE 2.

RESULTS OF ACRIVOS [53]

Prandtl Number	Forced convection negligible	Free convection negligible
0.73	$Gr_H/Re^2 > 2$	$Gr_H/Re^2 < 0.02$
10	$Gr_H/Re^2 > 5$	
100	$Gr_H/Re^2 > 30$	

Acrivos adds that the choice of velocity and temperature profiles in his **analysis** is somewhat arbitrary. Other profiles would give different ranges of (Gr_H/Re^2) within which both free and forced convection are important. The results obtained by Acrivos are only applicable to the case of aiding free and forced convective flow.

Sparrow and Gregg[54] assumed velocity and temperature profiles which were functions of (Gr_H/Re^2) in series form. These were substituted in the boundary layer equations and the energy equation to obtain a set of ordinary differential equations. These equations were then solved numerically at Prandtl numbers of 0.01, 1.0 and 10.0. By comparing the heat flux predicted by these solutions with that predicted for forced convection alone, they concluded that, for both aiding and opposing flows, free convection is negligible when :

$$(Gr_H/Re^2) \leqslant 0.225 \qquad 0.01 < Pr < 10.0 \qquad (2.46)$$

Sparrow, Eichhorn and Gregg [55] also analysed the equations of motion and energy using assumed velocity and temperature profiles. Their solution may be summarised in tabular form as :

TABLE 3.

RESULTS OF SPARROW, EICHHORN AND GREGG[55]

	Forced convection negligible	Free convection negligible
Aiding flow Pr = 0.7	$Gr_H/Re^2 > 16$	$Gr_H/Re^2 < 0.3$
Opposing flow Pr = 0.7	Separation occurs and no solution is presented	$Gr_H/Re^2 < 0.3$

Van der Hegge Zijnen [56] proposed that if heat transfer were occurring in a horizontal air stream, then the interaction of free and forced convection could be represented vectorially as :

$$Nu^2_{resultant} = Nu^2_{free} + Nu^2_{forced} \qquad (2.47)$$

Apparently on the basis of earlier experimental work, he claims that Nu_{free} and Nu_{forced} may be represented by the expressions :

$$Nu_{free} = 0.35 + 0.24\ Gr_H^{1/8} + 0.41\ Gr_H^{1/4} \qquad (2.48)$$

$$Nu_{forced} = 0.35 + 0.5\ Re^{1/2} + 0.001\ Re \qquad (2.49)$$

From equations (2.48) and (2.49) he obtained :

$$(Nu_{resultant}-0.35)\sqrt{1-\left(\frac{0.24Gr_H^{1/8}-0.41Gr_H^{1/4}}{Nu_{resultant}-0.35}\right)^2} = 0.5Re^{0.5} + 0.001\ Re \qquad (2.50)$$

The results of his experiments performed with a platinum wire at $Gr_H = 0.0066$ and $0.95 < Re < 79.3$, and with a brass cylinder at $Gr_H = 4412$ and $44.5 < Re < 8150$, are presented as separate logarithmic plots of Nu vs. Re. The data are seen to be better represented by the equation for combined free and forced convection, equation (2.50), than by that for forced convection alone, equation (2.49).

It is interesting to note that for the platinum wire, the curves for forced convection alone and for combined free and forced convection predict Nusselt numbers less than 5% different for $Re > 4$. The corresponding value for the brass cylinder is $Re > 936$. If the corresponding values of the group Gr_H/Re^2 are calculated the results obtained are :

for the platinum wire, free convection negligible if

$$Gr_H/Re^2 < 0.0004 ;$$

for the brass cylinder, free convection negligible if

$$Gr_H/Re^2 < 0.0005 .$$

In an experimental programme, Yuge [57] investigated both transient and steady state heat transfer from spheres in a wind tunnel. The experiments covered the Reynolds number range $3.5 < Re < 1.44 \times 10^5$, and the Grashof number range $1 < Gr_H < 1.05 \times 10^5$.

A plot of (Nu - 2) vs. Re on logarithmic co-ordinates indicates that at Reynolds numbers above 10

the data may be correlated by :

$$Nu = 2 + 0.493\ Re^{1/2} \qquad (2.51)$$

At Reynolds numbers below 10, however, the data begin to fall below the correlating line of equation (2.51). This was interpreted by Yuge as an effect of free convection. For Reynolds numbers below 10 the author proposed a graphical procedure to relate the interacting effects of free and forced convection. By consideration of the results of previous workers [30,58,59] for free convection alone, Yuge obtained the correlation :

$$Nu_{free} = 2 + 0.392\ Gr_H^{1/4} \qquad 1 < Gr < 10^5 \qquad (2.52)$$

Defining

$$N_R = 0.493\ Re^{1/2} \qquad (2.53)$$

$$N_G = 0.392\ Gr_H^{1/4} \qquad (2.54)$$

$$N_K = Nu - 2 \qquad (2.55)$$

Yuge plotted his data as N_K vs. N_R. The resultant graph shows a series of similar curves for different values of the parameter N_G. The Nusselt number for combined free and forced convection heat transfer may therefore be read from this graph if the Nusselt numbers for free and forced convection alone can be predicted.

Pei [60] investigated the interaction of free and forced convective heat transfer from spheres in a vertical wind tunnel. The air stream could be directed either

upwards or downwards thus permitting both opposing and aiding flow.

The results of this work are presented as logarithmic plots of $(Nu/Re^{1/2})$ vs. (Gr_H/Re^2) and $(Nu/Gr_H^{1/4})$ vs. (Gr_H/Re^2). In both cases the data for opposing and aiding flow fall on a single curve except in the range $0.3 < (Gr_H/Re^2) < 10$. In the case of opposing flow minima occur at $(Gr/Re^2) \triangleq 1$ whilst for aiding flow $(Nu/Re^{1/2})$ increases and $(Nu/Gr^{1/4})$ decreases over the complete range of the investigation i.e. $60 < Re < 6000$; $2 \times 10^{-3} < (Gr_H/Re^2) < 10$.

Apparently by comparison of the experimental data with the asymptotic solutions of Acrivos [53], Pei concludes that free convection is negligible when $(Gr_H/Re^2) < 0.05$ and forced convection negligible when $(Gr_H/Re^2) > 100$.

Of the heat transfer correlations presented for the interaction of free and forced convection, those based upon the group Gr_H/Re^2 have the greatest theoretical justification. The analogous nature of the heat and mass transfer processes suggests that data for interacting free and forced convective mass transfer may also be successfully correlated in terms of the group (Gr/Re^2).

CHAPTER 3.

THEORETICAL CONSIDERATIONS.

3.1. EQUATIONS OF MOTION AND DIFFUSION.

In theoretical attempts to predict mass transfer from a single drop to the surrounding medium, it is common to represent the drop as non-oscillating, non-vibrating, of constant volume, and with an initial temperature equal to that of its surroundings. Although some attempts have been made to derive a model allowing for internal circulation, it is common to examine theoretically the situation in which the drop surface may be considered rigid. Further, if the heat of dissolution is small, and if velocity gradients are not large so that the heat generated by viscous dissipation is small, the system may be assumed to be isothermal.

With the additional assumptions of :

i) no influence of magnetic, nuclear, or electrical forces;

ii) a Newtonian fluid;

iii) a two component system;

the equations of continuity, momentum, and diffusion for the system may be written in vector notation as :

continuity equation [61]:

$$\frac{D\rho}{Dt} + \rho (\nabla . \bar{v}) = 0 \qquad (3.1)$$

momentum equation [61]:

$$\rho\frac{D\bar{v}}{Dt} = -\nabla P + \rho\bar{g} + \mu\nabla^2\bar{v} + 1/3\,\mu\nabla(\nabla.\bar{v}) + 2(\nabla\mu).\nabla\bar{v} + (\nabla\mu)x(\nabla x\,\bar{v}) - 2/3(\nabla\mu)(\nabla.\bar{v}) + K\nabla(\nabla.\bar{v}) + \nabla K(\nabla.\bar{v}) \tag{3.2}$$

diffusion equation [62]:

$$\frac{DC_A}{Dt} + C_A(\nabla.\bar{v}) = \nabla.\rho D_v\left(\nabla\frac{C_A}{\rho}\right) \tag{3.3}$$

In principle, since the temperature is constant, equations (3.1), (3.2), and (3.3), together with :

$$\rho = f(P, C_A) \tag{3.4}$$

$$\mu = f(P, C_A) \tag{3.5}$$

$$K = f(P, C_A) \tag{3.6}$$

$$D_v = f(P, C_A) \tag{3.7}$$

could be solved to give C_A, ρ, P, μ, D_v, K, and $\bar{v}$ as functions of position and time. The concentration gradient at a point on the body surface, and hence the local mass transfer rate, could then be obtained at a particular instant of time. A double integration over surface and time would then give the total amount of mass transferred in any specified time interval.

The calculation of mass transfer by this procedure is dependent upon a solution of equations (3.1)

to (3.7). The complexity of these equations is such that an analytical solution is impossible while a numerical solution, even if possible, would require so much labour that it would be impracticable. It is therefore necessary to consider the possibility of simplification of these equations in such a way that they are rendered soluble without making the mathematical model too far removed from the true physical situation.

For free and forced convection to interact, the bulk velocity must be low; of the same order of magnitude as the velocities encountered in free convective motion. At these low velocities the continuous phase, even if a gas, may be considered incompressible. The density, ρ, may therefore be considered independent of pressure. In many mass transfer operations the concentration and pressure gradients are small and the diffusion coefficient, D_v, and the viscosity, μ, which are weak functions of concentration and pressure, may be considered constant. It is important to note, however, that when free and forced convection interact, density cannot be considered independent of concentration. Free convective forces are solely due to density differences which exist between the solvent and the solution formed by mass transfer. Except in cases of fluids subject to rapidly varying forces, such as

ultrasonic vibrations, the bulk viscosity, K, may be taken as zero [61].

On introduction of the above simplifications, equations (3.1) to (3.7) reduce to :

$$\frac{D\rho}{Dt} + \rho(\nabla.\bar{v}) = 0 \qquad (3.8)$$

$$\rho\frac{D\bar{v}}{Dt} = \rho\bar{g} - \nabla P + 1/3\mu\nabla(\nabla.\bar{v}) + \mu\nabla^2\bar{v} \qquad (3.9)$$

$$\frac{DC_A}{Dt} + C_A(\nabla.\bar{v}) = \rho D_v \nabla.(\nabla \frac{C_A}{\rho}) \qquad (3.10)$$

where μ and D_v are constants and

$$\rho = f(C_A) \qquad (3.11)$$

Equations (3.8) to (3.11) are still too complex to be useful in obtaining solutions to mass transfer problems. Further simplification is therefore necessary.

The major influence of the density differences is upon body forces, represented by the term $\rho\bar{g}$ in equation (3.9). In order to achieve further simplification of equations (3.8) to (3.11), density variations may be neglected elsewhere in these equations. Writing the constant density of the bulk fluid as ρ_o and the variable density of the body force term as ρ, equations (3.8) to (3.11) reduce to :

$$\nabla.\bar{v} = 0 \qquad (3.12)$$

$$\rho_o \frac{D\bar{v}}{Dt} = \rho \bar{g} - \nabla P + \mu \nabla^2 \bar{v} \qquad (3.13)$$

$$\frac{DC_A}{Dt} = D_v \nabla^2 C_A \qquad (3.14)$$

$$\rho = f(C_A) \qquad (3.15)$$

Equation (3.13) may be rewritten as :

$$\rho_o \frac{D\bar{v}}{Dt} = (\rho - \rho_o) \bar{g} + \rho_o \bar{g} - \nabla P + \mu \nabla^2 \bar{v} \qquad (3.16)$$

If the quantity P_o, the pressure at a point in the fluid when the fluid is at rest, is introduced then, since :

$$\nabla P_o = \rho_o \bar{g} \qquad (3.17)$$

equation (3.16) becomes :

$$\rho_o \frac{D\bar{v}}{Dt} = (\rho - \rho_o) \bar{g} - \nabla (P - P_o) + \mu \nabla^2 \bar{v} \qquad (3.18)$$

In equation (3.18) the quantity $(\rho - \rho_o) \bar{g}$ represents the buoyancy force due to density differences. Writing $(P-P_o)$ as P', the set of equations representing the system becomes :

$$\nabla . \bar{v} = 0 \qquad (3.19)$$

$$\rho_o \frac{D\bar{v}}{Dt} = (\rho - \rho_o) \bar{g} - \nabla P' + \mu \nabla^2 \bar{v} \qquad (3.20)$$

$$\frac{DC_A}{Dt} = D_v \nabla^2 C_A \qquad (3.21)$$

$$\rho = f(C_A) \qquad (3.22)$$

In the case of free convection or forced convection alone, equation (3.20) may be further simplified; for free convection alone there is no bulk flow and $\nabla P'$ is very small and may be neglected; for forced convection alone buoyancy forces are negligible and the term $(\rho - \rho_o)\,\bar{g}$ may be omitted. Thus for situations in which mass transfer is by free convection or forced convection alone, the equations describing the system are more simple than for the general case where the two effects interact. In addition, when mass transfer is by free convection or forced convection alone, equations (3.20) and (3.21) may often be further simplified by means of the boundary layer concept. When mass transfer from a rigid drop occurs in the presence of interacting free and forced convection, these two effects are normally opposed and the flow patterns around the drop may be expected to be complex and inherently unstable. In this situation the assumption of a thin boundary layer is unlikely to be valid. Therefore, for the situation at present under investigation, i.e. mass transfer from a rigid drop with interacting free and forced convection, it is not possible to solve equations (3.19) to (3.22) as has been done for forced convection and free convection alone.

It is possible, however, by consideration of the dimensionless forms of equations (3.19) to (3.22), to

decide which dimensionless groups may be expected to be of importance in the correlation of mass transfer data. In order to do this the following substitutions are introduced :

$$\bar{v}^* = \frac{\bar{v}}{U_{inf.}} \; ; \quad t^* = \frac{t\, U_{inf.}}{d_{Ch}} \; ; \quad P'^* = \frac{P'}{\rho U^2_{inf.}} \; ;$$

$$C_A^* = \frac{C_A - C_{Ao}}{C_{As} - C_{Ao}} \; ; \quad \rho^* = \frac{\rho - \rho_o}{\rho_s - \rho_o} \; .$$

The operator ∇ is made dimensionless by multiplication by d_{Ch}, i.e.

$$\nabla^* = d_{Ch} \nabla \quad \text{and} \quad (\nabla^*)^2 = d^2_{Ch} \nabla^2 \; .$$

In the above dimensionless quantities U_{inf} is the undisturbed bulk velocity, C_{As} the saturation concentration, C_{Ao} the bulk concentration, and ρ_s the density of the saturated solution. With the above substitutions equations (3.19) to (3.21) become :

$$\nabla^* \cdot \bar{v}^* = 0 \tag{3.23}$$

$$\frac{D\bar{v}^*}{Dt^*} = \left(\frac{Gr}{Re^2} \right) \frac{\bar{g}}{g} \rho^* - \nabla^* P'^* + \frac{1}{Re} (\nabla^*)^2 \bar{v}^* \tag{3.24}$$

$$\frac{DC_A^*}{Dt^*} = \frac{1}{Re.Sc} (\nabla^*)^2 C_A^* \tag{3.25}$$

where $Gr = \dfrac{\rho_s - \rho_o}{\rho_o} \cdot \dfrac{d^3_{Ch}\, \rho^2_o\, g}{\mu^2}$; $Re = \dfrac{U_{inf.}\, \rho_o\, d_{Ch}}{\mu}$;

and $Sc = \dfrac{\mu}{\rho_o D_v}$.

From this analysis it may therefore be concluded that :

$$C_A = f\left(\frac{Gr}{Re^2}, Re, Re.Sc, t, \text{position}\right) \quad (3.26)$$

The mass flux of component A at the surface is given by :

$$q_A = -D_v \left.\frac{\partial C_A}{\partial N}\right|_{surface} \quad (3.27)$$

where $\frac{\partial}{\partial N}$ denotes differentiation in the direction of the normal to the surface. This mass flux may also be defined in terms of the local mass transfer coefficient, k_{loc}, by :

$$q_A = k_{loc}\,(C_{As} - C_{Ao}) \quad (3.28)$$

where the surface concentration is taken to be the saturation concentration, C_{As}. Combination of equations (3.27) and (3.28) gives :

$$\frac{k_{loc}}{D_v} = -\frac{1}{(C_{As} - C_{Ao})} \cdot \left.\frac{\partial C_A}{\partial N}\right|_{surface} \quad (3.29)$$

Introduction of the following dimensionless substitutions :

$$C_A^* = \frac{C_A - C_{Ao}}{C_{As} - C_{Ao}} \quad ; \quad N^* = \frac{N}{d_{Ch}} \quad \text{leads to :}$$

$$\frac{k_{loc}}{D_v} = -\frac{1}{d_{Ch}} \left.\frac{\partial C_A^*}{\partial N^*}\right|_{surface} \quad (3.30)$$

or :

$$\frac{k_{loc} \cdot d_{Ch}}{D_v} = Sh_{loc} = - \frac{\delta C_A^*}{\delta N^*} \Bigg|_{surface} \qquad (3.31)$$

Equation (3.31) shows that the local Sherwood number, Sh_{loc}, at a point on the surface is the dimensionless concentration gradient normal to the surface at that point. From equations (3.26) and (3.31) it may therefore be concluded that :

$$Sh_{loc} = f\ (Re,\ Gr/Re^2,\ Re.Sc,\ \overset{position}{on\ surface},\ t) \qquad (3.32)$$

The overall Sherwood number, Sh, for the whole surface is then given by :

$$Sh = f\ (Re,\ Gr/Re^2,\ Re.Sc,\ t\ ) \qquad (3.33)$$

If the mass transfer is considered to be steady state in the time average, the equation (3.33) reduces to :

$$Sh = f\ (Re,\ Gr/Re^2,\ Re.Sc\ ) \qquad (3.34)$$

Equation (3.34) may also be expressed in the more general form :

$$Sh = f\ (Re,\ Gr,\ Sc\ ) \qquad (3.35)$$

As a result of the above analysis, the dimensionless groups Re, (Gr/Re^2), (Re.Sc), and Sh, are expected to be of importance in the correlation of mass transfer data for situations in which free and forced convection interact. The group (Gr/Re^2) represents the ratio of buoyancy forces to inertia forces. When

(Gr/Re^2) is very small, buoyancy forces are negligible compared with inertia forces i.e. the effects of free convection are negligible. Conversely, when (Gr/Re^2) is very large, inertia forces are negligible compared with buoyancy forces and the effects of forced convection are negligible.

From the above considerations it is evident that the group (Gr/Re^2) provides a criterion for deciding whether free or forced convection may be neglected in the prediction of mass transfer rates or whether both must be taken into account.

3.2. CHARACTERISTIC DIMENSIONS.

In principle, mass transfer data for any series of geometrically similar shapes may be represented by a single correlation in terms of the dimensionless Reynolds, Sherwood, Schmidt, and Grashof numbers. In these dimensionless groups any representative dimension may be used as a characteristic dimension. For example, data for a series of oblate spheroidal shapes of different size, but the same eccentricity i.e. ratio of minor to major axis, could be uniquely correlated by use of the major axis as the characteristic dimension.

If the data have been obtained from experiments using a set of geometrically related though not

geometrically similar, shapes, the problem becomes more complex. In this case it is necessary to introduce a further dimensionless group reflecting the shape variation. The present investigation, mass transfer from oblate spheroids of various eccentricities, falls into this latter category, the shape eccentricity, e, being the obvious choice of additional dimensionless group in this case.

Previous workers have attempted to account for the effect of shape by use of a shape dependent characteristic dimension in the Reynolds, Sherwood, and Grashof numbers, rather than by basing these groups on a shape independent characteristic dimension and introducing an additional dimensionless group to account for the shape variation. Dimensions which have been used in this manner are the following :

1) the diameter of the sphere of the same volume as the body[2,5,7,6,9,63,64];

2) the length of the minor axis [9,11];

3) the surface area of the body divided by the perimeter normal to flow [9,11,35];

4) the diameter of the sphere with the same surface area as the body [9,11];

5) the arithmetic mean of the major and minor axes [9,11];

6) the diameter of the sphere of the same volume as the body multiplied by the sphericity of the body [9,11,65];

7) the length of the major axis [9];

8) the cube root of the product of all three axes [3].

A further possible characteristic dimension, which may be added to the above is the geometric mean of the major and minor axes.

The diameter of the sphere of the same volume has been widely used since it is particularly useful when the total drop volume and the number of drops are known. The drop volume and hence the characteristic dimension can be estimated without a knowledge of drop shape. For this reason it is also common to base the associated mass transfer coefficient upon the surface area of the spherical drop of the same volume, although the true surface area may also be used if available.

The volume of an oblate spheroid is related to the semi-major and semi-minor axes, g and f, by the expression :

$$V = (\tfrac{4}{3})\ \pi\ f\ g^2 \qquad (3.36)$$

The diameter of the sphere of the same volume as the spheroid is therefore given by :

$$d_1 = (8\ f\ g^2)^{1/3} \qquad (3.37)$$

In terms of the spheroid major axis, d_M, and the eccentricity, e, this may be written :

$$d_1 = d_M \, e^{1/3} \qquad (3.38)$$

The spheroid minor axis, d_2, was considered as a potentially useful characteristic dimension by Skelland and Cornish [9]. It is related to f by :

$$d_2 = 2f \qquad (3.39)$$

and to the major axis by :

$$d_2 = d_M \, e \qquad (3.40)$$

The total surface area divided by the perimeter normal to flow, d_3, was successfully employed by Pasternak and Gauvin [35] to correlate mass transfer data for spheres, cylinders, prisms, hemispheres, and cubes, by the single expression :

$$Sh_3 = 0.692 \, Re_3^{0.514} \, Sc^{1/3} \qquad (3.41)$$

This expression correlated the experimental results with a "deviation" of 15% although no mention is made of whether this deviation is average, standard, or maximum. Pasternak and Gauvin also successfully applied this dimension to the results of other workers notably Williams [66], Powell [52], Linton and Sherwood [28], Maisel and Sherwood [29], and Krischer and Loos [25].

From the expression for the surface area of a spheroid, i.e. :

$$A = 2\pi g^2 + \frac{\pi g f^2}{(g^2-f^2)^{\frac{1}{2}}} \ln\left(\frac{g + (g^2-f^2)^{1/2}}{g - (g^2-f^2)^{1/2}}\right) \qquad (3.42)$$

d_3 can be shown to be related to f and g by the following expression :

$$d_3 = g + \frac{f^2}{2(g^2-f^2)^{\frac{1}{2}}} \ln\left(\frac{g + (g^2-f^2)^{\frac{1}{2}}}{g - (g^2-f^2)^{\frac{1}{2}}}\right) \qquad (3.43)$$

In terms of the major axis this becomes :

$$d_3 = d_M\left[1/2 + \frac{e^2}{4(1-e^2)^{\frac{1}{2}}} \ln\left(\frac{1 + (1-e^2)^{\frac{1}{2}}}{1 - (1-e^2)^{\frac{1}{2}}}\right)\right] \qquad (3.44)$$

The diameter of the sphere of the same surface area as the spheroid, d_4, has the obvious advantage that the true surface area is retained. In terms of f and g and of d_M and e it may be written :

$$d_4 = \left[2g^2 + \frac{f^2 g}{(g^2-f^2)^{\frac{1}{2}}} \ln\left(\frac{g + (g^2-f^2)^{\frac{1}{2}}}{g - (g^2-f^2)^{\frac{1}{2}}}\right)\right]^{\frac{1}{2}} \qquad (3.45)$$

$$d_4 = d_M\left[\frac{1}{2} + \frac{e^2}{4(1-e^2)^{\frac{1}{2}}} \ln\left(\frac{1 + (1-e^2)^{\frac{1}{2}}}{1 - (1-e^2)^{\frac{1}{2}}}\right)\right]^{\frac{1}{2}} \qquad (3.46)$$

The equivalent expressions for d_5, the arithmetic mean of major and minor axes is :

$$d_5 = g + f \qquad (3.47)$$

$$d_5 = d_M\left(\frac{1 + e}{2}\right) \qquad (3.48)$$

The sphericity multiplied by the diameter of the sphere of the same volume as the spheroid has been successfully employed in the field of multiparticle technology [67]. The sphericity is defined by :

$$\phi = \frac{\text{Surface area of sphere with same volume as spheroid}}{\text{Surface area of spheroid}}$$

The characteristic dimension, d_6, is related to d_1 by :

$$d_6 = \phi\, d_1 \tag{3.49}$$

It may also be written :

$$d_6 = \frac{8\, f\, g}{2g + {f^2}/{(g^2-f^2)^{\frac{1}{2}}}\ \ln\left(\frac{g + (g^2-f^2)^{\frac{1}{2}}}{g - (g^2-f^2)^{\frac{1}{2}}}\right)} \tag{3.50}$$

$$d_6 = d_M\left[\frac{1}{2e} + \frac{e}{4(1-e^2)^{\frac{1}{2}}}\ln\left(\frac{1 + (1-e^2)^{\frac{1}{2}}}{1 - (1-e^2)^{\frac{1}{2}}}\right)\right]^{-1} \tag{3.51}$$

It is interesting to note that this characteristic dimension, d_6, is identical to that defined by :

$$d_{Ch} = \frac{6V}{A} \tag{3.52}$$

and used by Tsubouchi and Sato [65].

Use of the major axis itself as a characteristic dimension is equivalent to the assumption that shape has no effect on mass transfer. Nevertheless, for completeness it may be expressed as a further characteristic dimension, d_7, where :

$$d_7 = 2g \tag{3.53}$$

$$d_7 = d_M \tag{3.54}$$

The geometric mean of the major and minor axes, d_8, may be written :

$$d_8 = (2g.2f)^{\frac{1}{2}} = 2(f.g)^{\frac{1}{2}} \quad (3.55)$$

$$\text{or :} \quad d_8 = d_M\, e^{\frac{1}{2}} \quad (3.56)$$

The cube root of the product of all three axes of the spheroid has been used by Lewis, Jones, and Pratt [3]. When expressed in terms of f and g or d_M and e it reduces to the same expressions as for d_1 : the diameter of the sphere of the same volume as the spheroid.

As shown above the characteristic dimensions d_1 to d_8 may be expressed as the product of the major axis, d_M, and a particular function of the eccentricity, e. If in general, mass transfer from oblate spheroids may be expressed as :

$$Sh = f\,(Re, Sc, Gr, e) \quad (3.57)$$

where the groups Sh, Re, and Gr are based upon the major axis of the oblate spheroid, the choice of a particular characteristic dimension is equivalent to rewriting equation (3.57) as :

$$[Sh.\psi(e)] = f\,[Re.\psi(e), Sc, Gr.(\psi(e))^3] \quad (3.58)$$

where the particular characteristic dimension employed is related to the eccentricity by :

$$d_{Ch} = d_M.\,\psi\,(e) \quad (3.59)$$

Although this approach somewhat limits the generality of equation (3.56)[7], a single correlation for

mass transfer data for oblate spheroids of different eccentricities in terms of a simple characteristic dimension would be extremely convenient. Such correlations have been presented by other workers and an attempt will be made to correlate the data of the present work in this manner.

CHAPTER 4.

EXPERIMENTAL APPARATUS AND TECHNIQUES.

4.1. INTRODUCTION.

In Chapter 3 consideration was given to the possibility of the theoretical prediction of mass transfer rates from drops to a surrounding medium in the presence of interacting free and forced convection. It was shown that, although the dimensionless forms of the equations of motion and diffusion may be used to obtain useful information concerning the dimensionless groups likely to be of interest in this situation, the complexity of the equations describing the system is such that a solution cannot be obtained without the introduction of assumptions which would make the equations no longer representative of the physical situation.

From these considerations it it evident that, with mass transfer theory in its present rudimentary state, the prediction of the mass transfer rates from drops to the surrounding medium in the presence of interacting free and forced convection must rely mainly upon empirical correlations. The survey of the literature, Chapter 2, shows, however, that a great deal of confusion and contradictory evidence exists concerning

the effect of the interaction of free and forced convection upon mass transfer rates. Furthermore, although there is much evidence to suggest that drops of one liquid falling or rising through a second liquid are frequently oblate spheroidal, rather than spherical, in shape, previous workers who have been concerned with the prediction of mass transfer rates from a single drop or solid particle in situations in which free and forced convection interact, have concentrated solely upon the spherical model.

In the light of the above considerations it was decided to carry out an experimental programme to obtain data for mass transfer from oblate spheroidal bodies in the presence of interacting free and forced convection. In order that the effects of shape and Reynolds number could be accurately studied, the oblate spheroidal bodies were to be rigidly supported in a fluid stream flowing at a controlled velocity. This model represents the fall or rise of liquid drops through a second liquid but eliminates the effects of oscillations, deformations, and internal circulation, which may be present in liquid-liquid systems.

The system selected for the experimental study was benzoic acid - water. This system has been

successfully employed by previous workers [24,26,38,44,47] for mass transfer studies at low Reynolds numbers and has the advantage that most of its physical properties are well established. The Grashof number of this system is high at room temperatures and it is therefore particularly suitable for studies in which the effects of free convection are to play an important role. Benzoic acid has the added advantage that it may be formed into accurately reproducible solid shapes. This subject is discussed in more detail in Section (4.3.1).

When drops of one liquid rise or fall through a second liquid the effects of free and forced convection are normally opposed. In order to represent this situation for the benzoic acid - water system, in which free convective forces act vertically downwards, the oblate spheroidal benzoic acid bodies were to be supported in a water tunnel in which the flow was vertically upwards. The oblate spheroidal bodies were to be supported with their minor axes parallel to the direction of flow. The range of Reynolds numbers to be investigated was $0 \leqslant Re_S \leqslant 200$; the data of other workers [24,26] suggest that this is the range of greatest interest with regard to the interaction of free and forced convection in benzoic acid - water systems.

An attempt was also to be made, by means of the schlieren technique, to photograph the flow patterns around the dissolving test bodies. If such photographs could be obtained they would provide useful qualitative evidence concerning the velocity distribution in the neighbourhood of dissolving bodies in situations in which free and forced convection interact.

4.2. WATER TUNNEL.

4.2.1. DESIGN CONSIDERATIONS.

The major difficulties in the design of water tunnels to operate at low Reynolds numbers lie in the creation of a stable velocity profile and the measurement of local velocities. Steinberger and Treybal [26] established known Poiseuille parabolic profiles by the use of very tall, small diameter columns. Use of such columns meant that the ratio of the sphere diameter to the column diameter was very high; in one case 0.497. There is much evidence [61,68,69,70,71] to indicate that, at such high values of this ratio, the containing wall has a profound effect upon the flow patterns around the test body. This effect becomes particularly important at low Reynolds numbers. When conditions of "creeping flow" exist, i.e. when $Re \ll 1$, theoretical analyses of

the simplified equations of motion are possible. The results of such analyses, summarised by Happel and Brenner [61], show that the wall effect is significant even at ratios as low as 0.1. Experimental observations [69] of the terminal falling velocity of liquid drops in a second liquid indicate that, in the Reynolds number range $3 \leqslant Re \leqslant 1200$, the effect of the wall on the terminal falling velocity is less than 1% for values of the ~~drop~~ diameter ratio less than 0.1. It is evident that, for low Reynolds number investigations, this ratio should be as low as possible. In the light of these considerations, it was decided to use a 1:12 ratio in the present work. Furthermore, in order to approach as closely as possible the ideal of an infinite medium, it was decided to employ a flat velocity profile rather than a parabolic one.

In order to obtain a flat profile with little turbulence, Garner and Keey [24] used a contraction section in conjunction with screens and honeycombs. Although they used a mean velocity based on volumetric throughput and cross-sectional area of the test section, these workers do not appear to have made any attempt to verify that the velocity profile was, in fact, flat. The use of the mean velocity was necessitated by the extreme difficulty of measuring the very low local velocities used

in their work. Nevertheless some qualitative check on the velocity profile would have been useful.

The large scatter of Garner and Keey's data is primarily due to the photographic technique used to determine the amounts of mass transferred. However, the increase of this scatter with decrease of the Reynolds number suggests that instability of the velocity profile may have been a contributory cause. A new approach to the design of low speed water tunnels was therefore used in the present work in an attempt to produce a flat velocity profile that would be stable down to $Re_S < 5$. This new design was based upon the use of a packed bed.

The use of packed beds to produce flat velocity profiles was suggested by the work of Arthur, Linnett, Raynor and Sington [72]. These workers measured the velocity profile across an air stream leaving a bed of carbon granules. The profile was determined by several methods and the effects of packing size, pre-bed air distribution and volumetric throughput investigated. The results indicated that the bed always tended to flatten the velocity profile and that decrease of particle diameter to column diameter ratio and decrease of volumetric throughput improved the "flatness". The pre-bed air distributors were quite crude but served to

illustrate that the better the pre-bed distribution the flatter the post-bed velocity profile.

Although the velocities used by Arthur et al. were high (of the order of 3 ft./sec.) the general trend of their work suggested that a packed bed could be successfully employed in the design of a low speed water tunnel, particularly since considerable improvements to their apparatus, in respect of pre-bed distribution and particle diameter to column diameter ratio, were possible.

The use of packed beds in the design of low speed water tunnels considerably simplifies construction as it obviates the need for a bulky contraction section and, as a stream of low intensity of turbulence is provided, it also eliminates the need for a series of gauzes to reduce turbulence intensity. It was felt, therefore, that if such a design were proved to be successful the concept would be of value to future workers.

4.2.2. STRUCTURAL DETAILS.

The water tunnel used in the present work had an overall height of 4 feet 1 inch and an internal cross-section of 1 ft. x 1 ft. As schlieren photography was to be an important part of the work, a tunnel of square

cross section was necessary in order to avoid the distortion caused by wall curvature. A drawing of the water tunnel is included, fig. (1), and a photograph, fig. (2), shows a general view of the equipment.

The water tunnel was constructed of 16 gauge mild steel flanged sections and incorporated a viewing section of 1/2 inch thick perspex. The metal sections were coated with a phenolic resin, "P/N Lithcote", to prevent corrosion. Samples of the material had been tested in saturated solutions of benzoic acid for several weeks without any sign of corrosion. The sectional construction of the column allowed flexibility when preliminary investigations of packing size, type and depth were carried out. The packing finally selected, on the basis of the post-bed velocity profile (Section 4.5.3), was a coarse grain sand, 8 to 12 mesh. A depth of $16\frac{1}{2}$ inches was used.

Care was taken when packing the column to ensure that no air was trapped in the bed. The column was filled with water before the thoroughly washed, wet sand was introduced. The bed was continuously stirred as the packing was added. When all the packing had been introduced the top of the bed was levelled. Muskat [73] points out that packing sand in the above

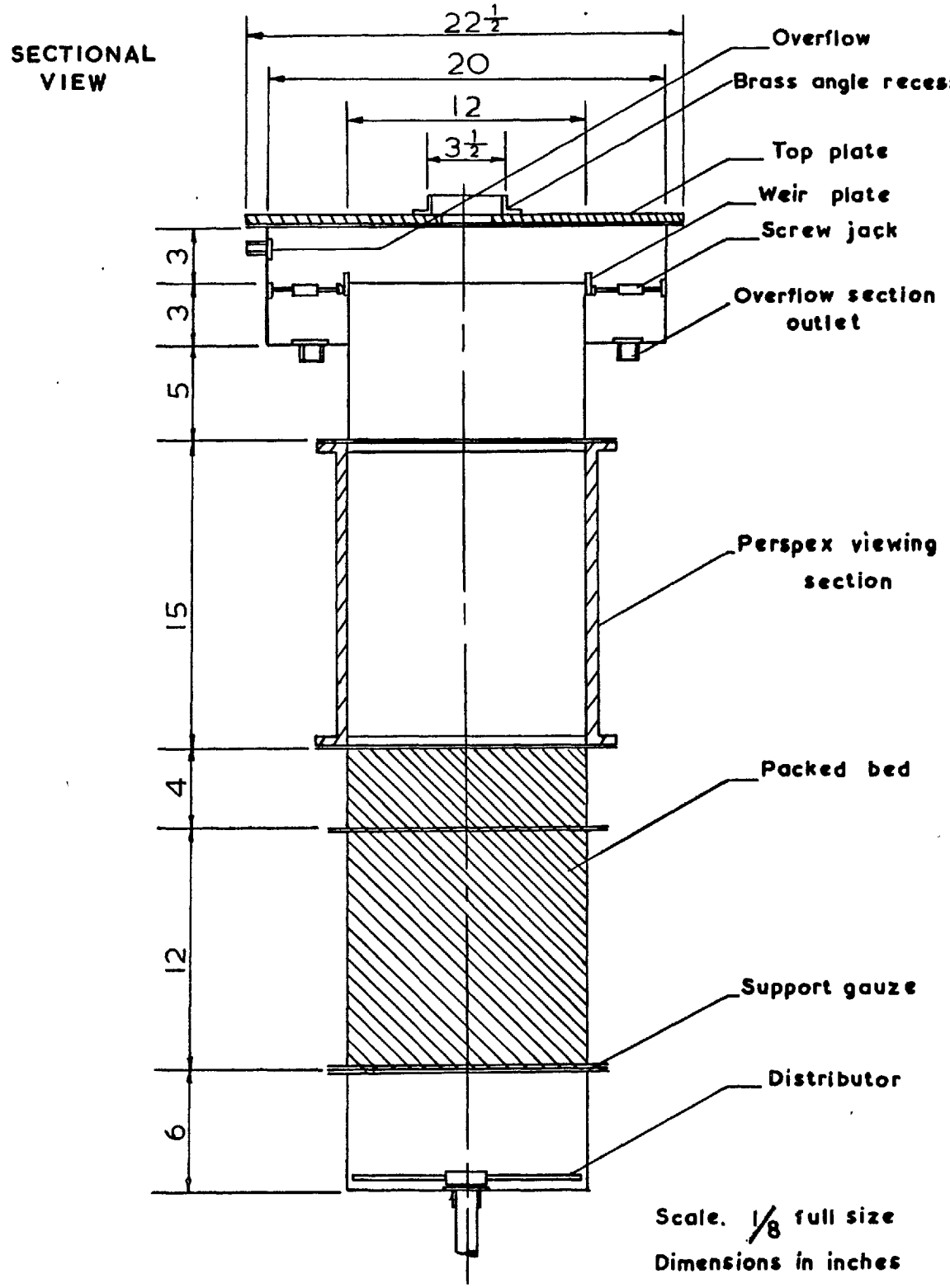

FIG. 1 WATER TUNNEL

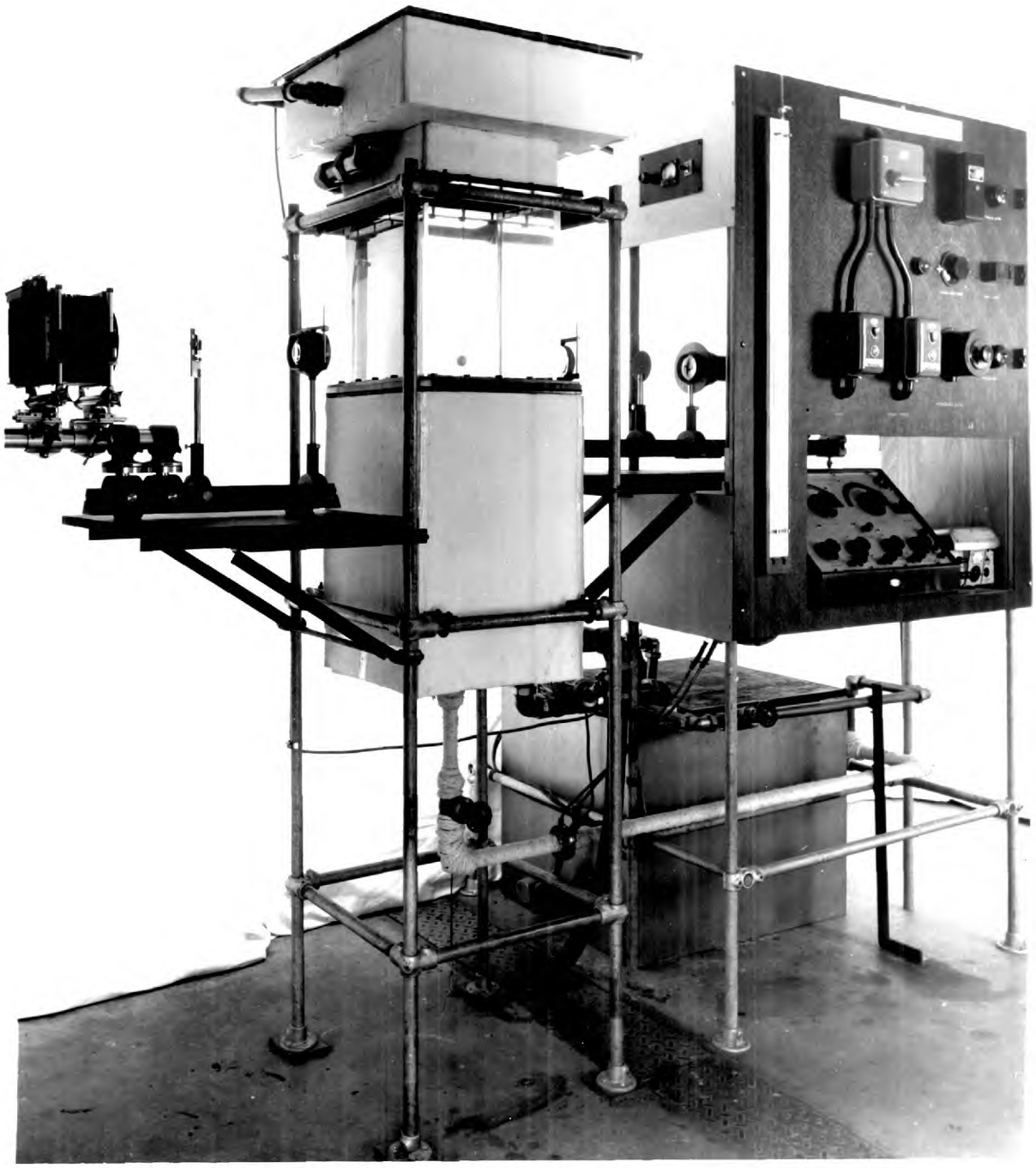

FIG. 2 GENERAL VIEW OF THE APPARATUS

manner results in an assemblage so nearly equal to the minimum porosity that further agitation or compression produces an almost inappreciable decrease. The structure of the bed was not, therefore, changed during the experimental work by settling.

Water entered at the base of the column through an eight armed distributor, fig. (3), constructed of 5/16 inch outside diameter brass tubing soldered into a central, 2 inch diameter, copper manifold. The 3/64 inch diameter outlet holes were on the underside of the distributor arms so that the emerging jets impinged onto the bottom of the column thus improving distribution. The exact number of these holes and their distance from the column centre line was such that the volumetric output per unit column cross-section was, as nearly as possible, constant. The distributor was tested in air, holes being added or blocked with solder in order to achieve as good a distribution as possible.

The bottom six inches of the column were not packed and acted as a calming section. This section was followed by the packed bed supported on a heavy gauge wire gauze bolted between flanges. On leaving the packed bed the water passed through the perspex

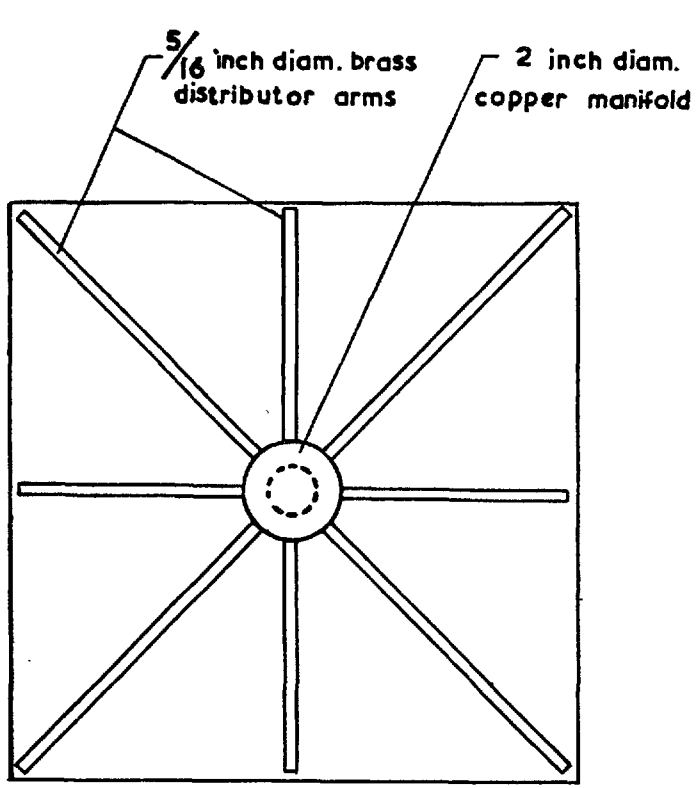

Scale. 1/4 full size

FIG. 3 INLET DISTRIBUTOR

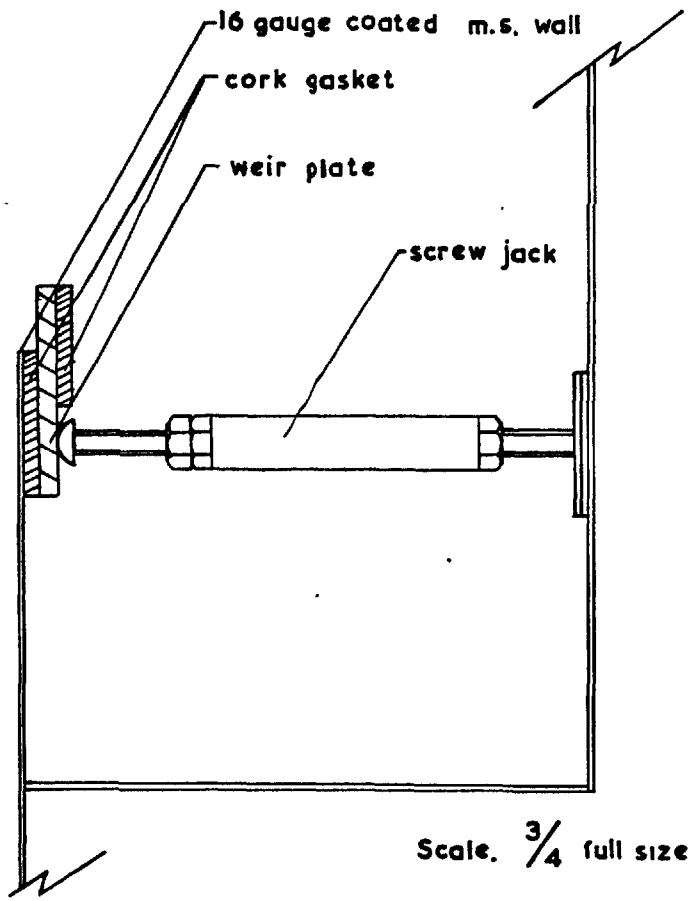

Scale. 3/4 full size

FIG. 4 WEIR PLATE & SCREW JACK

viewing section and left the column over a weir. The weir was fitted with adjustable plates clamped against the outside of the column wall by 16 screw jacks, fig. (4). The use of these plates allowed the weir to be critically levelled, thus preventing disturbance of upstream flow patterns by preferential flow of water over only part of the weir. The weir plates were of 1/8 inch x $1\frac{1}{2}$ inch brass strip. A cork gasket prevented leakage between the plates and the column wall.

Even when the plates were perfectly level, a surface tension effect caused channelling over the weir at low flow rates. To overcome this, a strip of the cork gasket material was glued to the outside of the weir plates and trimmed flush with the top. This modification proved highly successful and once the cork was thoroughly wet, uniform flow occurred over the whole length of the weir even at the lowest flow rates used. The open topped column design allowed the test body to be easily introduced with little disturbance to flow. Water flowing over the weir was collected in an overflow section from whence it returned by gravity to the feed tank.

A 1/2 inch thick, 1 ft. $10\frac{3}{4}$ inch square, aluminium plate, shown in fig. (1), covered the column

top and overflow sections. A $2\frac{1}{2}$ inch diameter hole at the centre of this plate permitted entry of the test object. Four $3\frac{1}{2}$ inch lengths of 1 inch x 1 inch x 1/8 inch thick brass angle were screwed to the top of the plate to form a $3\frac{1}{2}$ inch square that was concentric with the $2\frac{1}{2}$ inch diameter hole. To ensure positive and accurate positioning of the test body, the square end of the spheroid support rod, fig.(6), Section (4.2.4), fitted into the brass angle recess. Also cut into the top plate was a 6 inch diameter view hole which was provided with a perspex dust cover.

The water tunnel assembly was supported on a frame constructed of 1 inch outside diameter galvanised piping and "Keeklamp" fittings. Lemich and Levy [74] have shown that free convective mass transfer is unaffected by vibrations unless the amplitude or frequency of the vibrations is large. As a precautionary measure, however, the water tunnel frame was mounted on "Tico" antivibration pads to damp out any vibrations which might be transferred from other equipment through the structure of the building. The pump used was also mounted on a "Tico" pad and was connected to the rest of the apparatus by short lengths of rubber hose.

The working temperature used, $25.0^{\circ}C$, was

close to room temperature, but as a precaution against heat losses the metal sections of the column were insulated with 1/2 inch thick sheets of "Spandoplast" expanded polystyrene. The 1 inch delivery line between the feed tank and the column was lagged with asbestos rope.

4.2.3. ANCILLARY EQUIPMENT.

The feed tank was made of copper and measured 2 ft. 6 inches x 2 ft. x 2 ft. high. A mercury-toluene switch controlled a 1 kW. heater to maintain the tank temperature at 25.0°C. Water in the tank was efficiently mixed by a propeller type stirrer driven by a small electric motor. In consequence, the temperature could be easily controlled within limits of $\pm$ 0.1°C. To permit operation at 25.0°C. when the ambient temperature was in excess of this value, the tank was fitted with a cooling coil made of 1/2 inch diameter copper tubing. The flow of cooling water from the mains was controlled by a gate valve. A 4½ kW. boost heater enabled the system to be brought rapidly to the working temperature. A wooden cover was fitted to the tank to prevent the entry of dust from the atmosphere.

Water was pumped from the feed tank to the

column by a Stuart-Turner No.21 centrifugal pump. A fine copper gauze in the pump suction line acted as a filter. The stainless steel impeller was designed to deliver 500 Imp.gall./hr. against a 35 ft. head. As shown in fig. (5), a 1 inch nominal diameter by-pass line allowed water to be returned from the pump outlet to the feed tank without passing through the column. By combined operation of the gate valves on the by-pass and delivery lines the column throughput could be accurately controlled without heavy throttling of the pump. Some throttling was advisable, however, since this mimimised fluctuations in delivery rate.

The delivery line was fitted with flanges between which was bolted one of five interchangeable orifice plates. The pressure tappings were connected directly to an inverted U-tube manometer. The volumetric throughput was calculated from the pressure difference by use of the calibration curve of the appropriate orifice. The manometer recorded pressure differences of up to 3 ft. of water. To cover the range $3 < Re_S < 200$, orifices of diameters 0.15 inches, 0.33 inches, 0.44 inches, 0.60 inches, and 0.75 inches were used.

Water was returned from the column to the feed

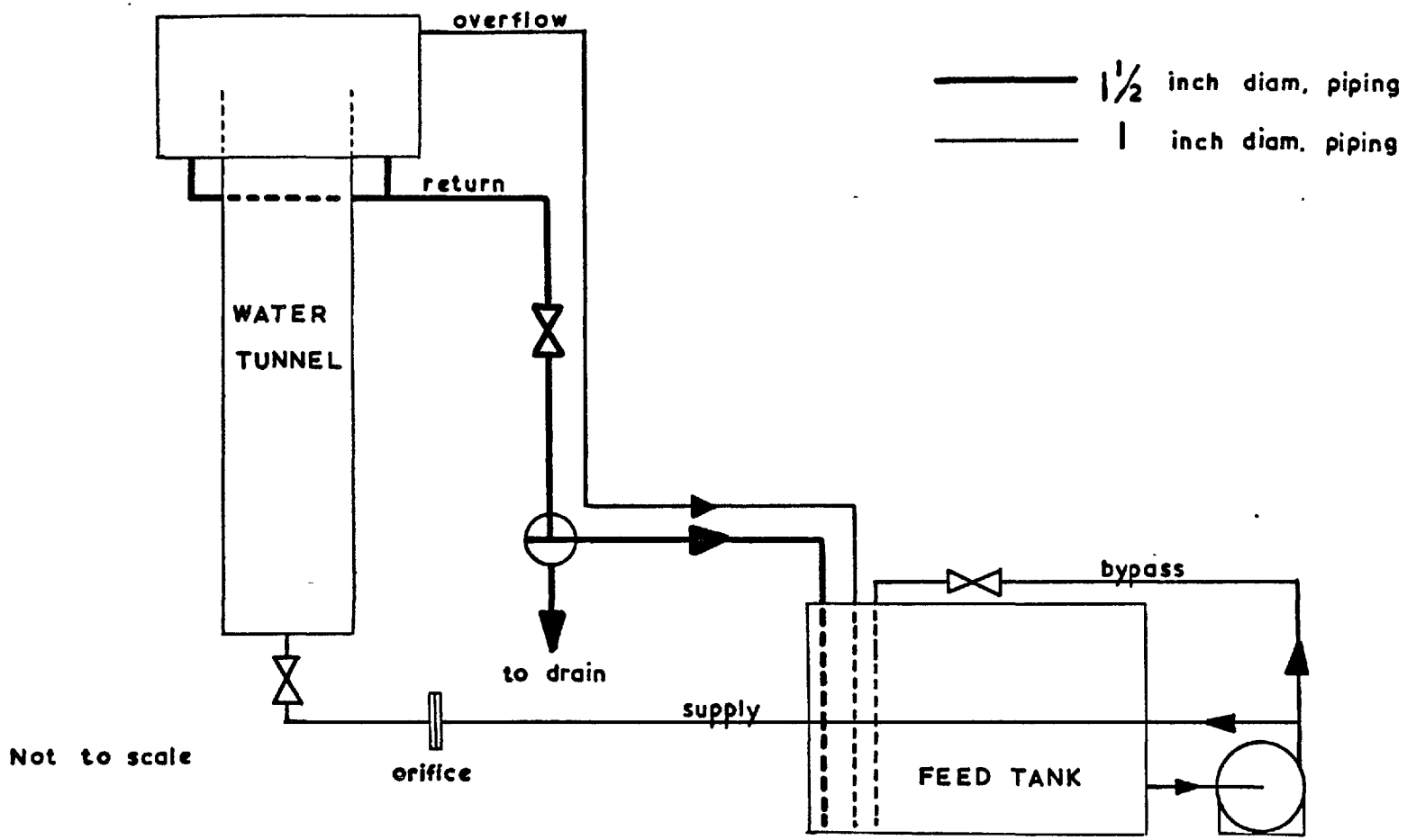

FIG. 5 PIPING DIAGRAM (Schematic)

tank by a 2 inch nominal diameter pipe. By adjustment of a valve on the return line, a constant head of water was maintained in the overflow section. This prevented the introduction of air bubbles into the feed tank by entrainment. The return line, together with all other piping, was of copper. Brass "Instantor" fittings were used throughout.

4.2.4. SPHEROID POSITIONING AND SUPPORT.

The spheroid support rod, fig. (6), was designed to provide rigid support for the test body with minimum disturbance to flow. A $2\frac{3}{4}$ inch long, 16 gauge, stainless steel rod was attached to the test body during casting and provided the final section of the support. The threaded end of this rod was screwed into a tapped hole in the lower end of the main support rod which, in turn, consisted of a 13 inch long, 1/4 inch diameter, stainless steel rod, turned down to 1/8 inch diameter for the final 3 inches. The 1/4 inch diameter to 1/8 inch diameter transition was smoothly accomplished over a 1/2 inch length. The upper end of this rod screwed into the centre of the plane face of a $2\frac{1}{2}$ inch long x $2\frac{1}{2}$ inch diameter aluminium cylinder. A $3\frac{1}{2}$ inch square x 1/2 inch thick aluminium plate was secured by four

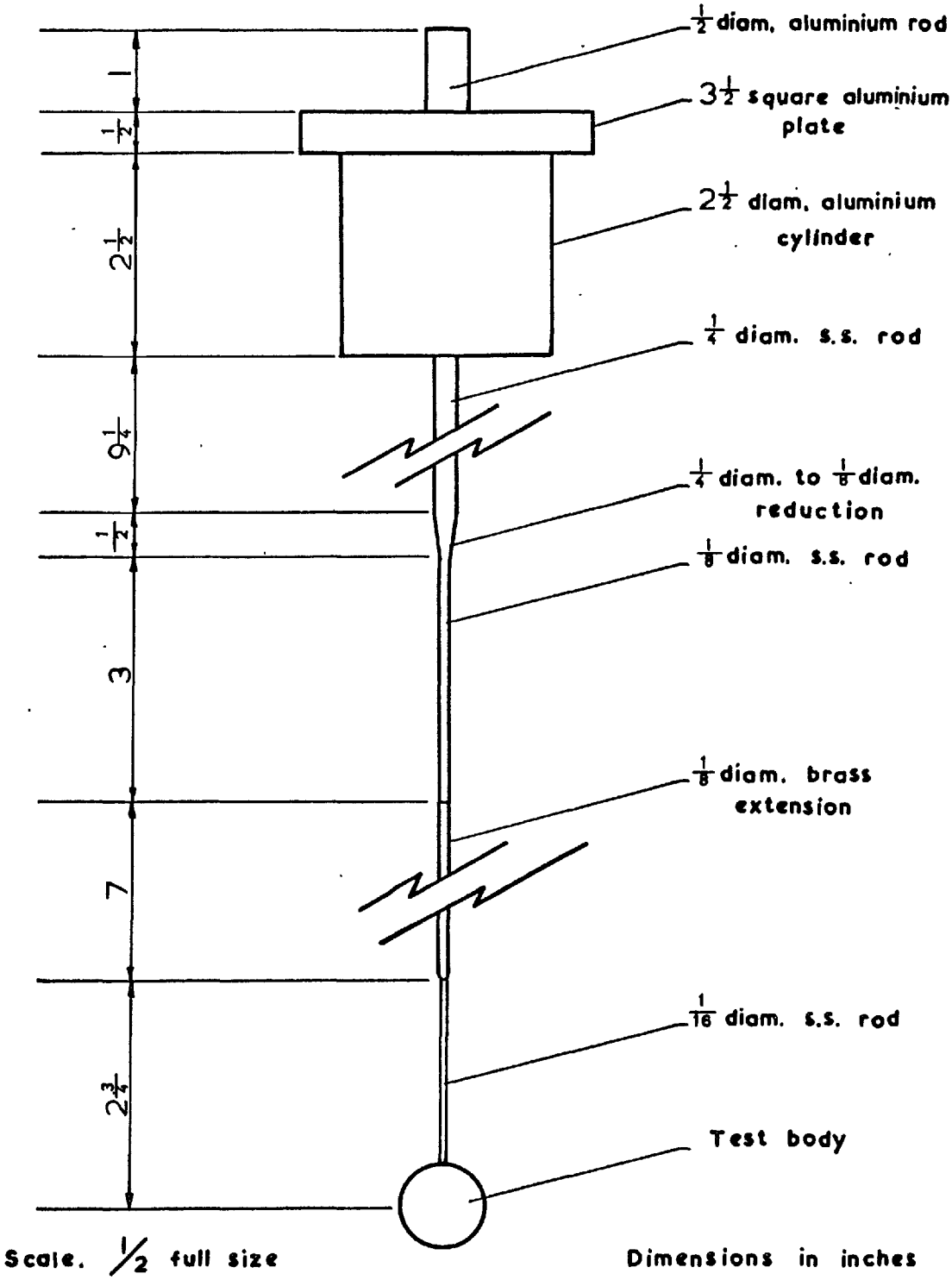

FIG. 6 SPHEROID SUPPORT ROD

Allen screws to the top of the cylinder. When the spheroid was in the test position, the aluminium cylinder and plate mated with the hole and brass angle square on the water tunnel top plate. A short length of 1/2 inch diameter aluminium rod projected from the 3½ inch square aluminium plate and served as a handle.

The above design positioned the test body on the centre line of the water tunnel at a level approximately half way up the viewing section. After preliminary investigation of flow patterns, section (4.5.3), an extension piece was added in order to position the test body at a lower point, 1½ inches above the packed bed. The extension consisted of a 7 inch long brass rod of 1/8 inch diameter. By means of a tapped hole at one end and a turned down, threaded section at the other, this rod was connected between the two sections of support rod already discussed.

4.3. PRODUCTION OF BENZOIC ACID SHAPES.

4.3.1. PRODUCTION METHOD.

Four possible methods of producing solid benzoic acid shapes were considered. These methods were compression, lapping, machining and casting.

Trial attempts to machine simple shapes from solid benzoic acid showed this to be a very time consuming operation even for a skilled machinist. Production of oblate spheroidal shapes by this method is, therefore, only practicable if no simpler method is available. The compression and lapping techniques have been successfully employed in the production of spheres by Garner et al.[24,44,47] and Rowe, Claxton and Lewis [38] respectively. Both methods depend, however, upon the random rotation of the shape during production and are therefore not suitable for the manufacture of oblate spheroids.

Casting, after the initial manufacture of the moulds, provides a simple method of making accurate and reproducible oblate spheroidal bodies. The casting technique also allows a support to be rigidly and accurately attached to the body during casting. This technique was chosen for the present work.

4.3.2. EXPERIMENTAL MOULDS.

Since molten benzoic acid is a highly corrosive substance, readily attacking brass, aluminium and ordinary steels, the moulds were machined from 58J acid resistant stainless steel. All accessory parts such as bolts and support rods were also made of stainless steel.

Because the effects of both shape and Reynolds number, upon mass transfer were to be investigated, five sets of moulds were manufactured, to produce oblate spheroids with eccentricities (ratio of lengths of minor to major axes) of 4:16, 7:16, 10:16, 13:16, and 16:16. The major axis was one inch in each case. The shapes were sufficiently large to enable accurate measurements of the weight losses to be made. A detailed drawing of a mould, fig. (7), is included.

The hemispheroidal cavities were cut in the die halves with specially made, quarter-elliptical tools; the stainless steel blanks being $2\frac{3}{4}$ inches in diameter and 3/4 inch thick. The surfaces of these cavities were polished to produce a mirror finish with a tolerance of $\pm$ 0.002 inches.

Incorporated in the mould assembly, together with the two die sections, was a top plate, 1/2 inch thick and $2\frac{3}{4}$ inches in diameter, fitted with an L-shaped bracket. This bracket allowed the spheroid support rod to be accurately positioned along the line of the minor axis. A 3/4 inch diameter hole at the centre of the top plate served as a reservoir for excess benzoic acid during casting. When assembling the mould a special jig was used to ensure correct alignment of the two die

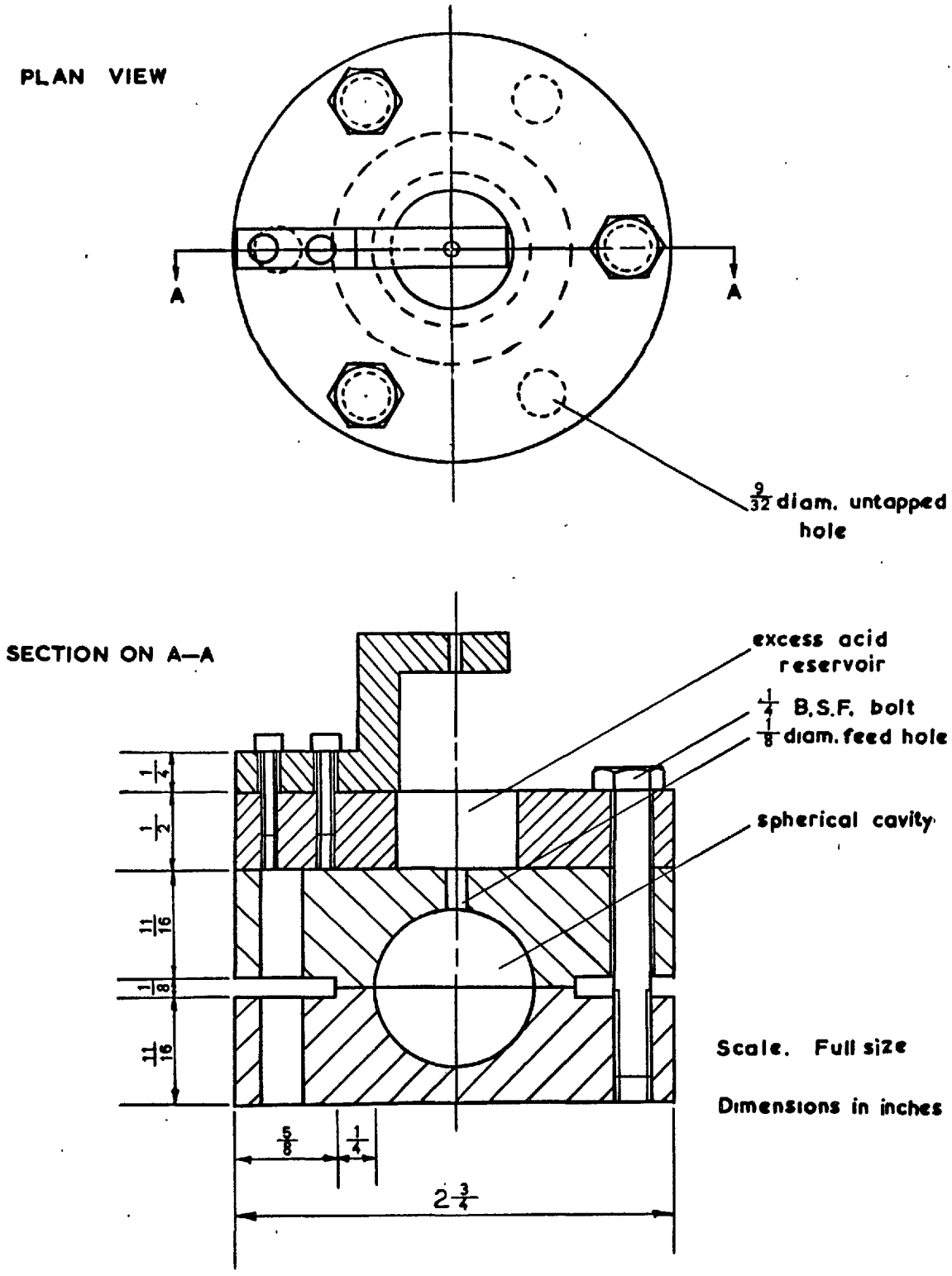

FIG. 7 MOULD ASSEMBLY

halves. This jig consisted of a flat plate to which three perpendicular pins, set at 120° to each other, were attached; two of these pins were permanently fixed to the plate, the third was adjustable. The loosely assembled mould was held firmly against the two fixed pins and the adjustable pin pushed against the mould and screwed down. The bolts of the mould assembly were then tightened. An assembled mould is shown in fig. (8) together with its various components and samples of the five oblate spheroidal shapes produced.

4.3.3. CASTING TECHNIQUE.

Much preliminary experimental work was necessary to develop a procedure for casting bodies with homogeneous, crack-free surfaces, which separated cleanly from the mould. The following proved to be the most successful technique.

The assembled mould was placed in an oven, set at 145°C, together with a funnel, the tip of which projected into the mould cavity through the 1/8 inch diameter hole in the upper die section. The funnel was made from a stainless steel capillary, cemented with "Araldite" into a 25 cc. glass syringe. The capillary was bent slightly so that, when its end was pushed into

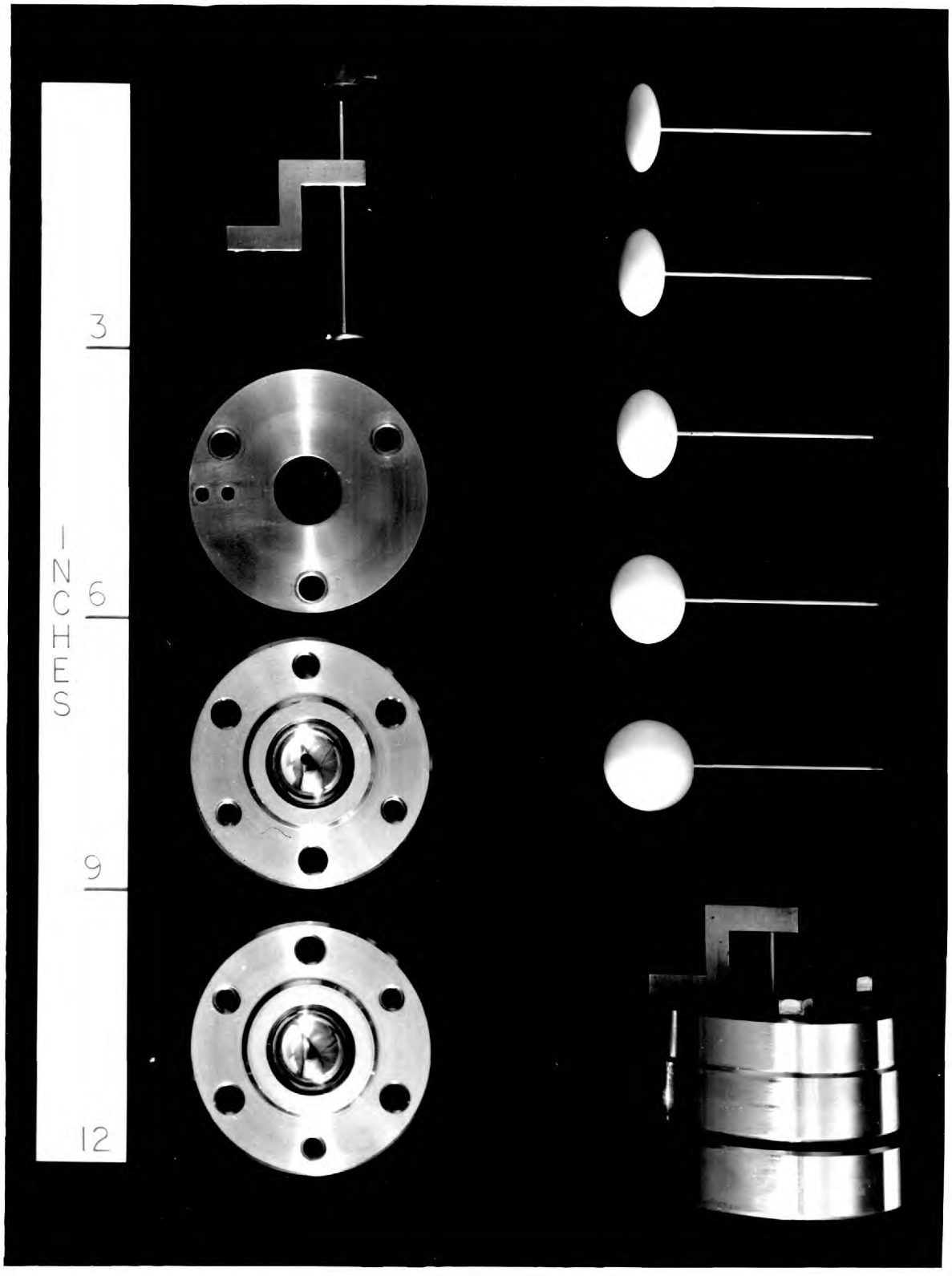

FIG. 8 MOULDS AND SPHEROIDS

the mould cavity, the body of the syringe remained in an upright position resting against the L-shaped bracket. The syringe body was insulated with asbestos string.

After three or four hours, when the oven had reached the set temperature, a glass phial containing a weighed quantity of benzoic acid crystals was placed in the oven. After a further hour, the benzoic acid, now molten, was poured into the funnel from whence it drained into the mould cavity. The oven was switched off after a further five minutes and allowed to cool overnight. The spheroid was then removed from the mould.

By this procedure up to four shapes were cast at one time, the limitation being oven size. The shapes thus produced, with a success rate of about 80%, separated easily from the moulds and had, smooth, opaque, crack-free surfaces. Even small deviations from this procedure caused a rapid increase in the failure rate; the most critical factors were casting temperature and the length of time for which the oven was left on after pouring the molten acid.

After removal from the mould the small amount of flash was carefully trimmed with a razor blade and the shapes, wrapped in paper tissues, stored in bottles containing some benzoic acid crystals.

Garner et al.[44,47] claimed that the crystal structure of cast shapes would cause irregular dissolution. Examination of the cross sections of the shapes produced by the above technique showed, however, that the crystals near the surface were small, dense, compact, and of uniform structure. Only towards the centre of the bodies did the crystals become larger and have a more open structure. This accounted for the densities of the bodies being slightly less than the literature[75] value of 1.266 g./cc. for solid benzoic acid. In the present work the mass transferred was always less than 5% of the mass of the body and the uniform, dense surface region was not penetrated. It was thought that the slight variations in crystal structure which may have existed in the surface region would have had only a negligible effect upon mass transfer rates. This effect would possibly be less than that caused by the stratified structure produced by the compression techniques of Garner et al.

4.4. PHOTOGRAPHIC EQUIPMENT.

It is common practice in present day research work to devise mathematical models to fit experimental data. For the mathematical model to be of any true

value it is essential that, as well as predicting experimental results, the model should be closely related to the physical situation which it is used to describe. In order to obtain a better understanding of the mechanism of mass transfer from solid shapes when free and forced convection interact, a schlieren technique [76] was employed to photograph the flow patterns around the dissolving test bodies. This technique depends upon the deflection of a ray of light by refractive index gradients normal to the ray.

Light from a 1 kW. mercury vapour lamp, fig. (9), was focussed onto a pinhole by means of a $2\frac{1}{2}$ inch diameter convex lens of 6 inches focal length. The pinhole acted as a point source and was situated at the focal length, $9\frac{1}{4}$ inches, of a 3 inch diameter achromatic doublet. The parallel beam leaving this lens passed through the test section and was focussed onto a knife edge by a 2.3 inch diameter compound lens of 8 inches focal length. The knife edge was positioned such that, in the absence of refractive index gradients, part of the light was cut off.

When the dissolving benzoic acid spheroid was in position in the test section, density gradients, and hence refractive index gradients, were set up in the

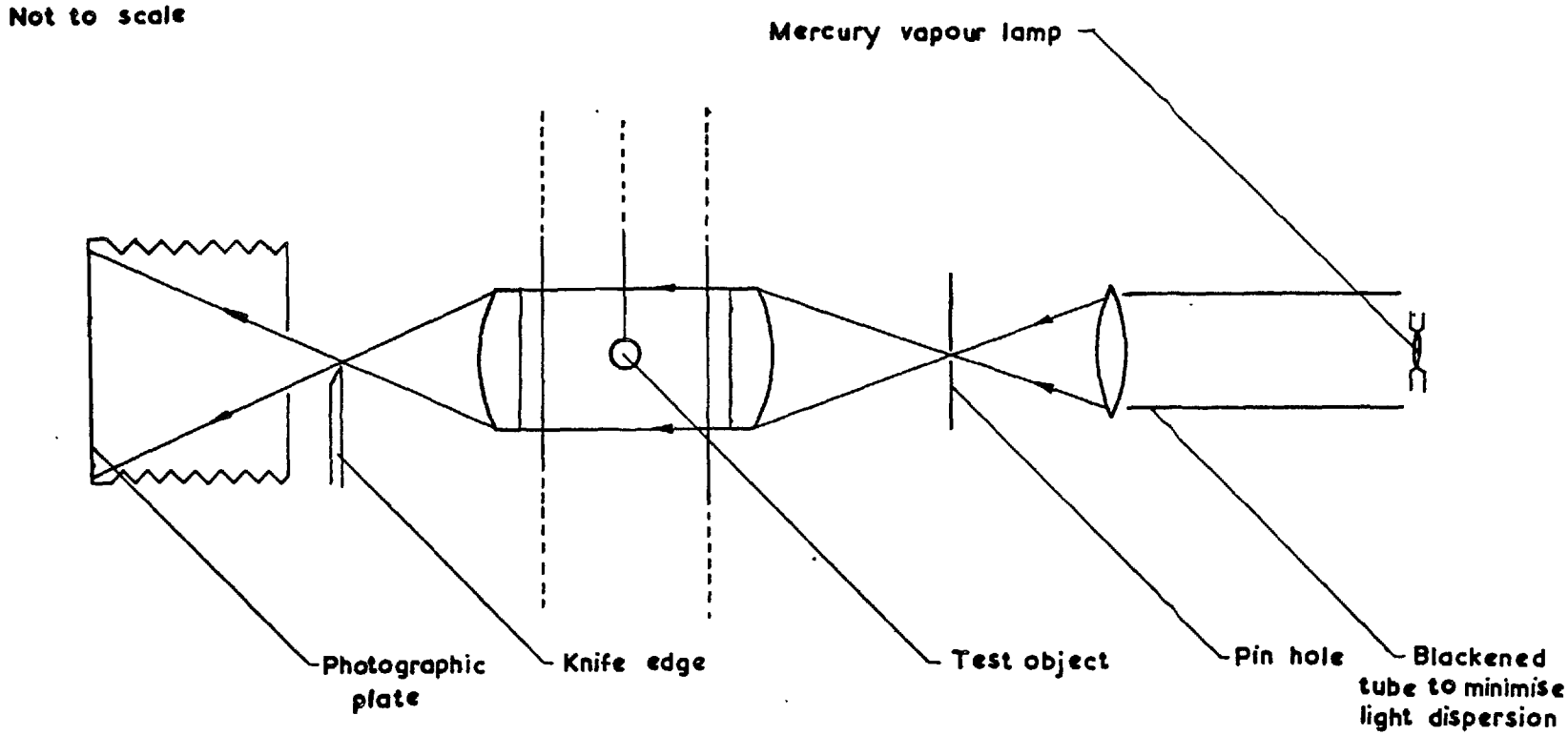

FIG. 9 SCHLIEREN APPARATUS (Schematic)

surrounding fluid, causing deflection of the light rays by amounts dependent upon local benzoic acid concentrations. The deflected rays either increased or decreased local light intensity according to whether deflection was away from or towards the opaque side of the knife edge. This resulted in light or dark areas when the image of the light source was focussed onto a screen or photographic plate.

A Sinar bellows camera was used to photograph the flow patterns. The lens was removed and the camera merely acted as a support for the photographic plate and as the shutter, the image being focussed onto the plate by the lens immediately preceding the knife edge. This lens and the camera were positioned so that the image formed filled the 5 inch by 4 inch photographic plates used. The plates, which were Kodak 0.800 "ortho-superspeed", were developed with Kodak D-76 developer.

The optical system was mounted on two lengths of optical bench supported on platforms fixed either side of the water tunnel. This arrangement is shown in fig. (2).

4.5. PRELIMINARY EXPERIMENTAL WORK.

4.5.1. ORIFICE PLATE CALIBRATION.

The orifice plates were designed closely, although not exactly to British Standard Specifications and calibration was necessary.

By operation of a three-way cock in the water tunnel return line water was collected for measured time intervals and weighed. The diversion of water from the feed tank resulted in a slight change of head at the pump inlet and hence in a small change in the flow rate; this in turn caused a small change in the manometer reading. The mean of the pressure differences before and after removal of water from the recirculating system was used in the calibration. To minimise these variations not more than 40 lb. of water were removed in a single collection and the water level was adjusted to a constant datum in the feed tank before each collection and before each experimental run. Water was collected for a period of time recorded on a stop clock and weighed to the nearest ounce on a calibrated laboratory spring balance. All calibrations were carried out at 25.0°C.

Approximately 35 calibration points were

recorded for each of the five orifices and the data for each fitted by an equation of the form :

$$F = C_7 (\Delta H)^{3/2} + C_8 (\Delta H) + C_9 (\Delta H)^{1/2} + C_{10} \qquad (4.1)$$

where F is the throughput in lb./min., (ΔH) the manometer reading in centimetres, and C_7 - C_{10} are constants. The data were fitted by a least squares library programme for the University of London Atlas computer. The mean error between the measured volumetric throughputs and those predicted by the correlating equation (4.1) was less than 1% for each of the five orifices. The values of the constants in equation (4.1) for each of the five orifices calibrated are included in Appendix 2.

4.5.2. TEST SECTION TEMPERATURE DISTRIBUTION.

A copper-constantan thermocouple, projecting from a 2 ft. length of stainless steel capillary, was used to explore the temperature profiles in the test section. The thermocouple junction was coated with "Araldite" which served to insulate the junction from the water and to cement the wires to the stainless steel sheath.

The local temperature measurements were carried out at various flow rates with the feed tank temperature constant at 25.0°C. Although the thermocouple could detect very small temperature changes, estimated at ± 0.05°C, no temperature variations were recorded within the whole of the test section. Investigations over a 5 hour period showed no temperature variation with time.

In view of the constancy of temperature with position and time, a single mercury-in-glass thermometer was used to measure the test section temperature during the main series of experimental runs. Two readings, one before and one after the runs, were taken. Except for the free convection runs where the temperature fell by a maximum of 0.3°C during the run, the temperature was constant at 25.0°C before and after all runs. The calibrated mercury-in-glass thermometer employed had scale divisions of 0.1°C and a range of from 0°C to 50°C. The thermometer was as accurate as the thermocouple and considerably simpler to use.

4.5.3. TEST SECTION VELOCITY PROFILE.

The combination of relatively large bodies, the low range of Reynolds number investigated, and the use of water as the continuous phase fluid, resulted in

very small velocities in the test section (0.02 to 0.69 cm./sec. for sphere Reynolds numbers of 4.8 to 195).

As has already been pointed out in Section (4.2.1), the absolute measurement of very low velocities is extremely difficult. Use of a pilot-static tube would have resulted in head differences of from 10^{-7} to 10^{-4} inches of water for sphere Reynolds numbers of from 5 to 200. Since the micro-manometers and gauges used to record low pressure differences have accuracies variously reported as [77,78] $\pm$ 2 x 10^{-4} inches of water and [79] $\pm$5 x 10^{-5} inches of water, they were clearly of no use in the work described.

Attempts were made to construct a sensitive measuring device of the vane anemometer type. A brass foil disc with an 1/8 inch diameter hole at the centre was reduced with emery paper to the minimum thickness compatible with rigidity. Segmental cuts were made in the disc and the segments twisted to form eight equally spaced vanes. A hub was machined from a 1/4 inch diameter polytetrafluoroethylene rod. The top of the hub was turned down to 1/8 inch diameter and was a push fit into the hole at the centre of the vanes, the whole being balanced on a needle projecting into a cavity machined into the bottom of the hub. Various

combinations of vane angle and length, and cavity depth and shape were tried but although rotation of the vanes required very little force, no rotation was observed in the water tunnel even at the maximum flow rate and after motion had been initiated mechanically.

Exploratory work was also carried out with a dye injection technique but the uncertainties of injection velocity, dye density, and dispersion by diffusion, rendered this technique unsuitable for measurement of the low velocities encountered.

Observation of the dissolving test bodies showed that the streams of benzoic acid solution photographed by the schlieren technique, (Section 4.4), were also clearly visible to the naked eye. The form of these flow patterns was very sensitive to changes in velocity over the range of Reynolds number investigated i.e. $0 \leqslant Re_S \leqslant 195$. The form of these flow patterns is discussed in more detail in Chapter 5 where representative photographs, figs. (10-14), are also presented. At Reynolds numbers above approximately 30, the flow separation angle for flow round the sphere varied with flow velocity. At lower Reynolds numbers the flow patterns, although complex, varied characteristically with velocity. For example, the proportion of time

spent in upflow or downflow, the frequency of collapse of the wake region, and the strength of disturbances of the tail when this type of pattern existed, were all related to flow velocity. It was therefore possible to obtain a qualitative indication of the test section velocity profile by observation of these patterns.

With the water tunnel top plate removed, the spheroid support rod was temporarily supported by two lengths of metal strip laid across the top of the overflow section. Thus the test body was located at the desired points in the column, the vertical position being achieved by the removal or addition of support rod extension pieces (Section 4.2.4) or by packing placed under the metal strips.

Early investigations of thus type with Raschig ring packings, together with results of work by Arthur et al.[72], indicated that the packing size should be as small as possible within the limitations of the pressure drop imposed by the pump delivery characteristics and the minimum fluidisation velocity of the bed. From these considerations an 8 to 12 mesh sand was chosen for investigation. The flow patterns in a 4 inch zone immediately above the $16\frac{1}{2}$ inch deep bed of this sand were unaffected by the position of the test body in the

test section. At the top of this zone, i.e. 4 inches above the bed, the first indications of a wall effect were noticed at Reynolds numbers less than ten. As the flow rate was increased, so did the height above the bed at which the wall effect was first detectable. This is in agreement with the concept of the flat velocity profile leaving the bed gradually changing into a fully developed laminar flow profile [80].

As a result of the velocity profile investigations it was decided to use the 7 inch support rod extension, discussed in Section (4.2.4), in the main series of experimental runs. The test bodies were thus positioned in the 4 inch zone where there was no wall effect.

In the absence of a reliable means of determining the absolute local velocities, and on the evidence of the velocity profile investigations, mean velocities based upon volumetric throughput and cross-sectional area were used in the calculation of the Reynolds numbers.

Evaluation of the errors involved in the calculation of Reynolds numbers by this procedure was not possible. The observations of the flow patterns suggested that at Reynolds numbers greater than ten the error was small. At very low flow rates, however, more

uncertainty exists. This probably accounts for the slightly increased scatter of the data points at these low flows.

4.6. EXPERIMENTAL PROCEDURE.

4.6.1. WATER TUNNEL OPERATION.

The boost heater was used as necessary to bring the feed tank water temperature to approximately 25.0°C. The controlled heater was then switched on, the pump started, and the delivery and bypass valves adjusted to give the maximum flow rate measurable by the manometer. The water level in the overflow section was kept above the level of the weir for two or three minutes to ensure wetting of the weir plates. The return line valve was then adjusted to maintain a steady water level of 1 to 2 inches in the overflow section. This level was easily controlled and was followed from outside the column by means of a ⋂-shaped glass tube. One limb of this glass tube passed through the top plate and dipped below the water surface in the overflow section while the other end was open to the air.

It was normally found necessary to use the cooling coil to remove heat created by friction in the

pump and in the flow circuit, even when the ambient temperature was below 25.0°C. Temperature in the test section was measured with the mercury-in-glass thermometer described in Section (4.5.2). When this thermometer indicated a steady temperature of 25.0°C (normally after 1 to 2 hours), the delivery and bypass valves were adjusted to give the required manometer reading, and the return valve readjusted to keep the overflow level constant. A further period of 1/2 to 1 hour was allowed for the steady state to again be reached before the test section temperature was recorded and the thermometer removed. The spheroid, which had previously been stored in a desiccator, was weighed, attached to the main support rod, and carefully introduced into the water tunnel.

During the experimental runs the manometer reading was recorded at intervals of 15 to 30 minutes. Fluctuations in the manometer reading were small; the mean change of reading during a complete run, averaged over the 117 experimental runs, was 0.8percent. Time weighted means of the recorded manometer readings were used in the calculation of the volumetric throughputs from the calibration curves.

After the required time of immersion, of from

50 minutes to 4½ hours, the spheroid was removed, excess water removed from its surface with a paper tissue, and stored in a desiccator to await weighing (Section 4.6.2). After the thermometer was replaced and the test section temperature recorded, the bypass valve was fully opened, the delivery valve closed, and the pump stopped. Finally the controlled heater was switched off and the cooling water control valve closed.

After each run approximately two cubic feet of water were pumped to waste and replaced by fresh, distilled water; the three-way cock on the return line allowed direct return to the feed tank or delivery to drain. This in itself was sufficient to keep the benzoic acid concentration in the circulating water below 1 percent of the saturation level. However, to ensure against the build up of dust or other extraneous material, the feed tank was periodically drained, cleaned, and refilled with fresh distilled water.

In order to change an orifice plate, the manometer tap was opened and water drained from the manometer, the delivery line, and the bypass line into the feed tank. After the orifice plate had been changed air was purged from the delivery line through a small bore copper bleed tube. To avoid the introduction of air into the packed bed the packed portion of the column was never drained.

4.6.2. WEIGHING THE SPHEROID.

The spheroids were weighed before immersion to ± 0.1 mg. on a Mettler H.16 automatic, constant load balance. After removal from the water tunnel the shapes were dried in a desiccator for 24 hours and reweighed; this weight was taken as the final dry weight. Further weighings showed an approximately constant weight loss of 0.5 mg. per 24 hours, indicating that drying was complete before the end of the first 24 hour period.

Attempts to obtain a more precise final weight, by weighing against time over the first 24 hours, were unsuccessful due to the uncertainties introduced by repeated handling and the interruption of the overnight period. Typical total weight losses were 80 mg. for the smallest shape (4:16 eccentricity) increasing to 300 mg. for the largest (16:16 eccentricity). Both these figures represent between 3 percent and 4 percent of the original weight of the body.

4.7. PHYSICAL PROPERTIES AND DIMENSIONLESS GROUPS.

The dimensionless groups of interest in correlating the data of the work described are the Sherwood, Schmidt, Grashof, and Reynolds numbers as shown in Chapter 3. The choice of physical property data for

use in calculating these groups is not always obvious and is treated in detail below.

Schmidt Number $\quad \dfrac{\mu}{\rho D_v}$

Since the bulk stream benzoic acid concentration was always less than 1 percent of the saturation value the density and viscosity in the Schmidt number were taken as those of pure water. The values obtained from the literature for the density [81] and viscosity [82] of pure water at 25.0°C were 0.99707 g./cm^3 and 0.8937 centipoise respectively.

No comprehensive diffusivity data for the benzoic acid - water system has been published and it is usual for research workers requiring such data to use one of the semi-empirical correlations that have been reported [83,84]. Of these the Wilke-Pin Chang [84] correlation has been the most favoured. This correlation, which, with viscosity in centipoise units, is of the form :

$$D_v = \frac{7.4 \times 10^{-8} \, M^{\frac{1}{2}} \, T}{\mu \, V_m^{0.6}} \qquad (4.2)$$

where V_m is the molal volume of the solute at its normal boiling point, M is the molecular weight of the solvent, μ is the viscosity of the solvent and T is the absolute temperature, gives the value of D_v in the units cm^2/sec.

Wilke and Pin Chang found that equation (4.2) correlated the experimental data for 123 systems with an average deviation of 12 percent. They incorporated a parameter, X_p, to compensate for the solution properties of associated solvents, to produce a modified form of equation (4.2), i.e.

$$D_v = \frac{7.4 \times 10^{-8} (X_p M)^{\frac{1}{2}} T}{\mu V_m^{0.6}} \qquad (4.3)$$

The parameter X_p was given values of 1.5, 1.9, and 2.6 for ethanol, methanol, and water respectively, whilst for non-associated solvents its value was 1.0. The modified equation correlated the experimental results for aqueous solutions with an average deviation of 6 percent.

The isolated experimental values of diffusivity which have been reported for benzoic acid - water systems at 25.0°C show considerable inconsistency. Hixson and Wilkens's [85] value of 11.5×10^{-6} cm.²/sec. was 23.6% higher than that predicted by equation (4.3), whilst Vasudev [86] reported a value of 9.07×10^{-6} cm.²/sec. at 25.25°C.

In view of the lack of consistent experimental values and in order to maintain continuity with previous workers, the Wilke - Pin Chang correlation, equation (4.3),

was employed to obtain the value of the diffusion coefficient used in the present work. The value obtained for the benzoic acid - water system at 25.0°C by the use of equation (4.3) is 8.92×10^{-6} cm.²/sec. The value of molal volume used in equation (4.3), 134.8 cm.³/g.mole, was obtained from Perry [81]. The molecular weight of water was taken [82] as 18.016.

Reynolds Number $\dfrac{v \rho d_{Ch}}{\mu}$

The same viscosity and density values were used as for evaluation of the Schmidt number. The velocity, v, used was the mean velocity based upon volumetric throughput and test section cross-sectional area as described earlier.

The choice of characteristic dimension, d_{Ch}, for oblate spheroidal shapes is a subject of considerable importance and has been discussed separately elsewhere (Chapter 3). Values of the Reynolds number were obtained for each of the eight characteristic dimensions for each of the experimental runs.

Grashof Number $\dfrac{d_{Ch}^3 \rho^2 g}{\mu^2} \cdot \dfrac{(\rho_s - \rho)}{\rho}$

The value of ρ_s, the density of a saturated solution of benzoic acid, used was 0.99766 g./cm³ as reported by Sandoval [11]. Viscosity and density were

again taken as those of pure water as in the Schmidt number.

Sherwood Number $\frac{k_c d_{Ch}}{D_v}$

The evaluation of diffusion coefficient has already been discussed. The mass transfer coefficient, k_c, was determined from the results of the experimental work by use of the relationship :

$$W = k_c A (c_s - c_o) \qquad (4.4)$$

In this equation A is the surface area of the spheroid, tabulated in Appendix 1, c_s is the saturation concentration of benzoic acid which was evaluated from the literature [87] as 3.45 g./litre at 25.0°C, and c_o the concentration of benzoic acid in the recirculating water which was taken as zero. This latter assumption was justified since sufficient of the recirculating water was replaced to maintain the bulk stream concentration at less than 1 percent of the saturation concentration. The value of W in g./hr. was obtained from the total weight loss during an experimental run and the run duration.

CHAPTER 5.

DISCUSSION OF RESULTS.

5.1. SCHLIEREN PHOTOGRAPHS.

The schlieren photographs are useful in the interpretation of the experimental data and will therefore be considered first.

The schlieren photographs show that several flow regimes exist within the Reynolds number range investigated i.e. $0 \leqslant Re_3 \leqslant 195$. These regimes, which are illustrated by the representative photographs figs. (10-14), may be categorized as follows.

REGIME 1. Free convection. Downward motion of dense solution in the form of a tail streaming away from the body. The tail was thin for the spherical and near spherical bodies but it became thicker for the flatter shapes.

REGIME 2. Downward motion, basically in the form of a tail but with disturbances causing some scattering and occasional break up of the tail. The range of Reynolds numbers over which this regime existed was different for each shape. These ranges of Reynolds number, together with those for the other regimes, are included in tables (4-8). These tables are a qualitative analysis of the flow patterns observed during all the

$Re_3 = 0$

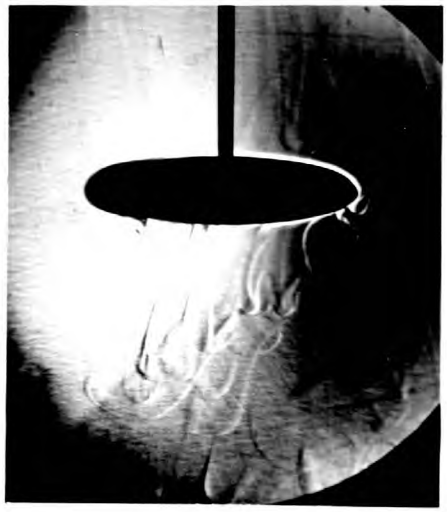

$Re_3 = 3 \cdot 8$

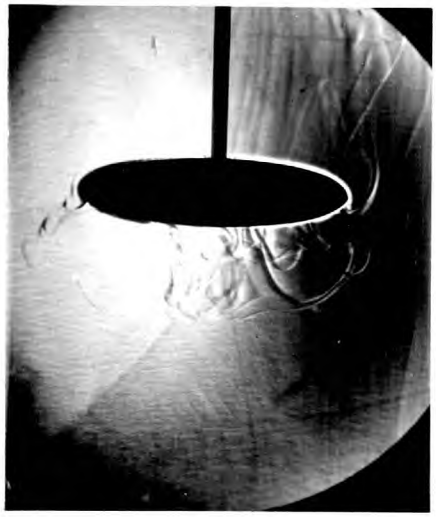

$Re_3 = 5 \cdot 3$

$Re_3 = 12 \cdot 2$

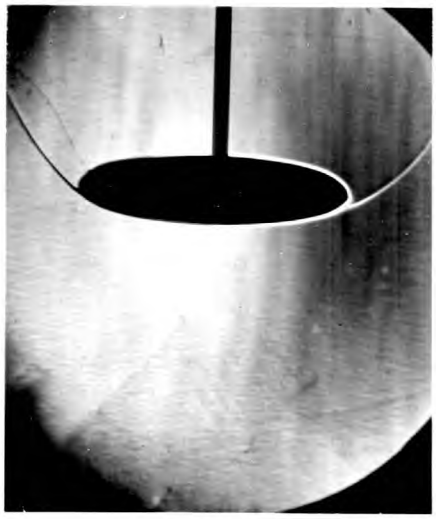

$Re_3 = 20 \cdot 6$

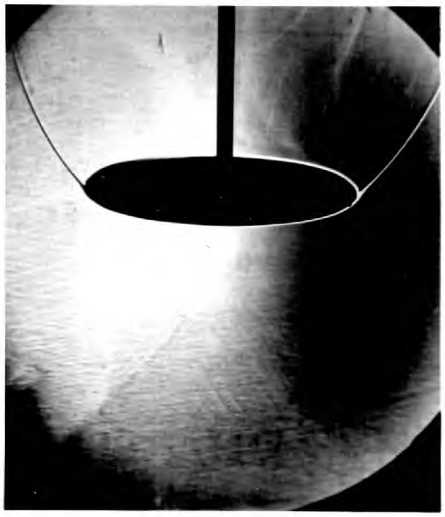

$Re_3 = 60 \cdot 8$

Fig. 10 SCHLIEREN PHOTOGRAPHS. $e = 4:16$

$Re_3 = 0$

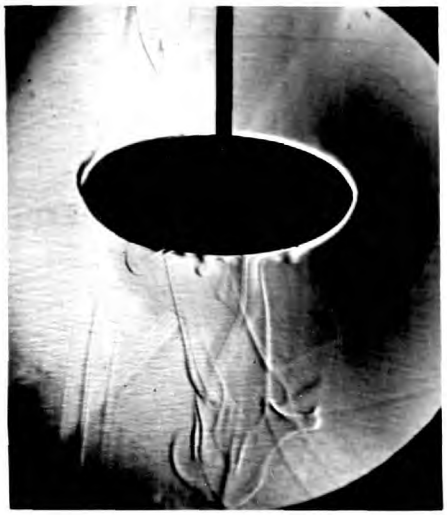

$Re_3 = 3 \cdot 6$

$Re_3 = 6 \cdot 2$

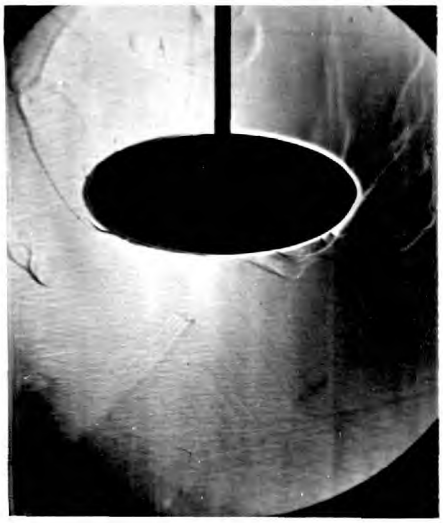

$Re_3 = 16 \cdot 7$

$Re_3 = 32 \cdot 1$

$Re_3 = 49 \cdot 3$

Fig. 11 SCHLIEREN PHOTOGRAPHS. $e = 7:16$

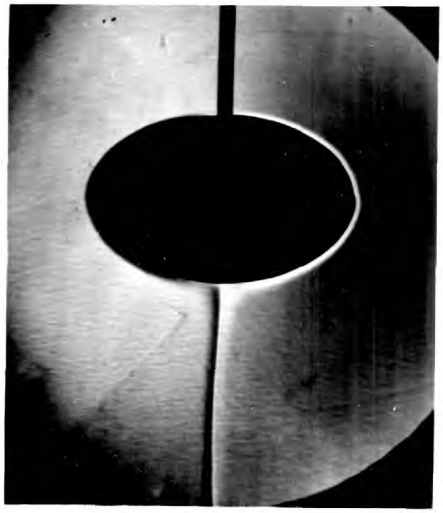

$Re_3 = 0$

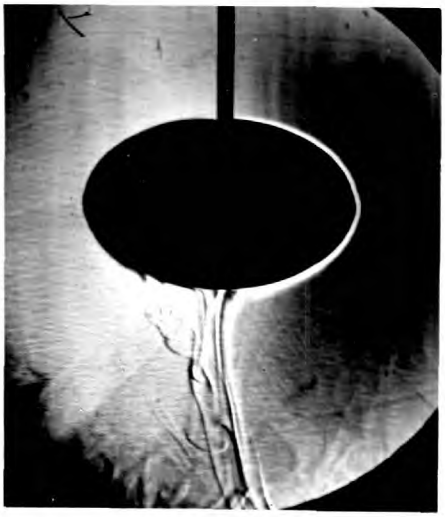

$Re_3 = 5{\cdot}2$

$Re_3 = 11{\cdot}0$

$Re_3 = 39{\cdot}7$

$Re_3 = 48{\cdot}0$

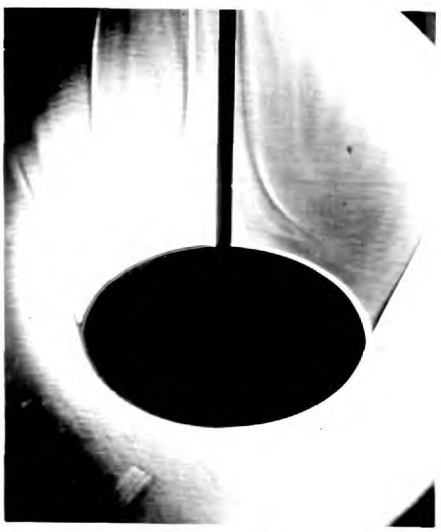

$Re_3 = 106$

Fig. 12 SCHLIEREN PHOTOGRAPHS. $e = 10{:}16$

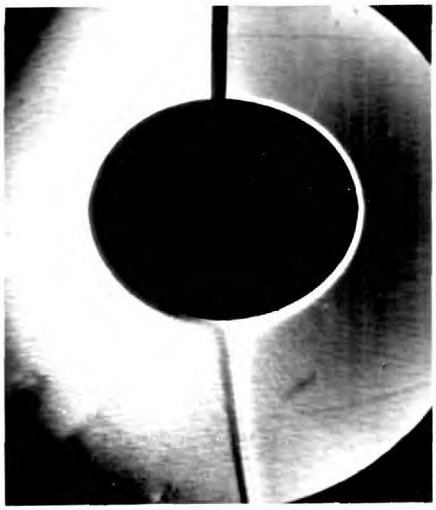

$Re_3 = 0$

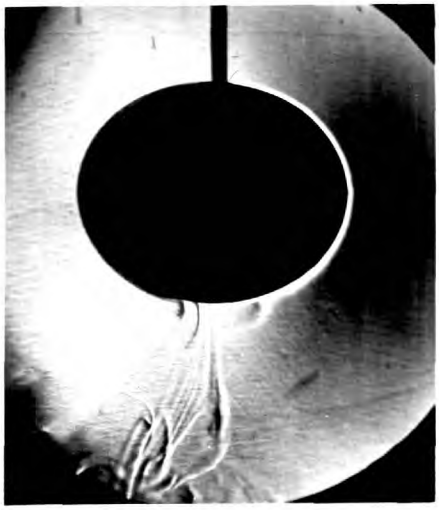

$Re_3 = 4{\cdot}5$

$Re_3 = 18{\cdot}2$

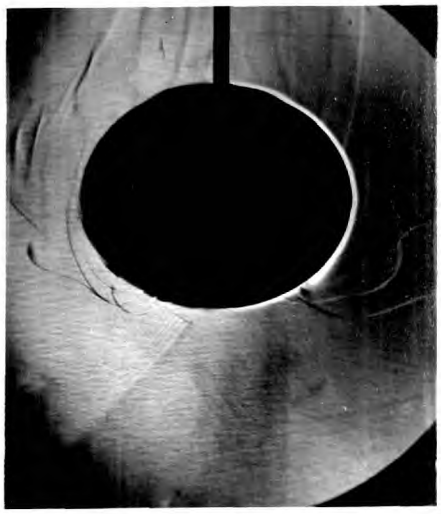

$Re_3 = 23{\cdot}3$

$Re_3 = 42{\cdot}4$

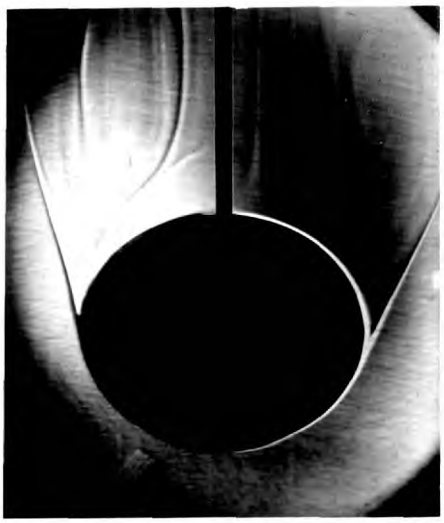

$Re_3 = 123$

Fig. 13 SCHLIEREN PHOTOGRAPHS. $e = 13:16$

$Re_3 = 0$

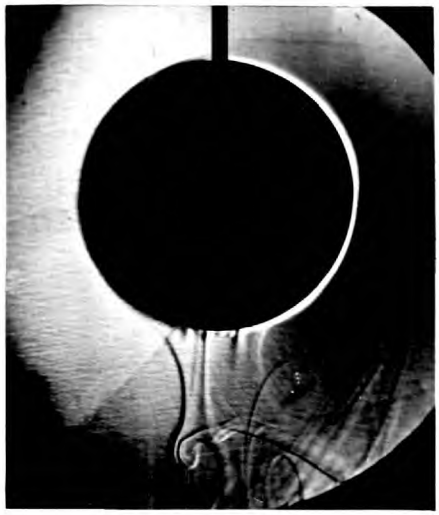

$Re_3 = 4{\cdot}8$

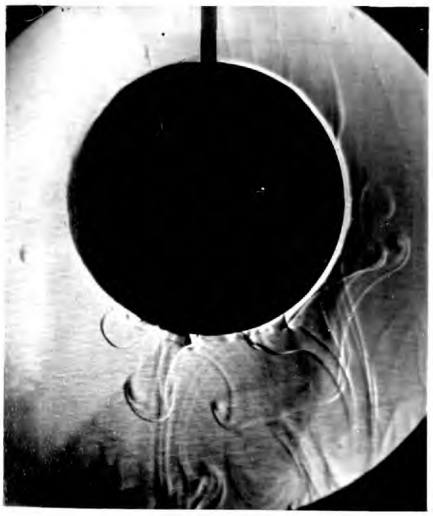

$Re_3 = 15{\cdot}4$

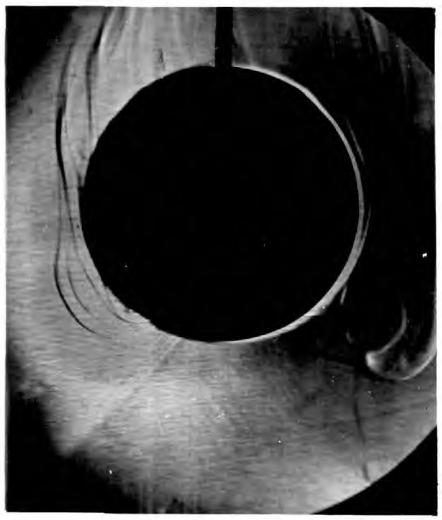

$Re_3 = 25{\cdot}7$

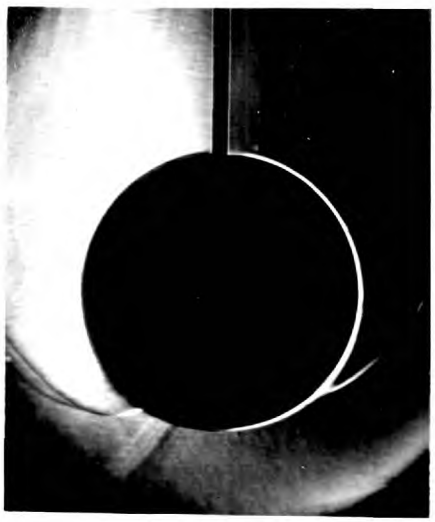

$Re_3 = 49{\cdot}0$

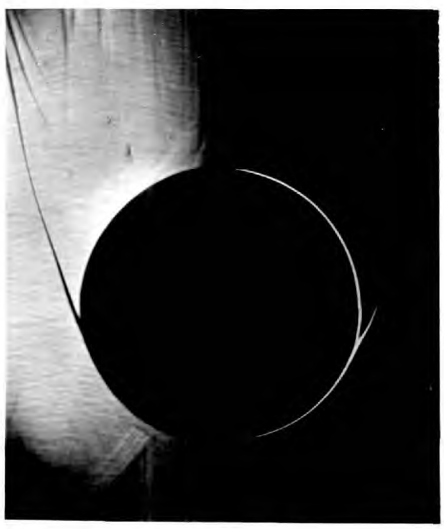

$Re_3 = 107$

Fig. 14 SCHLIEREN PHOTOGRAPHS. $e = 16{:}16$

TABLE 4. (e = 4 : 16)

Re_3	Sh_3	Gr_3/Re_3^2	FLOW REGIME	SEPARATION ANGLE $(\theta)_s$ (degrees)	RUN NO.
0	35.5	Infinite	1	-	51
0	36.1	Infinite	1	-	116
3.8	38.7	1940	2	-	107
6.5	45.7	502	3	-	3
10.4	40.7	196	3	-	54
13.3	42.9	121	4	<90*	2
13.4	45.6	119	4	<90*	4
16.6	43.3	76.6	4	<90*	5
16.6	42.7	77.0	4	<90*	7
21.2	47.4	47.8	4	<90*	1
26.0	47.6	31.6	4	<90*	11
33.3	51.0	19.3	4	90	17
40.8	57.8	12.1	4	90	15
52.6	65.5	7.72	4	90	22
64.8	74.2	4.88	4	90	28
76.6	81.2	3.50	4	90	34
89.1	88.5	2.54	4	90	41
98.0	92.5	2.10	4	90	38
112	100	1.61	4	90	50
125	108	1.30	4	90	43
137	112	1.01	4	90	46

* not stable.

TABLE 5. (e = 7 ; 16)

Re_3	Sh_3	Gr_3/Re_3^2	FLOW REGIME	SEPARATION ANGLE $(\theta)_s$ (degrees)	RUN NO.
0	41.7	Infinite	1	-	109
0	40.4	Infinite	1	-	117
3.6	46.5	2590	2	-	108
6.4	47.0	807	3	-	66
10.8	47.3	281	3	-	61
16.9	45.7	115	4	<40*	57
22.1	46.6	67.3	4	<40*	68
27.2	47.9	45.5	4	45	56
34.9	53.3	27.5	4	70	73
43.0	54.7	18.0	4	70	71
54.3	68.1	11.4	4	90	77
60.6	71.1	9.05	4	90	84
68.3	76.7	7.19	4	90	79
75.8	82.9	5.83	4	90	86
85.6	89.7	4.60	4	90	75
95.7	95.3	3.69	4	90	87
107	106	2.90	4	90	92
117	110	2.42	4	90	93
129	114	2.00	4	90	95
140	120	1.70	4	90	90
152	122	1.45	4	90	102
163	129	1.27	4	90	98

* not stable.

TABLE 6. (e = 10 : 16)

Re_3	Sh_3	Gr_3/Re_3^2	FLOW REGIME	SEPARATION ANGLE (θ_s)(degrees)	RUN NO.
0	46.2	Infinite	1	-	52
0	47.0	Infinite	1	-	115
6.3	47.9	1310	2	-	113
9.4	53.9	573	3	-	67
14.6	47.8	225	3	-	59
19.2	50.3	141	4	15	53
22.8	51.0	100	4	45	55
30.5	51.3	56.6	4	55	9
38.4	53.0	35.3	4	60	13
43.6	58.3	27.4	4	75	20
49.5	64.0	21.1	4	80	16
56.3	68.1	16.3	4	85	19
61.1	69.8	13.9	4	90	26
70.0	75.7	10.5	4	90	32
78.0	79.6	8.54	4	90	24
88.2	86.4	6.67	4	90	29
96.4	91.5	5.63	4	90	23
107	97.1	4.60	4	90	37
117	100	3.85	4	90	36
129	109	3.08	4	90	40
141	113	2.57	4	90	44
151	115	2.28	4	90	103
156	124	2.13	4	90	47
161	119	2.01	4	90	104
171	125	1.76	4	90	99
179	132	1.62	4	90	49
188	131	1.49	4	90	106

TABLE 7. (e = 13 : 16)

Re_3	Sh_3	Gr_3/Re_3^2	FLOW REGIME	SEPARATION ANGLE (θ_s)(degrees)	RUN NO.
0	54.0	Infinite	1	-	111
0	51.1	Infinite	1	-	114
4.5	55.3	4040	2	-	112
11.1	55.0	638	2	-	64
18.3	54.3	234	3	-	60
24.2	54.4	135	3	-	69
29.1	58.0	94.1	4	30	65
36.5	60.8	60.3	4	30	63
47.8	64.9	35.0	4	45	74
58.5	68.9	23.2	4	50	72
63.9	73.0	19.5	4	55	81
73.2	79.9	14.8	4	60	80
80.9	83.9	12.1	4	65	83
92.0	89.5	9.46	4	65	78
104	96.5	7.44	4	85	85
115	103	6.25	4	85	76
126	110	5.21	4	90	82
137	116	4.24	4	95	88
143	120	3.90	4	95	97
147	128	3.65	4	95	105
157	130	3.20	4	95	91
169	136	2.77	4	95	94
181	137	2.44	4	100	89
191	143	2.20	4	100	96

TABLE 8. (e = 16 : 16)

Re_3	Sh_3	Gr_3/Re_3^2	FLOW REGIME	SEPARATION ANGLE (θ_s)(degrees)	RUN NO.
0	59.9	infinite	1	-	48
4.8	62.4	5240	2	-	110
9.9	59.0	1180	2	-	62
14.8	61.9	534	2	-	70
21.0	58.6	263	2	-	58
26.1	60.5	173	3	-	10
33.2	64.5	107	4	15	8
41.6	65.6	68.3	4	40	6
52.0	69.8	43.7	4	40	12
60.1	74.7	32.7	4	45	21
66.0	76.4	27.0	4	50	14
73.8	82.4	21.4	4	60	18
83.1	84.2	17.1	4	70	25
94.6	90.1	13.2	4	80	31
107	96.9	10.3	4	85	33
121	108	8.18	4	90	27
135	113	6.53	4	90	30
155	122	5.03	4	90	35
166	131	4.28	4	95	100
174	135	3.87	4	95	39
183	144	3.49	4	95	101
192	146	3.20	4	100	45
195	145	3.13	4	100	42

experimental runs of the present work.

REGIME 3. High interaction with both upflow and downflow periodically predominant. Initially the upflow of the bulk fluid caused a build up of dense solution in the wake region behind the body. The bulk upflow velocity was insufficient to sweep this solution away from the vicinity of the dissolving body so that when the mass of dense solution was sufficient, the downward gravity forces overcame the upward forces due to bulk motion and the solution moved downwards, past the body, causing the temporary establishment of a highly disturbed tail. The dense solution was dispersed by this disturbance and swept from the vicinity of the body by the bulk motion. Upflow was then temporarily re-established and the cycle repeated. The length of the cycle was irregular, downflow was observed to predominate for periods of from one minute to one hour. The ratio of the total time spent in upflow to the total time spent in downflow increased with increase of Reynolds number.

REGIME 4. Upflow with a steady flow separation angle. The downward motion of dense solution in the wake region pushed forward the separation point, but instead of collapsing to form a disturbed tail as

in regime 3, equilibrium was reached with the upward forces due to bulk motion. Since the point at which equilibrium was reached depended upon the bulk velocity and the body shape, the separation angle was, at constant Grashof and Schmidt numbers, a function of Reynolds number. In the work described the only quantity that was varied in the Grashof number was the characteristic dimension and hence the Grashof number was constant for each shape. In the case of the sphere, steady separation angles, θ_s, (measured from the front stagnation point) of 15^o to 100^o were observed between Reynolds numbers (Re_3) of 33.2 and 195, the latter being the highest value of Re_3 used in the present work.

Above a particular Reynolds number the effect of free convection may be expected to be negligible and the separation angle that which would be observed in forced convection alone. The value of the separation angle in purely forced convective mass transfer, even for the case of the sphere, is still the subject of some research and no conclusive evidence has yet appeared in the literature. Frossling [21] has solved the boundary layer equations for flow round a sphere and his solution, which was based upon the theoretical pressure distribution, predicts separation in the absence of mass transfer at

109.6° irrespective of the Reynolds number. It is commonly assumed that the forced convective flow patterns and hence the angle of separation are not influenced by the mass flux away from the surface provided the mass flux is small. Thus, in this situation, the value of the separation angle in purely forced convective mass transfer may be assumed to be that which occurs in the absence of mass transfer.

Garner and Grafton [23] obtained experimental evidence concerning the value of the separation angle for dissolving benzoic acid spheres. They assumed that the position of the minimum local mass transfer rate on the surface of a dissolving sphere occurred at the separation point. Their experiments indicated that the separation angle was constant at 105° over the Reynolds number range 400 to 1,000. Garner and Keey [24] carried out similar experiments to those of Garner and Grafton and they also found that the separation point was constant at 105° over the Reynolds number range 100 to 500. Garner and Keey concluded from their mass transfer data that the effect of free convection could not be neglected at Reynolds numbers below 750. It is possible, therefore, that the value for the separation angle observed by both Garner and Keey and Garner and Grafton, i.e. 105°, did

not represent the limiting value of the separation angle for forced convection alone.

From the work of Garner and Keey, Garner and Grafton, and Frossling it appears that the maximum value of the separation angle for a sphere observed in the present work, i.e. 100°, may be less than the limiting value which would be observed in the absence of free convection. In view of the approximate nature of the values of the separation angle reported by Garner and Keey and Garner and Grafton it is not possible to conclude with certainty that the difference between the maximum value of the sphere separation angle observed in the present work i.e. 100° and the value of 105° observed by these workers was due to free convection.

From consideration of the separation angle alone it appears that the maximum value of the Reynolds number at which there is a significant effect of free convection upon the flow patterns around a dissolving benzoic acid sphere is close to the maximum value employed in the present work i.e. $Re_3 = 195$. It is possible, however, that, even when the separation angle reaches the limiting value for forced convection alone, there may be an effect of free convection upon the flow patterns in the wake region. For example the angle which is

formed between the stream line through the separation point and the tangent to the body surface at that point may be increased, relative to the value of this angle for forced convection alone, by the effects of free convection.

In the case of the flattest shape, (e = 4:16), the separation angle moved to the equator at very low values of Re_3; separation occurred at 90^o for $Re_3 > 30$. Experiments with oblate spheroidal bodies in the absence of free convection [10] indicate that for flatter shapes (e = 4:16, 7:16, and 10:16) the separation angle does not increase beyond 90^o even at Reynolds numbers as high as 32,000. As for the sphere, however, it is possible that free convection influenced the flow patterns in the wake region even when the separation angle reached the limiting value of 90^o. For Reynolds numbers in the range $10 < Re_3 < 30$ the separation angle for the flattest shape (e = 4:16) was between 0^o and 90^o but, as indicated in table 4, the separation was not stable and could not be assigned a specific value.

5.2. PLOTS OF SHERWOOD NUMBER vs. REYNOLDS NUMBER.

The feasibility of unifying the mass transfer data for the five oblate spheroidal shapes employed by choice of a suitable characteristic dimension was next

investigated.

The Sherwood and Reynolds numbers were calculated on the basis of the eight characteristic dimensions, d_1 to d_8, considered in Chapter 3. In the following discussion the Sherwood and Reynolds numbers are identified with the appropriate characteristic dimension by the subscripts 1 to 8. The values of the Sherwood and Reynolds numbers, Sh_1 to Sh_8 and Re_1 to Re_8, for the 117 experimental runs are included in Appendix 1. Figs. 15 to 22 show the various plots of the Sherwood numbers versus the Reynolds numbers on logarithmic co-ordinates.

Some previous workers [88] have attempted to correlate mass transfer data for drops in terms of a Sherwood number in which the mass transfer coefficient is based upon the surface area of the sphere of the same volume as the drop and the characteristic dimension is the diameter of the sphere with the same volume as the drop, d_1 in the present nomenclature. Such a correlation does not require a knowledge of drop shape, only drop volume being necessary. The values of the Sherwood numbers calculated on this basis from the data of the present work, Sh_{1f}, are also included in Appendix 1. The plot of Sh_{1f} vs. Re_1 on logarithmic coordinates is presented in fig.23.

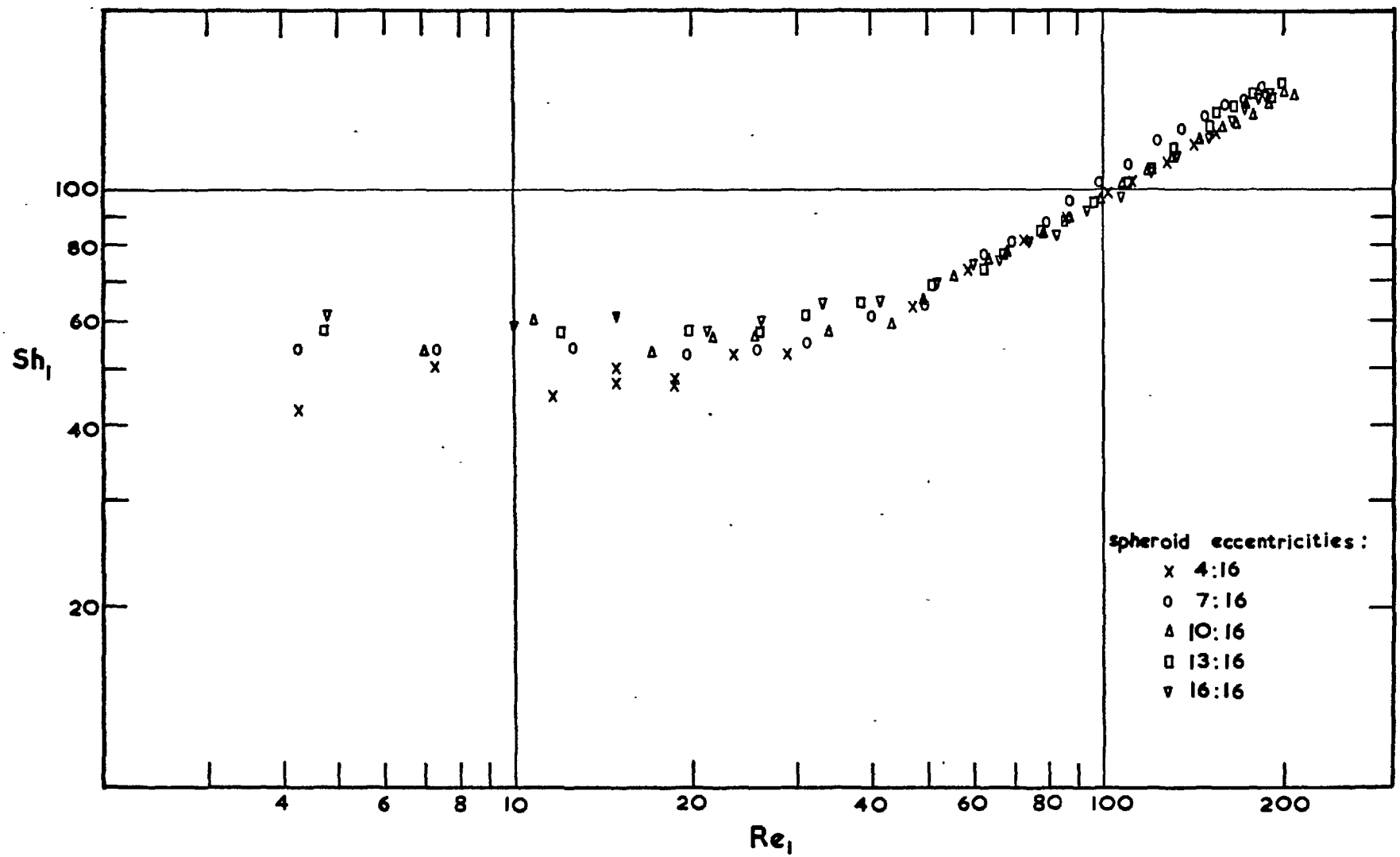
100
80
60
40
20
Sh_1
4
6
8
10
20
40
60
80
100
200
Re_1
spheroid eccentricities :
x 4:16
o 7:16
Δ 10:16
□ 13:16
▽ 16:16

FIG. 15

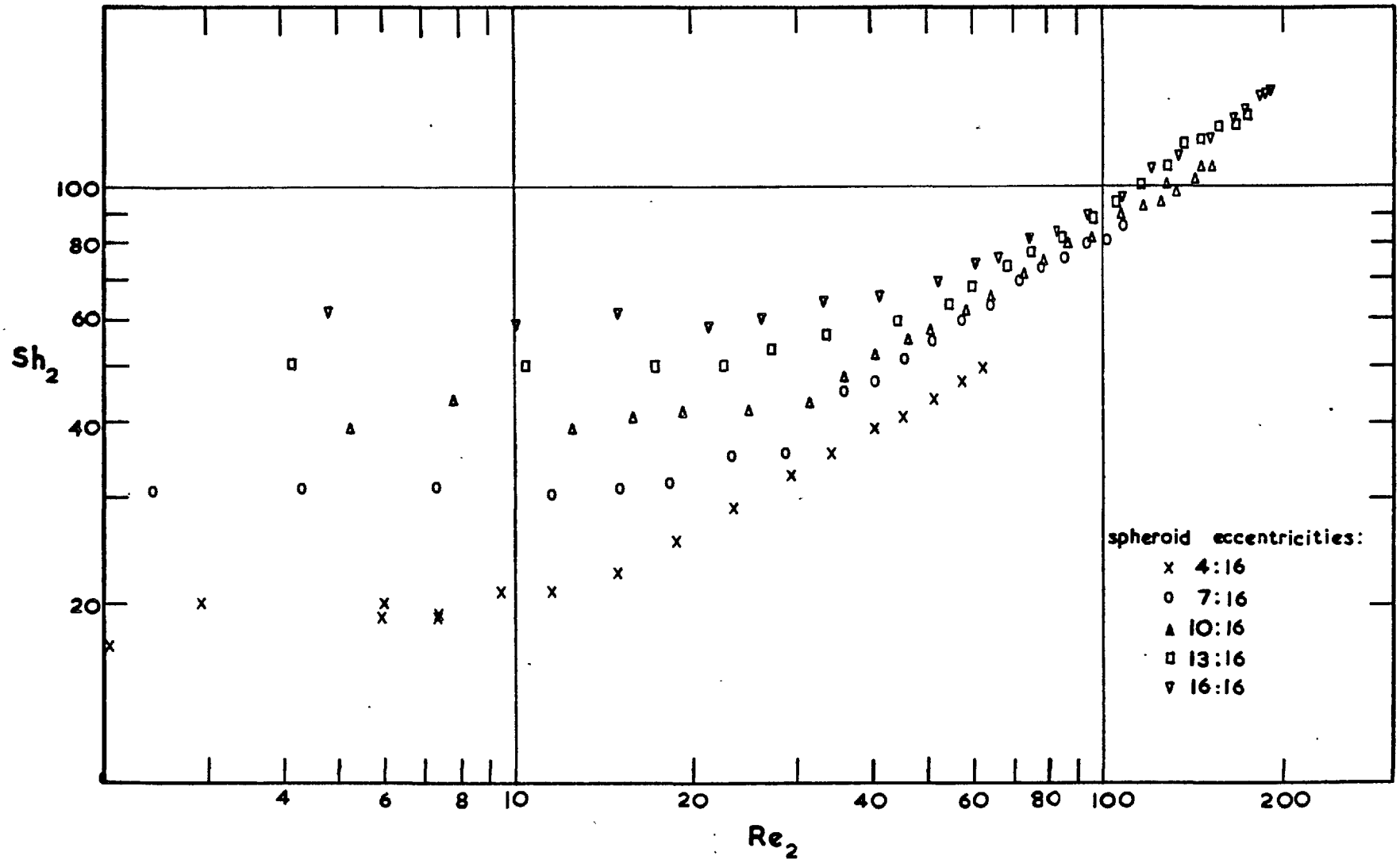
100
80
60
40
20
Sh_2
4
6
8
10
20
40
60
80
100
200
Re_2
spheroid eccentricities:
x 4:16
o 7:16
▲ 10:16
□ 13:16
▽ 16:16

FIG. 16

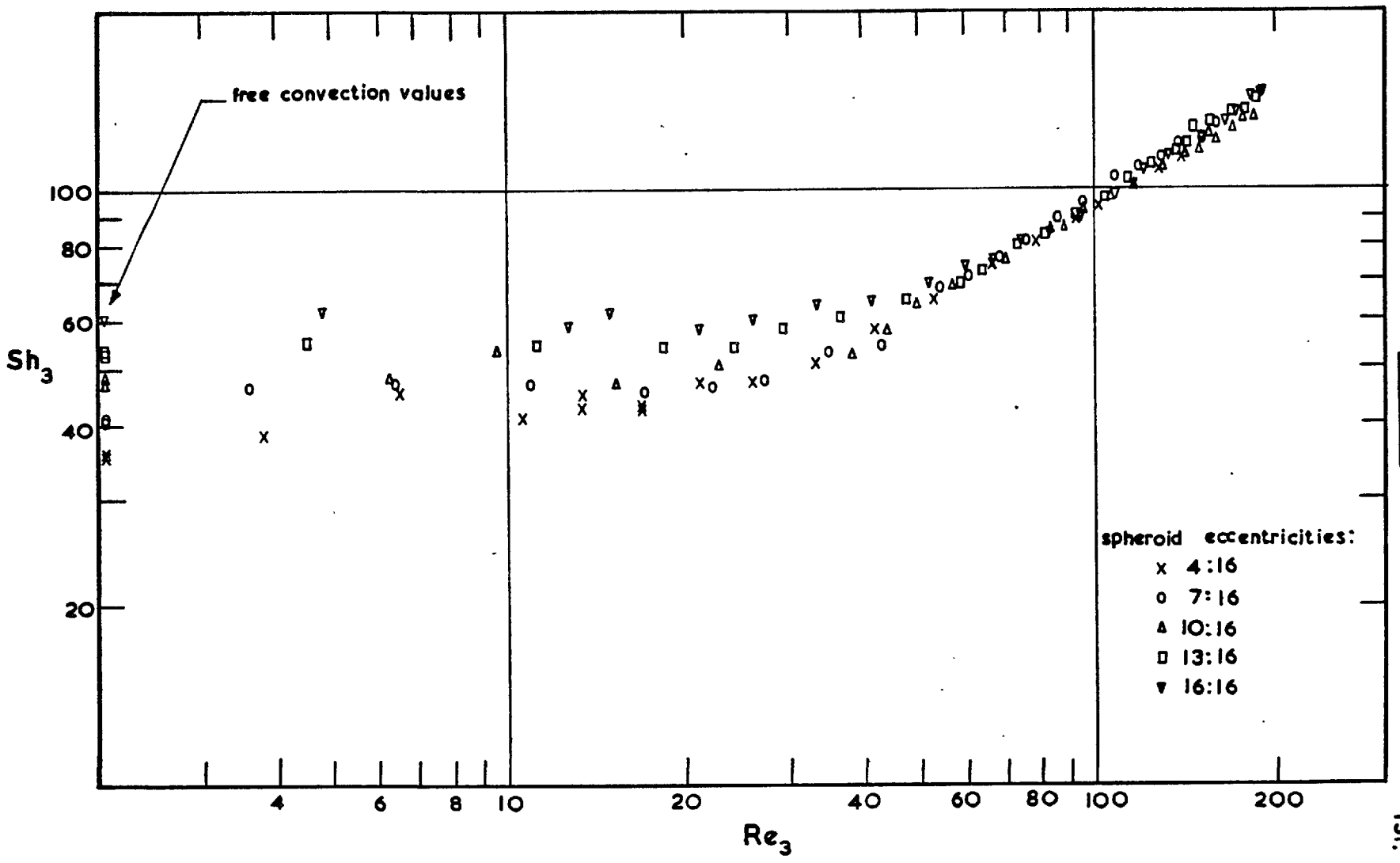
free convection values
100
80
60
40
20
Sh_3
4
6
8
10
20
40
60
80
100
200
Re_3
spheroid eccentricities:
x 4:16
o 7:16
Δ 10:16
□ 13:16
▽ 16:16

FIG. 17

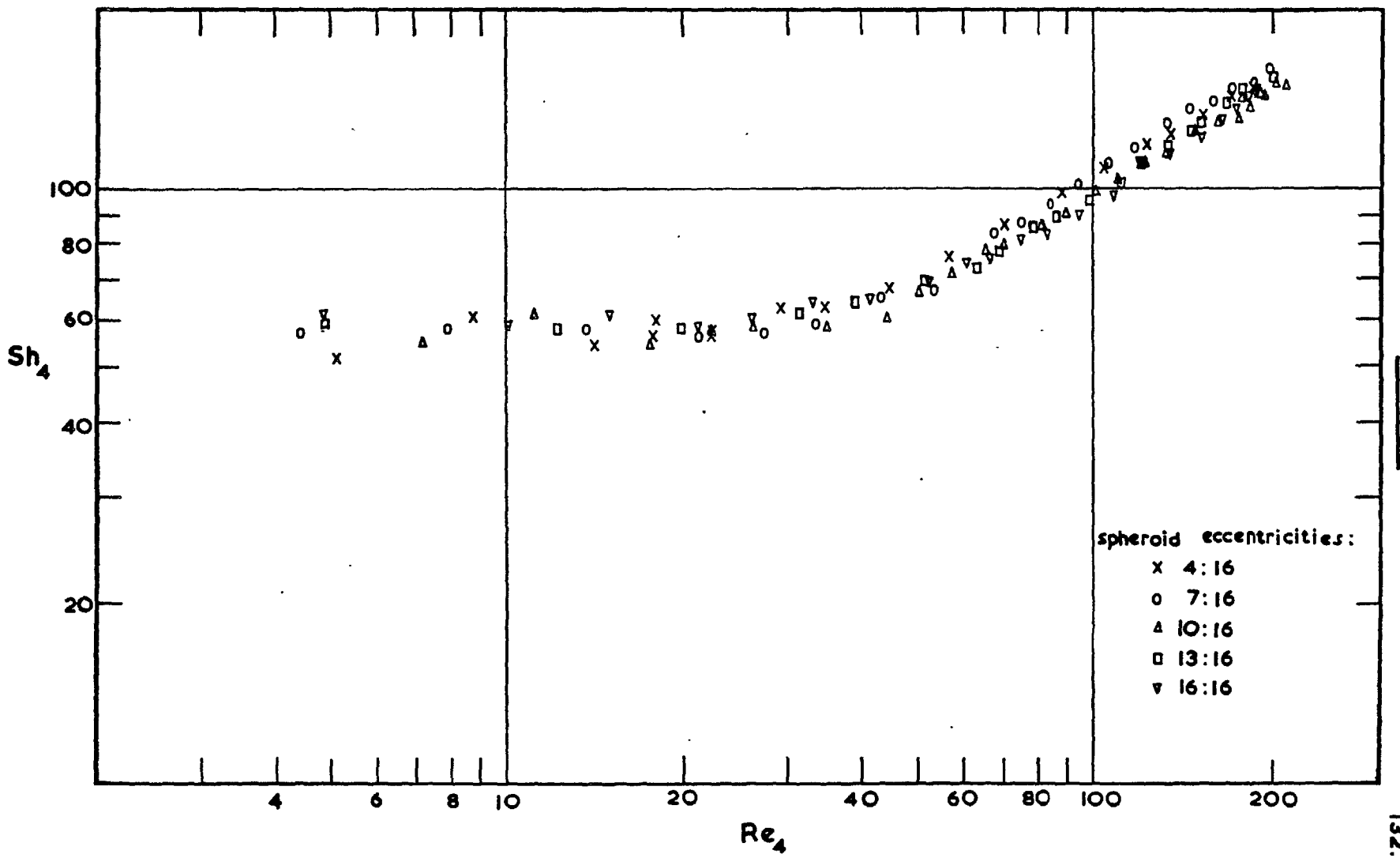
100
80
60
40
20
Sh_4
4
6
8
10
20
40
60
80
100
200
Re_4
spheroid eccentricities:
x 4:16
o 7:16
Δ 10:16
□ 13:16
▽ 16:16

FIG. 18

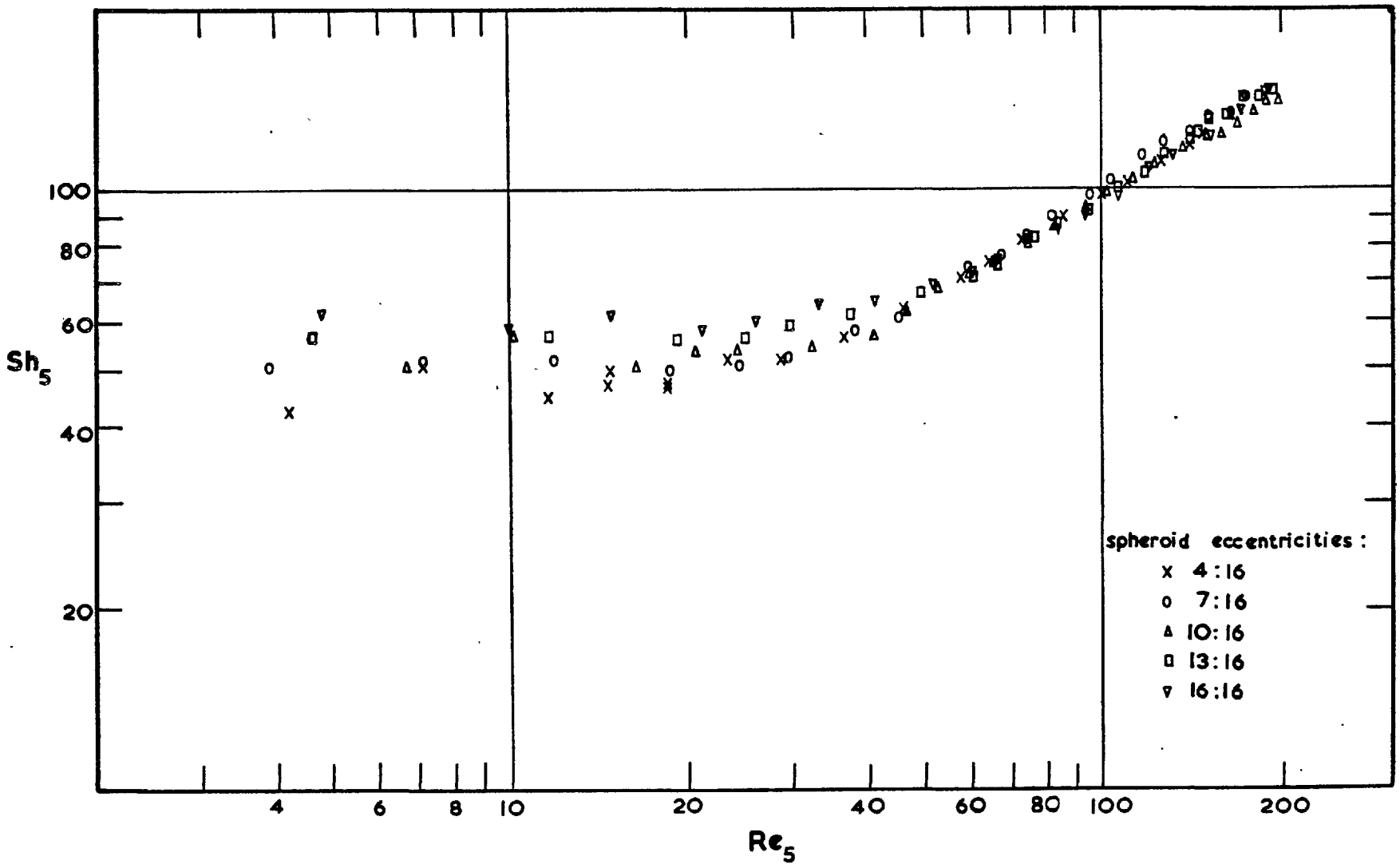
100
80
60
40
20
Sh_5
4
6
8
10
20
40
60
80
100
200
Re_5
spheroid eccentricities :
x 4:16
o 7:16
Δ 10:16
□ 13:16
▽ 16:16

FIG. 19

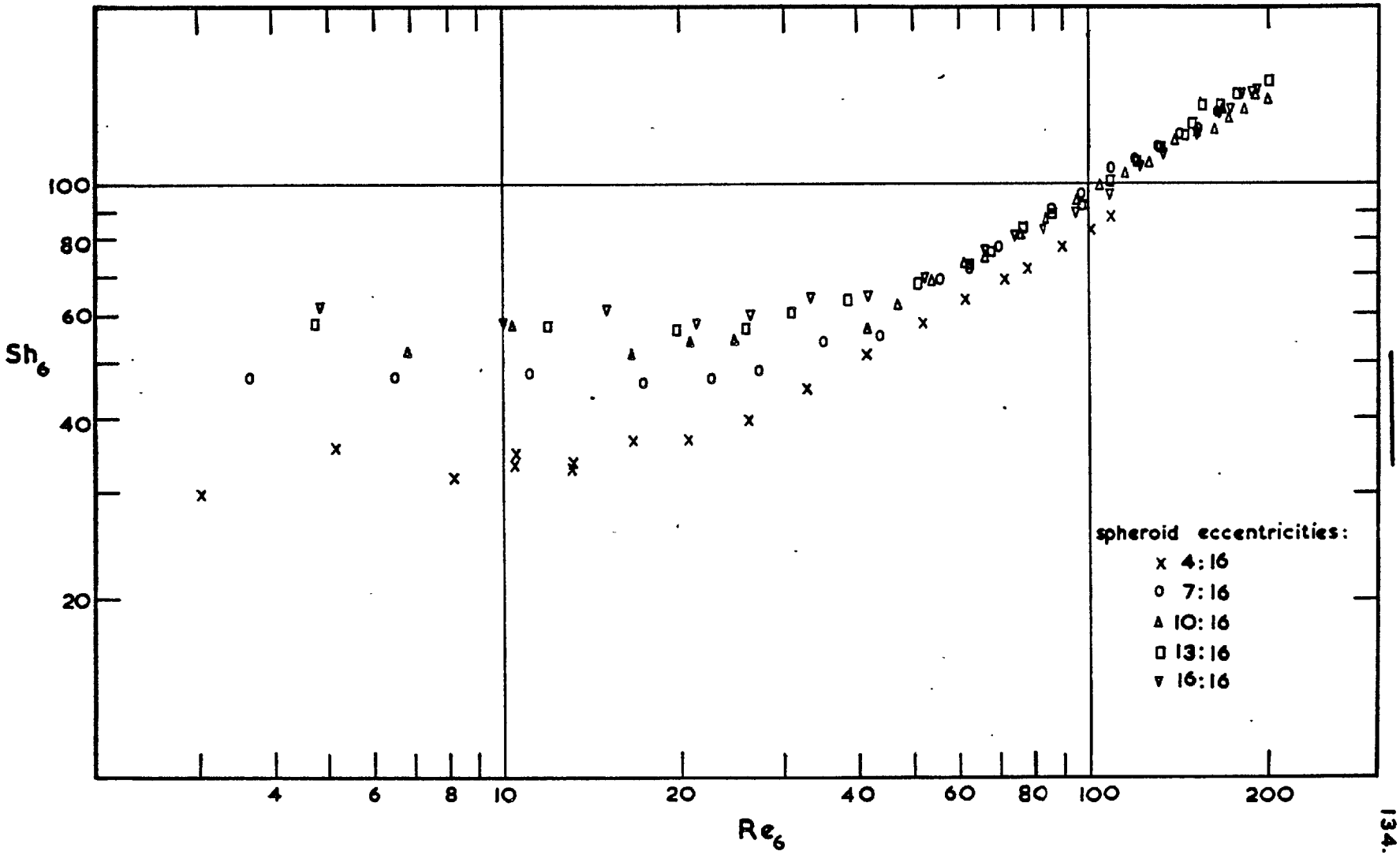
100
80
60
40
20
Sh_6
4
6
8
10
20
40
60
80
100
200
Re_6
spheroid eccentricities:
x 4:16
o 7:16
Δ 10:16
□ 13:16
▽ 16:16

FIG. 20

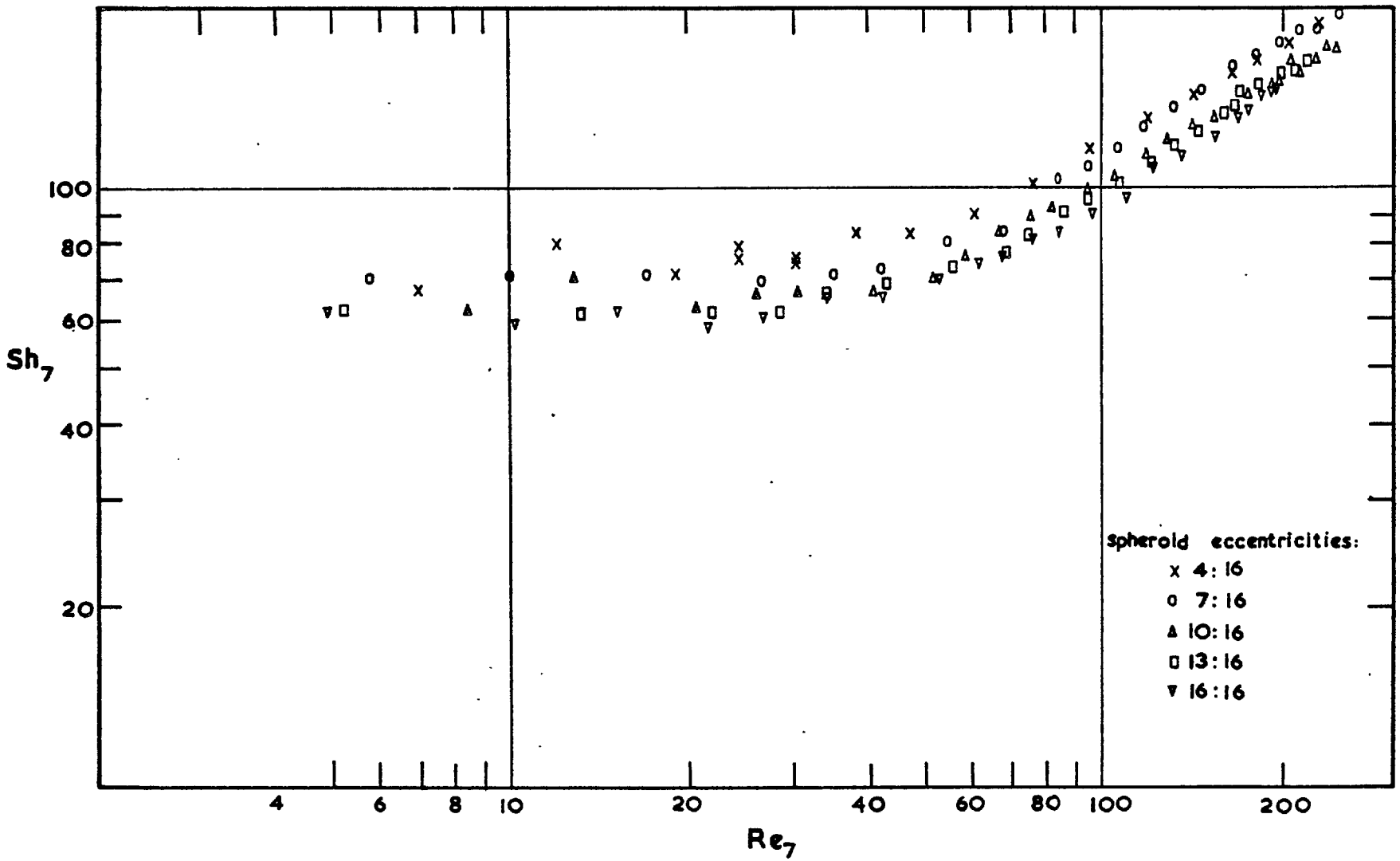
100
80
60
40
20
Sh_7
4
6
8
10
20
40
60
80
100
200
Re_7
Spheroid eccentricities:
x 4:16
o 7:16
Δ 10:16
□ 13:16
▽ 16:16

FIG. 21

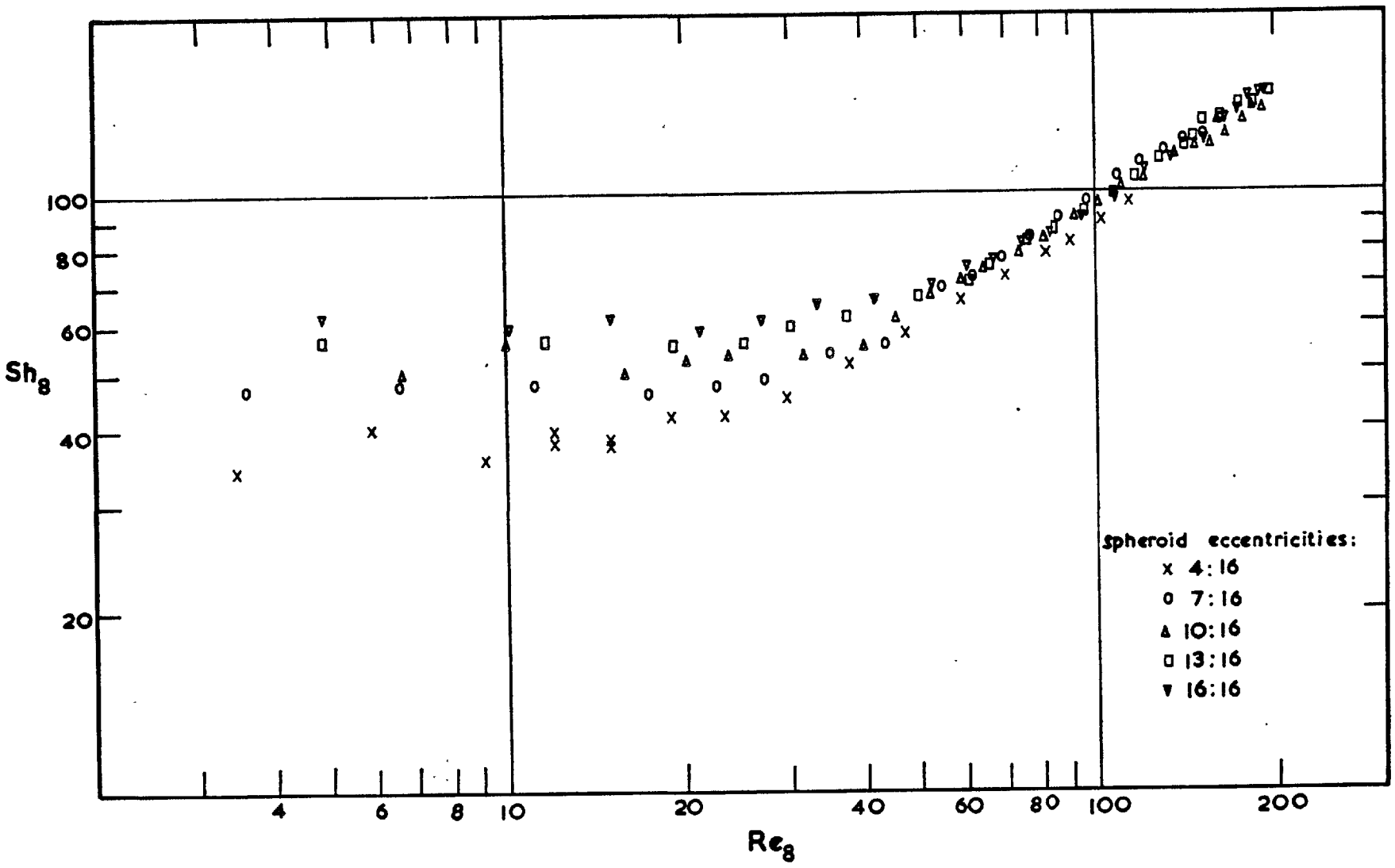
100
80
60
40
20
Sh_8
4
6
8
10
20
40
60
80
100
200
Re_8
spheroid eccentricities:
x 4:16
o 7:16
Δ 10:16
□ 13:16
▽ 16:16

FIG. 22

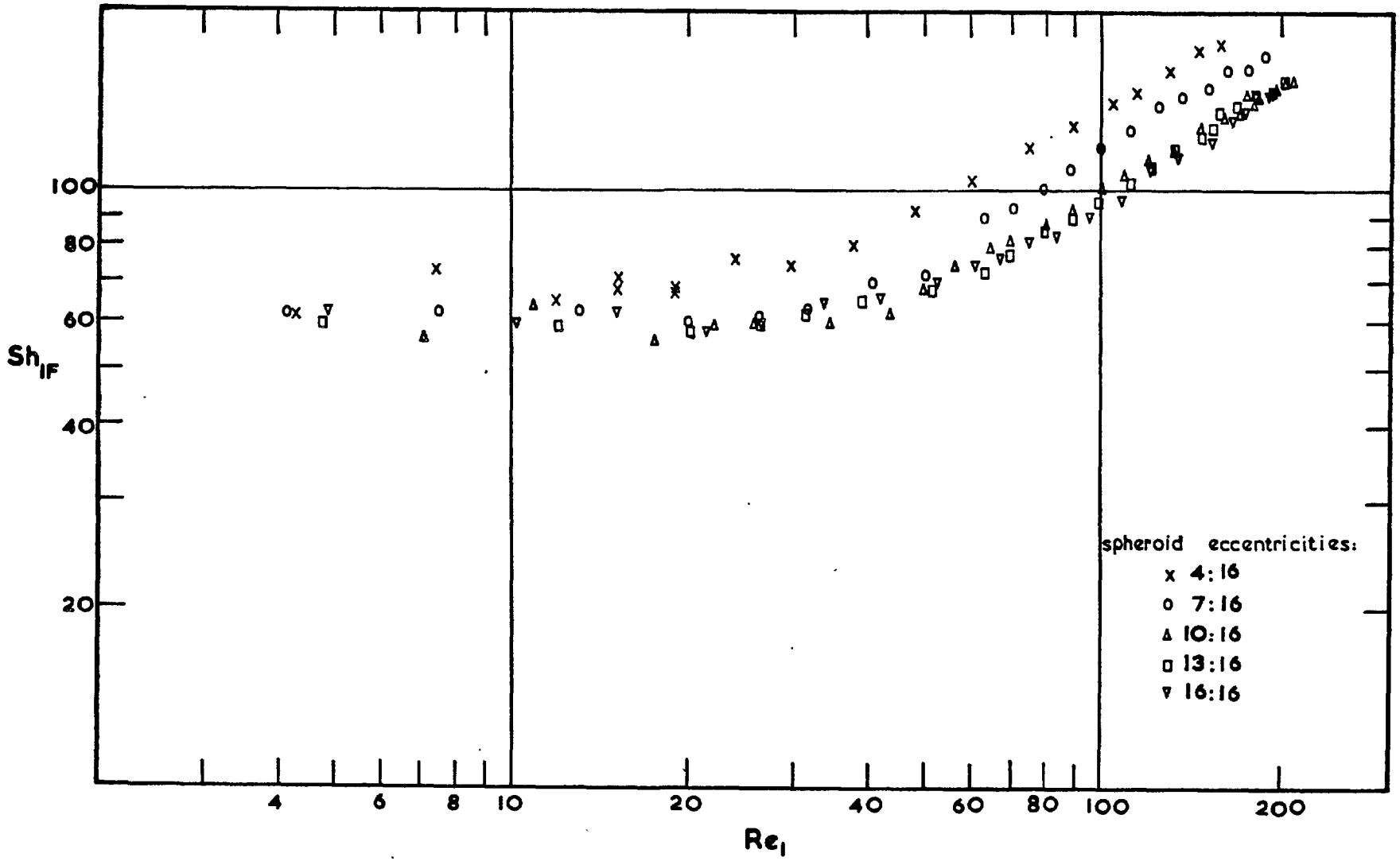
100
80
60
40
20
Sh_{IF}
4
6
8
10
20
40
60
80
100
200
Re_I
spheroid eccentricities:
x 4:16
o 7:16
Δ 10:16
□ 13:16
▽ 16:16

FIG. 23

It is evident from examination of figs. 15 to 22 that at high Reynolds numbers some of the characteristic dimensions employed, in particular d_3 and d_5, are very successful in unifying the data for all five oblate spheroidal shapes. For both these characteristic dimensions, however, the data for the five shapes begin to diverge below a Reynolds number, Re_3 or Re_5, of approximately 45. None of the eight characteristic dimensions is very successful in combining the data for all shapes at these lower Reynolds numbers. The characteristic dimension d_4, which is the most successful in this respect, fails to unify the data at the higher Reynolds numbers. Fig.23 shows clearly that unification of the data for all five oblate spheroidal shapes is not achieved by use of the Sherwood number based upon the surface area of the sphere with the same volume as the spheroid and the characteristic dimension d_1.

For the sake of discussion it is convenient to denote by Re_{TR} the value of the Reynolds number above which the data for all shapes are successfully unified by certain characteristic dimensions and to consider separately the regions above and below this value of the Reynolds number. The significance of this "transition" Reynolds number, Re_{TR}, with respect to the various flow regimes discussed in Section (5.1) is also considered below.

5.2.1. THE REGION ABOVE Re_{TR}.

As mentioned above, d_3 and d_5 are the most successful characteristic dimensions for combining the data in this region. The characteristic dimensions d_8, d_1, and d_6 each appear successful in unifying the data for four of the shapes but fail with the fifth. In the case of d_1, the data for the spheroid with eccentricity 7:16 is not unified with the data for the other four shapes whilst for the characteristic dimensions d_6 and d_8 the data for the spheroid with eccentricity 4:16 is not unified with the data for the other shapes.

Inspection of the data based upon the characteristic dimensions d_3 and d_5, as plotted in figs. 17 and 19, suggested that the data above Re_{TR} could be correlated in the form suggested by previous theoretical and experimental investigations of forced convective mass transfer from solid bodies, i.e.

$$Sh_3 = C_{1_3} + C_{2_3} Re_3^{n_3} Sc^{1/3} \qquad (5.1)$$

and

$$Sh_5 = C_{1_5} + C_{2_5} Re_5^{n_5} Sc^{1/3} \qquad (5.2)$$

In order to compare d_3 and d_5 on a statistical basis and also in an attempt to produce a correlation of

the data above Re_{TR} in the form of equations (5.1) and (5.2), use was made of the University of London Atlas computer. A modified library programme, Autocode programme 1000, was employed for the least squares method of data correlation. This programme was used to fit the observed values of two variables, X and Y, by a linear equation of the form:

$$\bar{Y}_m = A + B(X_m) \qquad (5.3)$$

where $\bar{Y}_m$ is the predicted value of Y_m for an observed value of X_m. The programme output included the values of the constants A and B obtained by minimisation of the sum of squares of the residual differences, $\sum_{m=1}^{m=T}(Y_m-\bar{Y}_m)^2$, where T is the total number of data points. The predicted values of $\bar{Y}_m$, corresponding to the input values of X_m, the residual differences, and the sum of the squares of the residual differences were also included in the programme output. The sum of the squares of the residual differences may be used to estimate the variance, $S^2(\bar{Y})$, of the observed values of Y_m from the predicted values, $\bar{Y}_m$, by use of the relationship:

$$\frac{\sum_{m=1}^{m=T}(Y_m - \bar{Y}_m)}{f} = S^2(\bar{Y}_m) \qquad (5.4)$$

where f = degrees of freedom = (T - 2).

The estimate of the variance, $S^2(\bar{Y})$, is a measure of the deviation of the data points from the correlating line. An estimate of the standard deviation of the data points from the correlating line is obtained by taking the square root of $S^2(\bar{Y})$.

Since equations (5.1) and (5.2) each contain three unknown constants it was necessary to adopt the following procedure in order to evaluate these constants by the use of the Autocode programme 1000. Considering firstly the correlation of the data based upon d_3 by equation (5.1), a value of n_3, n_{3_1} say, was selected and the product $(Re_3^{n_{3_1}} . Sc^{1/3})$ calculated. The groups Sh_3 and $(Re_3^{n_{3_1}} . Sc^{1/3})$ were then used as input data for Autocode programme 1000, the resultant output giving values of C_{1_3}, C_{2_3}, and $S^2(\overline{Sh}_3)$ at the selected value of n_3, n_{3_1}. A new value of n_3, n_{3_2} say, was then selected and the procedure repeated. The results of this analysis are given in table 9. An identical procedure was followed in correlating the data based upon d_5 and the results are given in table 10.

The confidence ranges of the true variance, $\sigma^2(\overline{Sh})$ at a probability level $(1-2\alpha)$, can be expressed [89] as:

TABLE 9.

CORRELATION OF DATA ABOVE Re_{TR} AS $Sh_3 = C_{1_3} + C_{2_3} Re_3^{n_3} Sc^{1/3}$

Equation No.	Assumed Value of n_3	C_{1_3}	C_{2_3}	$S^2(\overline{Sh}_3)$	90% confidence range of $\sigma^2(\overline{Sh}_3)$
5.6	0.10	-476	36.2	19.72	13.6 - 30.6
5.7	0.15	-285	19.2	18.53	12.8 - 28.8
5.8	0.20	-190	11.4	17.50	12.1 - 27.1
5.9	0.25	-132	7.24	16.43	11.3 - 25.4
5.10	0.30	-93.9	4.79	15.52	10.7 - 24.1
5.11	0.35	-66.6	3.26	14.70	10.1 - 22.8
5.12	0.40	-46.2	2.26	13.98	9.65 - 21.6
5.13	0.41	-42.6	2.10	13.85	9.55 - 21.4
5.14	0.42	-39.3	1.96	13.71	9.45 - 21.2
5.15	0.43	-36.2	1.83	13.59	9.36 - 21.0
5.16	0.44	-33.1	1.70	13.46	9.27 - 20.8
5.17	0.45	-30.2	1.59	13.34	9.20 - 20.7
5.18	0.46	-27.5	1.49	13.23	9.14 - 20.5
5.19	0.47	-24.8	1.39	13.12	9.05 - 20.4
5.20	0.48	-22.3	1.30	13.01	8.97 - 20.2
5.21	0.49	-19.8	1.21	12.90	8.90 - 20.0
5.22	0.50	-17.5	1.13	12.80	8.82 - 19.8
5.23	0.51	-15.3	1.06	12.70	8.75 - 19.7
5.24	0.52	-13.1	0.993	12.61	8.70 - 19.6
5.25	0.53	-11.0	0.930	12.52	8.65 - 19.4
5.26	0.54	-9.01	0.871	12.43	8.59 - 19.3
5.27	0.55	-7.08	0.816	12.35	8.51 - 19.1
5.28	0.56	-5.22	0.765	12.27	8.45 - 19.0
5.29	0.57	-3.42	0.717	12.19	8.40 - 18.9
5.30	0.58	-1.69	0.673	12.12	8.36 - 18.8
5.31	0.59	-0.01	0.632	12.05	8.31 - 18.7
5.32	0.60	+1.61	0.592	11.98	8.26 - 18.6
5.33	0.61	3.18	0.559	11.92	8.22 - 18.5
5.34	0.62	4.69	0.522	11.86	8.17 - 18.4

TABLE 9 (continued)

Equation No.	Assumed Value of n_3	C_{1_3}	C_{2_3}	$S^2(\overline{Sh}_3)$	90% confidence range of $\sigma^2(\overline{Sh}_3)$
5.35	0.63	6.16	0.490	11.81	8.15 - 18.3
5.36	0.64	7.58	0.460	11.76	8.10 - 18.2
5.37	0.65	8.96	0.433	11.71	8.08 - 18.2
5.38	0.66	10.3	0.407	11.66	8.04 - 18.1
5.39	0.67	11.6	0.382	11.62	8.02 - 18.0
5.40	0.68	12.9	0.359	11.59	7.99 - 18.0
5.41	0.69	14.1	0.338	11.55	7.96 - 17.9
5.42	0.70	15.3	0.318	11.52	7.95 - 17.9
5.43	0.71	16.4	0.299	11.50	7.93 - 17.8
5.44	0.72	17.5	0.281	11.47	7.91 - 17.8
5.45	0.73	18.6	0.265	11.45	7.90 - 17.8
5.46	0.74	19.7	0.249	11.44	7.90 - 17.8
5.47	0.75	20.7	0.234	11.43	7.90 - 17.7
5.48	0.76	21.7	0.221	11.42	7.89 - 17.7
5.49	0.77	22.7	0.208	11.41	7.88 - 17.7
5.50	0.78	23.7	0.196	11.41	7.88 - 17.7
5.51	0.79	24.6	0.184	11.41	7.88 - 17.7
5.52	0.80	25.5	0.174	11.42	7.89 - 17.7
5.53	0.85	29.7	0.129	11.49	7.92 - 17.8
5.54	0.90	33.5	0.0963	11.65	8.04 - 18.1
5.55	0.95	36.8	0.0720	11.89	8.20 - 18.4
5.56	1.00	39.9	0.0540	12.21	8.42 - 18.9
5.57	1.05	42.6	0.0406	12.61	8.70 - 19.5
5.58	1.10	45.1	0.0305	13.09	9.02 - 20.3
5.59	1.15	47.3	0.0230	13.65	9.41 - 21.2
5.60	1.20	49.4	0.0174	14.29	9.85 - 22.0
5.61	1.25	51.3	0.0131	14.99	10.3 - 23.2
5.62	1.30	53.1	0.00995	15.77	10.9 - 24.4
5.63	1.35	54.8	0.00754	16.62	11.5 - 25.8
5.64	1.40	56.3	0.00572	17.54	12.1 - 27.2
5.65	1.45	57.7	0.00435	18.52	12.8 - 28.7

TABLE 10.

CORRELATION OF DATA ABOVE Re_{TR} AS $Sh_5 = C_{1_5} + C_{2_5} Re_5^{n_5} Sc^{1/3}$

Equation No.	Assumed Value of n_3	C_{1_5}	C_{2_5}	$S^2(\overline{Sh}_5)$	90% confidence range $\sigma^2(\overline{Sh}_5)$
5.66	0.10	-483	36.8	18.74	13.2 - 28.8
5.67	0.15	-289	19.5	17.55	12.4 - 27.0
5.68	0.20	-192	11.6	16.47	11.6 - 25.4
5.69	0.25	-134	7.36	15.52	10.9 - 23.9
5.70	0.30	-94.7	4.86	14.69	10.3 - 22.6
5.71	0.35	-66.9	3.31	13.98	9.84 - 21.6
5.72	0.40	-46.1	2.29	13.39	9.43 - 20.6
5.73	0.41	-42.6	2.13	13.28	9.35 - 20.4
5.74	0.42	-39.2	1.99	13.18	9.28 - 20.3
5.75	0.43	-36.0	1.85	13.09	9.22 - 20.2
5.76	0.44	-32.9	1.73	12.99	9.15 - 20.0
5.77	0.45	-29.9	1.61	12.83	9.09 - 19.9
5.78	0.46	-27.1	1.51	12.75	9.04 - 19.8
5.79	0.47	-24.4	1.41	12.68	8.98 - 19.6
5.80	0.48	-21.8	1.32	12.61	8.93 - 19.5
5.81	0.49	-19.4	1.23	12.55	8.88 - 19.4
5.82	0.50	-17.0	1.15	12.50	8.84 - 19.3
5.83	0.51	-14.7	1.08	12.44	8.80 - 19.3
5.84	0.52	-12.5	1.01	12.38	8.76 - 19.2
5.85	0.53	-10.4	0.943	12.34	8.71 - 19.1
5.86	0.54	- 8.36	0.883	12.30	8.70 - 19.0
5.87	0.55	- 6.40	0.828	12.28	8.66 - 18.9
5.88	0.56	- 4.51	0.776	12.25	8.65 - 18.9
5.89	0.57	- 2.68	0.727	12.23	8.63 - 18.9
5.90	0.58	- 0.921	0.682	12.20	8.61 - 18.8
5.91	0.59	+ 0.782	0.640	12.19	8.59 - 18.8
5.92	0.60	2.43	0.600	12.18	8.58 - 18.8
5.93	0.61	4.02	0.563	12.17	8.58 - 18.7
5.94	0.62	5.56	0.529	12.17	8.57 - 18.7

TABLE 10 (continued)

Equation No.	Assumed Value of n_3	C_{1_5}	C_{2_5}	$S^2(\overline{Sh}_5)$	90% confidence range $\sigma^2(\overline{Sh}_5)$
5.95	0.63	7.05	0.496	12.17	8.57 - 18.7
5.96	0.64	8.50	0.466	12.17	8.57 - 18.7
5.97	0.65	9.90	0.438	12.17	8.57 - 18.7
5.98	0.66	11.3	0.412	12.19	8.58 - 18.8
5.99	0.67	12.6	0.387	12.20	8.59 - 18.8
5.100	0.68	13.9	0.364	12.22	8.61 - 18.8
5.101	0.69	15.1	0.342	12.25	8.63 - 18.9
5.102	0.70	16.3	0.322	12.27	8.65 - 18.9
5.103	0.71	17.5	0.302	12.31	8.67 - 19.0
5.104	0.72	18.6	0.284	12.34	8.70 - 19.0
5.105	0.73	19.7	0.268	12.39	8.72 - 19.1
5.106	0.74	20.8	0.252	12.42	8.75 - 19.1
5.107	0.75	21.9	0.237	12.48	8.79 - 19.2
5.108	0.76	22.9	0.223	12.54	8.84 - 19.3
5.109	0.77	23.9	0.210	12.59	8.86 - 19.4
5.110	0.78	24.8	0.198	12.66	8.91 - 19.5
5.111	0.79	25.8	0.186	12.73	8.97 - 19.6
5.112	0.80	26.7	0.176	12.80	9.01 - 19.7
5.113	0.85	31.0	0.130	13.22	9.32 - 20.4
5.114	0.90	34.8	0.0972	13.74	9.82 - 21.2
5.115	0.95	38.2	0.0726	14.37	10.1 - 22.1
5.116	1.00	41.3	0.0544	15.09	10.6 - 23.2
5.117	1.05	44.1	0.0408	15.92	11.2 - 24.6
5.118	1.10	46.6	0.0307	16.83	11.9 - 25.9
5.119	1.15	48.9	0.0231	17.84	12.6 - 27.5
5.120	1.20	51.0	0.0175	18.94	13.3 - 29.2

$$\frac{S^2(\overline{Sh})}{F_{\alpha,f,inf.}} \leqslant \sigma^2\ (\overline{Sh}) \leqslant F_{\alpha,inf,f}.S^2(\overline{Sh}) \qquad (5.5)$$

where f and inf. are the degrees of freedom at which the value of the F distribution is obtained. Tables 9 and 10 include the 90% confidence range of the true variance, $\sigma^2(\overline{Sh})$, calculated from equation (5.5). The significance of the 90% confidence range may be illustrated by reference to table 9 as follows. The minimum estimate of variance, $S^2(\overline{Sh}_3)$, occurs when the exponent of Re_3 is 0.78. This minimum estimate of variance has a value of 11.41 and a 90% confidence range of 7.88 to 17.7. If the value of $S^2(\overline{Sh}_3)$ at any other exponent of Re_3, n_{3_3} say, falls outside this confidence range then it may be concluded with 90% certainty that 0.78 is a significantly better exponent than n_{3_3} for correlating the data by an equation of the form of (5.1). Table 9 shows, however, that the estimates of variance for exponents of Re_3 ranging from 0.20 to 1.40 fall within the 90% confidence range of the exponent 0.78. Thus within this range it cannot be concluded with 90% certainty that any one exponent is better than another. When correlation is based upon Re_5 the minimum estimate of variance has a value of 12.17 and a 90% confidence range of 8.57 to 18.7 as shown in table 10.

By a similar analysis to that described above, Rowe, Claxton and Lewis [38] also found that their data for mass transfer from spheres could be correlated by an equation of the form :

$$Sh_S = C_{11} + C_{12} Re_S^{n} Sc^{1/3} \qquad (5.121)$$

using a large range of values of n. They report that their data can be equally well fitted by an equation of the form of (5.121) "with any desired value of n between about 0.2 and 0.8, provided the constants C_{11} and C_{12} are selected appropriately." Similar results have been found by Beg [10] in the analysis of forced convective mass transfer data for oblate spheroids.

It is interesting to note that when correlation of the present data is based upon d_5 the minimum estimate of variance, 12.17, occurs when the exponent of Re_5 is in the range 0.62 to 0.65 whereas when the correlation is based upon d_3, the minimum estimate of variance, 11.41, occurs when the exponent of Re_3 is in the range 0.77 to 0.79. This change of the exponent of the Reynolds number giving the minimum variance, the "best value of n", with change of characteristic dimension is explained as follows.

Consider the data for a single shape: a change from one characteristic dimension to another merely multiplies the Sherwood and Reynolds numbers by a constant factor so that the slope of the data on a logarithmic plot of Sh vs. Re will not be altered. However, if the data for a single shape were correlated by an expression of the form :

$$Sh_{Ch} = C_{13} + C_{14} \, Re_{Ch}^{n} \, Sc^{1/3} \qquad (5.122)$$

then, if the value of C_{13} were known, the value of n could be found from the slope of a plot of $\log(Sh_{Ch} - C_{13})$ vs. $\log Re_{Ch}$. In this case a change in characteristic dimension would result, as before, in multiplication of the Reynolds numbers by a constant factor but not, however, the values of $(Sh_{Ch} - C_{13})$. As a result, the slope of the data would be altered. Hence if the slopes of the data for the individual shapes are altered, it is highly probable that the slope of the combined data for all shapes would also be altered. The value of C_{13} is unknown for the data of the present work and the "best" value of n must be found by the use of various assumed values of n to determine the value which correlates the data with the minimum variance. A change of characteristic dimension which results in a change of the

slope of the data for a single shape when these data are plotted as $(Sh_{Ch} - C_{13})$ vs. Re_{Ch} would, therefore, result in a change of the "best" value of n for this shape. Hence if the "best" values of n for the individual shapes are altered by a change in characteristic dimension, it is highly probable that the "best" value of n for the combined data for all five shapes would also be altered.

A change of characteristic dimension would also increase or decrease the magnitude of the Reynolds and Sherwood numbers by different amounts for each shape. A change from d_3 to d_5, for example, increases the Sherwood number by a factor d_5/d_3. For shapes with an eccentricity of 4:16 the value of this factor is 1.1 whereas for shapes with an eccentricity 16:16 its value is 1.0. When the data for all shapes are correlated together, this would also result in a change in the "best" value of n, due to the increased weighting of the data for the bodies of eccentricity 4:16.

With the variances associated with exponents of Re_3 ranging from 0.20 to 1.40, and exponents of Re_5 from 0.15 to 1.15, falling within the 90% confidence range of the minimum variances when the data above Re_{TR} are correlated by equations (5.1) and (5.2), the

choice of which correlation should be presented to represent the experimental data is somewhat arbitrary. The fact that the minimum variance of the data based upon d_3, i.e. 11.41, is less than that when the data is based upon d_5, i.e. 12.17, does not necessarily mean that d_3 is a better charactertistic dimension for use in correlating the present data than d_5. The magnitude of the variance is dependent upon the magnitude of the Sherwood numbers of the data points, as well as their scatter about the correlating line. As previously mentioned, change from d_3 to d_5 increases the magnitude of the Sherwood numbers of some of the data points and will, therefore, increase the magnitude of the minimum variance even if the scatter is not increased by this change. This point may be illustrated by consideration of the ranges of values of the exponents of Re_3 and Re_5 which fall within the 90% confidence range of the associated minimum variances. Since the minimum variance for the d_3 data is less than that for the d_5 data it might be thought that the range of Re_3 exponents with variances within the 90% confidence range of this minimum variance would be narrower than the corresponding range of Re_5 exponents. Reference to tables 9 and 10 shows that this is not, in fact, the case. For the

data based on d_3, exponents of Re_3 from 0.20 to 1.40 have variances within the 90% confidence range of the minimum variance, 11.41, whereas for the data based on d_5, exponents of Re_5 from 0.15 to 1.15 have variances within the 90% confidence range of the minimum variance, 12.17. This marginally narrower range of exponents for the d_5 data might suggest that d_5 is a better characteristic dimension to use in correlating the present data than d_3, even though the minimum variance for the d_5 data is greater than that for the d_3 data. This apparent contradiction further illustrates the difficulty in choosing between d_3 and d_5 on a statistical basis.

The above statistical analysis has only been carried out for the data based upon d_3 and d_5, the characteristic dimensions which are shown by figs.(15-22) to be the most successful in unifying the data above Re_{TR}. It has been shown in Chapter 3, equation (3.44), that d_3 is a complex function of eccentricity while d_5, equation (3.48), is linearly related to eccentricity. It is not immediately obvious why these two apparently dissimilar characteristic dimensions should be successful in unifying the data while, d_4 say, is not.

In order to illustrate the relationships between the various characteristic dimensions a plot of eccentricity vs. characteristic dimension is included. This graph, fig.24, shows that d_3 is, in fact, almost linearly related to eccentricity within the range of eccentricity investigated in the present work i.e. 4:16 to 16:16. Furthermore, d_5, is similar in slope to d_3. Other dimensions are decreasingly less successful in unifying the data the further they are removed from the area contained by the lines:

$$d_3 = f(e) \tag{5.123}$$

$$d_5 = f(e) \tag{5.124}$$

It would appear that any characteristic dimension which, when plotted against eccentricity, lies within the area bounded by equations (5.123) and (5.124) would be at least as successful as either d_3 or d_5 in unifying the data above Re_{TR}.

In order to test whether this was in fact so, a line was drawn on fig. (24) lying in the area contained by equations (5.123) and (5.124). This line defined a new characteristic dimension, d_9, which is related to eccentricity by :

$$d_9 = \left(\frac{1.2}{2.54} + \frac{1.34}{2.54} e \right) d_M \tag{5.125}$$

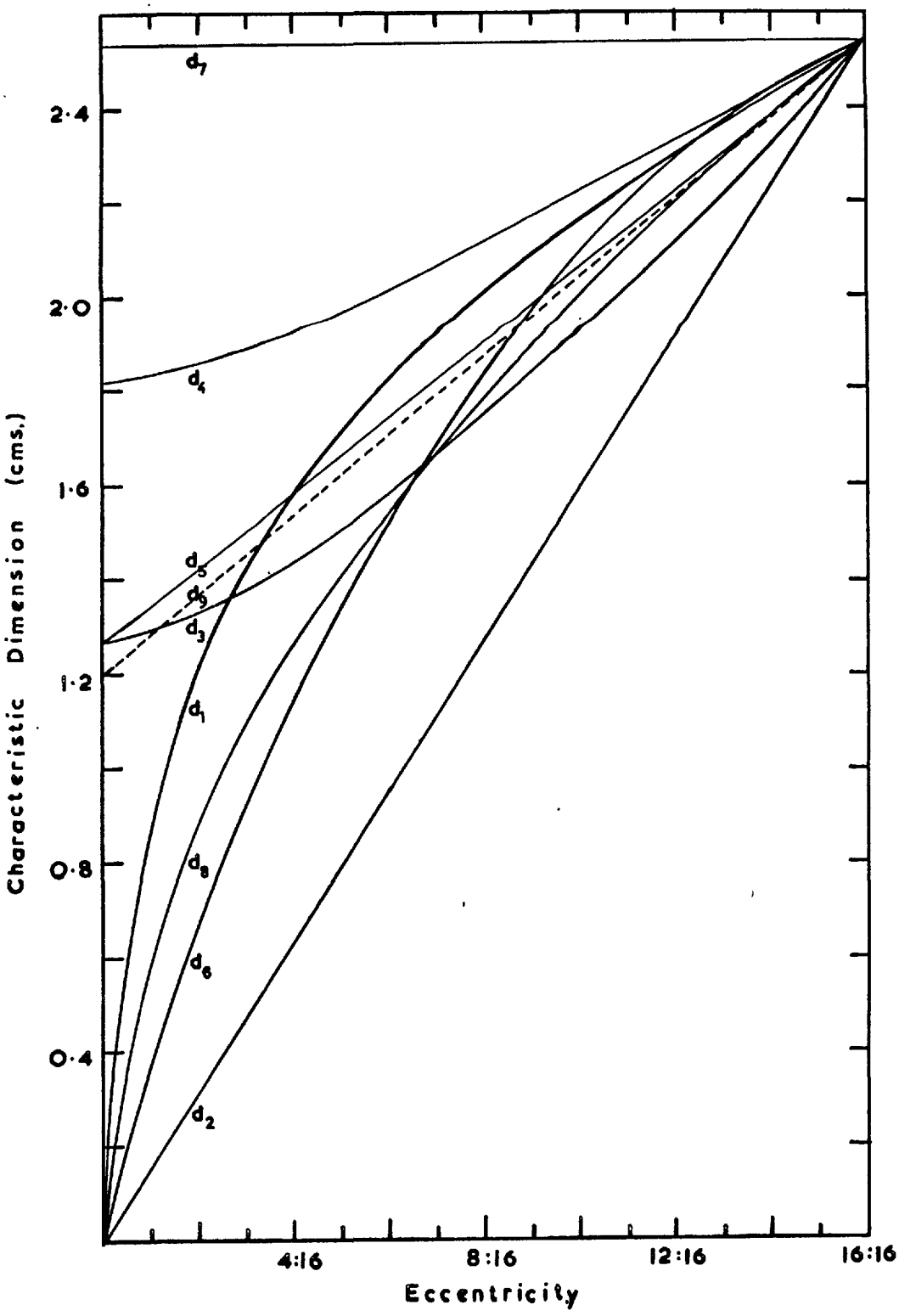
Characteristic Dimension (cms.)
2·4
2·0
1·6
1·2
0·8
0·4
d7
d4
d5
d3
d1
d8
d6
d2
4:16
8:16
12:16
16:16
Eccentricity

FIG. 24

Reynolds and Sherwood numbers based upon d_9 were calculated and correlated by the least squares procedure already described. The results are shown in table 11. Comparison of the estimates of variance, $S^2(\overline{Sh}_9)$, and 90% confidence ranges given in table 11 with the corresponding values given in tables 9 and 10 indicate that d_9 may also be successfully used to correlate the data. The minimum variance in table 11, when the exponent of Re_9 is 0.60, is in fact less than the minimum variances of tables 9 and 10.

It is evident from the considerations presented above that it is not possible to select the "best" characteristic dimension for correlating the present data on a purely statistical basis. From practical considerations the correlation presented should be based upon d_3 in order to preserve continuity with the correlations for oblate spheroids of Skelland and Cornish [9], for forced convection, and Sandoval [11], for free convection. However, even if it is decided to present a correlation in terms of d_3 from practical considerations it is not possible to decide on a statistical basis which of the equations (5.8) to (5.64) should be presented. Many previous workers have assumed a value of zero or 2

TABLE 11.

CORRELATION OF THE DATA ABOVE Re_{TR} AS $Sh_9 = C_{1_9} + C_{2_9} Re_9^{n_9} Sc^{\frac{1}{3}}$

EQUATION No.	ASSUMED Value of n_9	C_{1_9}	C_{2_9}	$S^2(\overline{Sh}_9)$	90% confidence range of $\sigma^2(\overline{Sh}_9)$
5.126	0.10	-479	36.4	18.14	12.18 - 28.0
5.127	0.15	-286	19.3	16.91	11.9 - 26.0
5.128	0.20	-190	11.5	15.80	11.1 - 24.4
5.129	0.30	-93.9	4.83	13.68	9.63 - 21.0
5.130	0.40	-45.9	2.28	12.58	8.85 - 19.4
5.131	0.50	-17.0	1.15	11.68	8.22 - 18.0
5.132	0.60	+2.20	0.598	11.26	7.92 - 17.3
5.133	0.70	15.9	0.321	11.28	7.94 - 17.4
5.134	0.80	26.2	0.175	11.74	8.28 - 18.1
5.135	0.90	34.3	0.0972	12.63	8.90 - 19.5
5.136	1.00	40.7	0.0544	13.93	9.81 - 21.5
5.137	1.10	45.9	0.0308	15.61	11.0 - 24.0
5.138	1.20	50.3	0.0175	17.66	12.4 - 27.2
5.139	1.30	54.0	0.0100	20.05	14.1 - 30.8

for C_{13} when correlating mass transfer data by an equation of the form of (5.122). It is interesting to note that the data of the present work above Re_{TR} may also be correlated on either of these assumptions with a variance falling within the 90% confidence range of equation (5.50). As shown in table 9, the assumption that $C_{13} = 0$ produces a value for the exponent of Re_3 of between 0.59 and 0.60, while the assumption that $C_{13} = 2$ produces an exponent of Re_3 between 0.60 and 0.61.

The correlation selected from equations (5.8) to (5.64) to represent the data of the present work above Re_{TR} is equation (5.50) i.e. the equation with the minimum variance :

$$Sh_3 = 23.7 + 0.196\ Re_3^{0.78}\ Sc^{1/3} \qquad 45 \leqslant Re_3 \leqslant 195 \qquad (5.50)$$

Equation (5.50) has mean and maximum deviations of 2.4% and 7.1% respectively.

Equally satisfactory, however, on the basis of the 90% confidence range, is equation (5.31) i.e.

$$Sh_3 = -0.01 + 0.632\ Re_3^{0.59}\ Sc^{1/3} \qquad 45 \leqslant Re \leqslant 195 \qquad (5.31)$$

which may be rounded off with negligible error to the more simple form :

$$Sh_3 = 0.632\ Re_3^{0.59}\ Sc^{1/3} \qquad 45 \leqslant Re \leqslant 195 \qquad (5.140)$$

From the theoretical considerations of Chapter 3, the absence of the Grashof number in correlations of the form of equation (5.122) indicates the absence of free convection. The schlieren photographs, figs. 10 to 14, show, however, that although correlation of the present data above Re_{TR} by equation (5.122) is possible, free convection has an influence upon the flow patterns at Reynolds numbers considerably greater than Re_{TR}, possibly even at $Re_3 = 195$, the highest Reynolds number investigated. If it is assumed that the presence of free convection, as evidenced by the schlieren photographs, has an influence upon mass transfer rates then clearly correlation of the data by equation (5.122) is an oversimplification. The exponent of the Reynolds number, may, for example, be a function of the Grashof number when free convection is present. When mass transfer data are correlated by equation (5.122), deviation of n from 0.5, the theoretical value for forced convection, may therefore be an effect of free convection. In a similar way the constants C_{13} and C_{14} of equation (5.122) may also be functions of Grashof number. It is not possible, however, to draw definite

conclusions concerning the effect of free convection upon the exponent of the Reynolds number and the constants C_{13} and C_{14} because of the large range of values of n which fall within the 90% confidence range of the value of n with the minimum estimate of variance.

5.2.2. THE REGION BELOW Re_{TR}.

As previously mentioned, none of the characteristic dimensions employed proved to be successful in unifying the data in this region. Since there is no preferred dimension on this basis discussion will be confined to fig. 17, based on d_3, in order to preserve continuity with the region above Re_{TR}.

Fig. 17 includes on the Sh_3 axis the limiting values of Sh_3 for free convection. These data, obtained in the present experimental work, are in close agreement with the values obtained from the correlation of Sandoval [11] whose apparatus was specifically designed to investigate free convection.

The data for spheres below Re_{TR}, including the limiting data point for free convection, indicate that in this region the overall mass transfer rates are independent of Reynolds number. These data may be represented by :

$$Sh_3 = 61 \qquad 0 \leqslant Re_3 \leqslant 45 \qquad (5.141)$$

Considering the evidence of the schlieren photographs, fig.14, which show a great variation of flow patterns in the Reynolds number range $0 \leqslant Re_3 \leqslant 45$, it is quite remarkable that the Sherwood number should remain constant over this range. It would appear that this constancy of the overall Sherwood number must be due to some compensatory variation of local mass transfer rates at different points on the sphere surface. At $Re_3 = 40$ the mass transfer rate at the front stagnation point must be increased relative to the mass transfer rate at this point at $Re_3 = 0$ due to the thinning of the boundary layer. At the flow separation point, approximately 40° at $Re_3 = 40$, the mass transfer rate will be reduced relative to the mass transfer rate at this point in free convection. Further investigation of this compensatory effect would require measurements of local mass transfer rates, possibly by a double exposure photographic technique. From the data of the present work it may only be concluded that, for the sphere, the effect of forced convection may be ignored below Re_{TR} and overall mass transfer rates calculated from correlations for free convection.

For the other shapes the situation is not so

simple. For the flattest shape, e = 4:16, the data continue to fall along the projection of the unified data above Re_{TR} until $Re_3 \doteq 30$. Below this value the scatter of the data is such that it is not possible to draw definite conclusions concerning the variation of the Sherwood number with Reynolds number. These data appear to indicate, however, that the true relationship between the Sherwood and Reynolds numbers below $Re_3 \doteq 30$ is a curve which is asymptotic to a horizontal line through the limiting value of the Sherwood number for free convection. Similarly the data for each of the shapes e = 7:16, e = 10:16, and e = 13:16, below Re_{TR} indicate that the true relationship between the Sherwood and Reynolds numbers for each of these shapes is a curve asymptotic to a horizontal line through the limiting free convection Sherwood number for that shape. The value of Re_3 at which the data for a particular shape begin to diverge from the projection of the unified data increases from $Re_3 \doteq 30$ for the shape with e = 4:16, to $Re_3 \doteq 45$ for the sphere. The scatter of the data in this region, however, is such that it is not possible to assign specific values of Re_3 to the point at which the data for each shape begin to diverge: it is evident, however, that this value increases with increase in

eccentricity. Similarly it is evident that as eccentricity increases so does the value of Re_3 below which the mass transfer rate may be taken to be that which occurs in free convection alone: again it is not possible to assign specific values to these Reynolds numbers.

From the above considerations it is clear that further research is necessary at $Re_3 < 45$ in order to determine the exact form of the relationships between the Sherwood and Reynolds numbers which may only be qualitatively deduced from the data of the present work. For spherical and near spherical bodies, however, the present data indicate that little error would be incurred if mass transfer rates at $Re_3 < 45$ were predicted on the basis of the correlation for free convection proposed by Sandoval i.e.

$$Sh_3 = 0.121\ (Gr.Sc)^{1/3} \qquad 2.1 \times 10^7 < Gr_3Sc < 2.1 \times 10^8 \tag{5.142}$$

It should be pointed out, however, that the value of Re_3 below which overall mass transfer rates for spheres may be predicted from correlations for free convection is a function of the Grashof number. Since the only quantity varied in the Grashof number in the present work was the characteristic dimension, the Grashof number was constant for each shape. The value of 45 for

the Reynolds number below which forced convection may be neglected is, therefore, only valid at the Grashof number employed in the present work for spheres i.e. 11.8×10^4. A more general criterion for deciding when forced convection may be neglected which involves both the Grashof and Reynolds numbers is discussed in the following section.

5.3. DISCUSSION OF THE PLOT OF Sh_3 vs. $\left(\frac{Gr_3}{Re_3^2}\right)$.

The importance of the group (Gr/Re^2) in the correlation of mass transfer data for interacting free and forced convection was suggested by analysis of the equations of motion and diffusion. A plot of Sh_3 vs. (Gr_3/Re_3^2) on logarithmic coordinates is presented in fig. 25. This plot shows that the data for each shape lie on a separate curve which is approximately parallel to the curves for the other shapes. The data based on d_5 follow similar parallel curves but when the other characteristic dimensions previously discussed are used the curves for the data of the individual shapes are less regularly related. The other characteristic dimensions are thus of less use in correlating the present data. This re-emphasises the importance of the

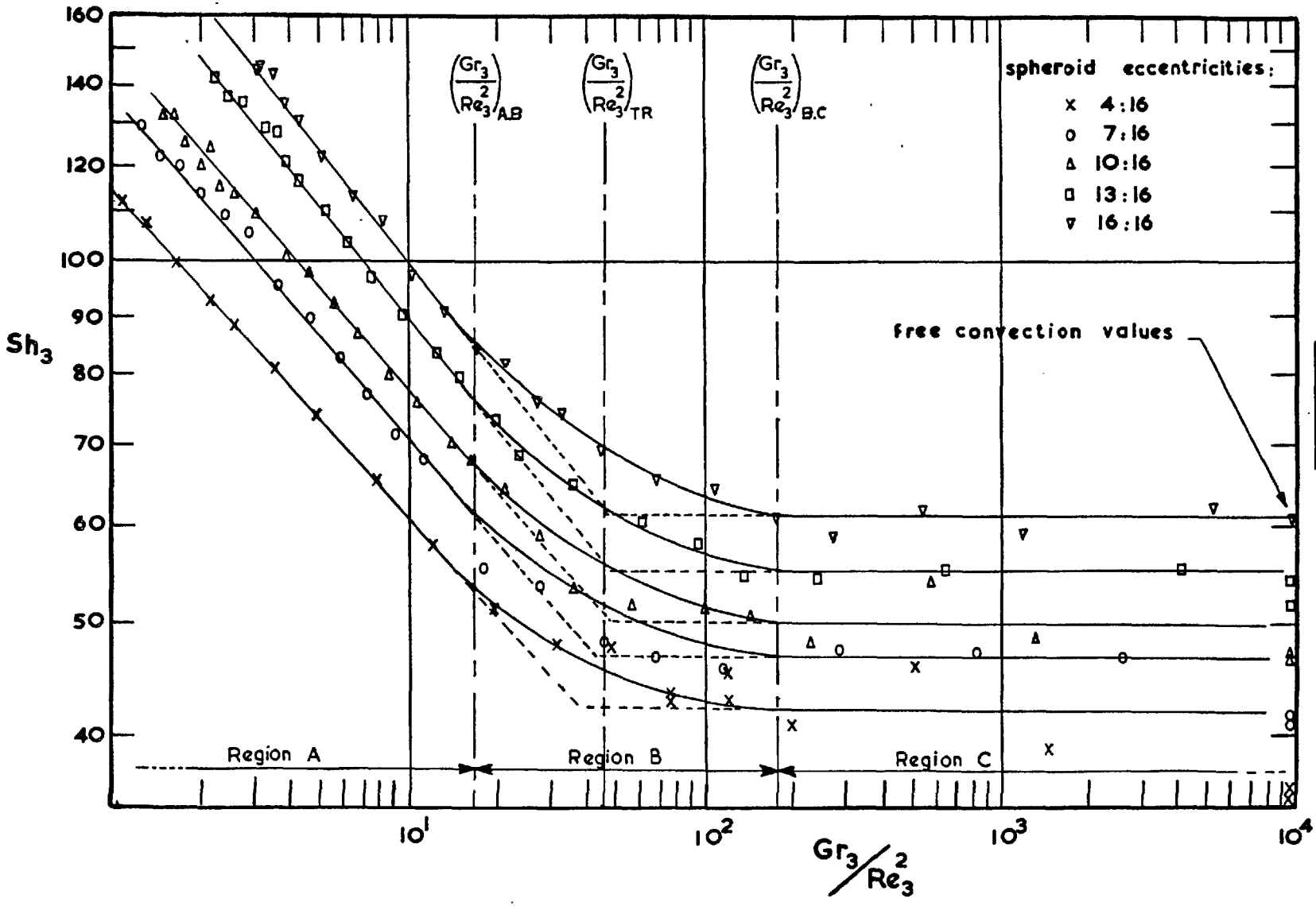
160
140
120
100
90
80
70
60
50
40
Sh_3
$\left(\frac{Gr_3}{Re_3^2}\right)_{A,B}$
$\left(\frac{Gr_3}{Re_3^2}\right)_{TR}$
$\left(\frac{Gr_3}{Re_3^2}\right)_{B,C}$
spheroid eccentricities:
x 4:16
o 7:16
Δ 10:16
□ 13:16
▽ 16:16
free convection values
Region A
Region B
Region C
10^1
10^2
10^3
10^4
Gr_3/Re_3^2

FIG. 25

characteristic dimensions d_3 and d_5 in correlating mass transfer data for oblate spheroids. The present discussion will be confined to the data obtained by the use of d_3 as the characteristic dimension which are plotted in fig.25.

The curves in fig.25 may be divided into three regions, designated for the sake of discussion, A, B, and C. As shown in fig.25, the transition values between these regions, $(Gr_3/Re_3^2)_{A.B}$ and $(Gr_3/Re_3^2)_{B.C}$, are independent of shape.

In regions A and C the data for individual shapes may be closely approximated by the straight lines shown in fig.25. Region B is clearly a transition region in which the data for each shape lie on a curve asymptotic to the limiting straight lines of regions A and C. The extrapolations of these straight lines into region B intersect at $(Gr_3/Re_3)_{TR} \doteq 45$, which is very nearly independent of shape.

The limiting free convection values for Sh_3 as $(Gr_3/Re_3^2) \longrightarrow$ infinity, are also shown in fig.25. In the case of the sphere, the limiting value for free convection lies close to the horizontal line through the data in region C. As eccentricity decreases from 16:16 to 4:16, the limiting values fall further and further

below the corresponding correlating line in region C. Thus whereas for a sphere it may be concluded that within region C the effect of forced convection upon the Sherwood number is negligible, this conclusion becomes increasingly less valid with decreasing eccentricity.

The relevance of regions A, B, and C, with respect to the flow patterns shown by the schlieren photographs may be discussed by reference to tables (4-8). These tables show that the transition from region B to region C, at $(Gr_3/Re_3^2)_{A.B} = 160$, corresponds to transition from flow regime 3 to flow regime 4. In the case of the sphere the Sherwood number is constant no matter whether flow regimes 1,2, or 3 predominates. For the other shapes Sh_3 is constant for flow regimes 2 (within the range of (Gr_3/Re_3^2) investigated) and 3 but is reduced in the limiting case of free convection i.e. regime 1. This suggests that the horizontal lines drawn through the data for the bodies with eccentricities 4:16, 7:16, 10:16, and 13:16 in region C are in fact an oversimplification. Although these horizontal lines represent the data over the range investigated it is probable that further research at higher values of (Gr_3/Re_3^2) would indicate that the data for each shape fall on a continuous curve asymptotic to the horizontal line through

the limiting free convection value of Sh_3.

The transition from region A to region B on fig.25 at $(Gr_3/Re_3^2)_{A.B} = 16$ cannot be related to a change in flow regime. For the oblate spheroidal bodies with eccentricities 4:16, 7:16, and 10:16 it corresponds to the flow separation angle first reaching 90^o, but in the cases of e = 13:16 and e = 16:16 the separation angles are 60^o and 70^o respectively.

Workers in the field of heat transfer have reported values of the group (Gr_H/Re^2) above or below which it is permissible to neglect forced or free convection. Although the reported values are for heat transfer and for various geometries other than oblate spheroids they may be usefully compared with the data of the present work. A synopsis of the reported values is given in table 12.

Fig.25 indicates that, in the calculation of overall Sherwood numbers for the sphere, forced convection may be neglected above $(Gr_3/Re_3^2) = 160$. For the other shapes mass transfer was increased, compared with the limiting free convection value, even at the highest values of (Gr_3/Re_3^2) employed in the present work.

In order to decide whether $(Gr_3/Re_3^2)_{A.B}$ represents the value of (Gr_3/Re_3^2) below which the effect

TABLE 12

LIMITING VALUES OF (Gr_H/Re^2) FOR INTERACTING FREE AND FORCED CONVECTION

Author	Free convection negligible	Forced convection negligible	Method of Analysis	Geometry	Sense of Flow	Prandtl Number
Acrivos[53]	$0.02 > Gr_H/Re^2$	$Gr_H/Re^2 > 100$	Theoretical	Vertical plate	Aiding	$0.73 \rightarrow 100$
Sparrow & Gregg[54]	$0.225 > Gr_H/Re^2$	---	Theoretical	Vertical Plate	Aiding and opposing	$0.01 \rightarrow 10.0$
Sparrow[55] Eichhorn & Gregg	$0.3 > Gr_H/Re^2$	$Gr_H/Re^2 > 16$	Theoretical	Vertical Plate	Aiding	0.7
	$0.3 > Gr_H/Re^2$	---	Theoretical	Vertical Plate	Opposing	0.7
Pei[60]	$0.05 > Gr_H/Re^2$	$Gr_H/Re^2 > 100$	Experimental	Sphere	Aiding and opposing	0.7

of free convection upon mass transfer rates may be neglected, it is necessary to compare the present data with those of other workers. This comparison is shown for spheres in fig.26. The dotted curves indicate extrapolation of correlations obtained outside the range of values of (Gr_3/Re_3^2) investigated in the present work.

Fig.26 shows that the correlations obtained for purely forced convection which are of the form :

$$Sh_3 = C_{15} \; Re_3^{n} \; Sc^{m} \qquad (5.143)$$

appear as straight lines: these correlations have been plotted using the Grashof number for 1 inch diameter benzoic acid spheres in water at 25.0°C. i.e. 11.8×10^4. Correlations for forced convection which are of the form :

$$Sh_3 = 2 + C_{16} \; Re_3^{n} \; Sc^{m} \qquad (5.144)$$

are also almost exactly straight lines on fig.26.

If the data of the present work below $(Gr_3/Re_3^2)_{A.B}$ were to fall along the extrapolation of the correlations obtained in the absence of free convection, then it could be concluded that free convection has negligible effect upon mass transfer rates in this region. Although there is great variation amongst the extrapolated correlations, it is clear that the data of the present work lie above all of these extrapolations.

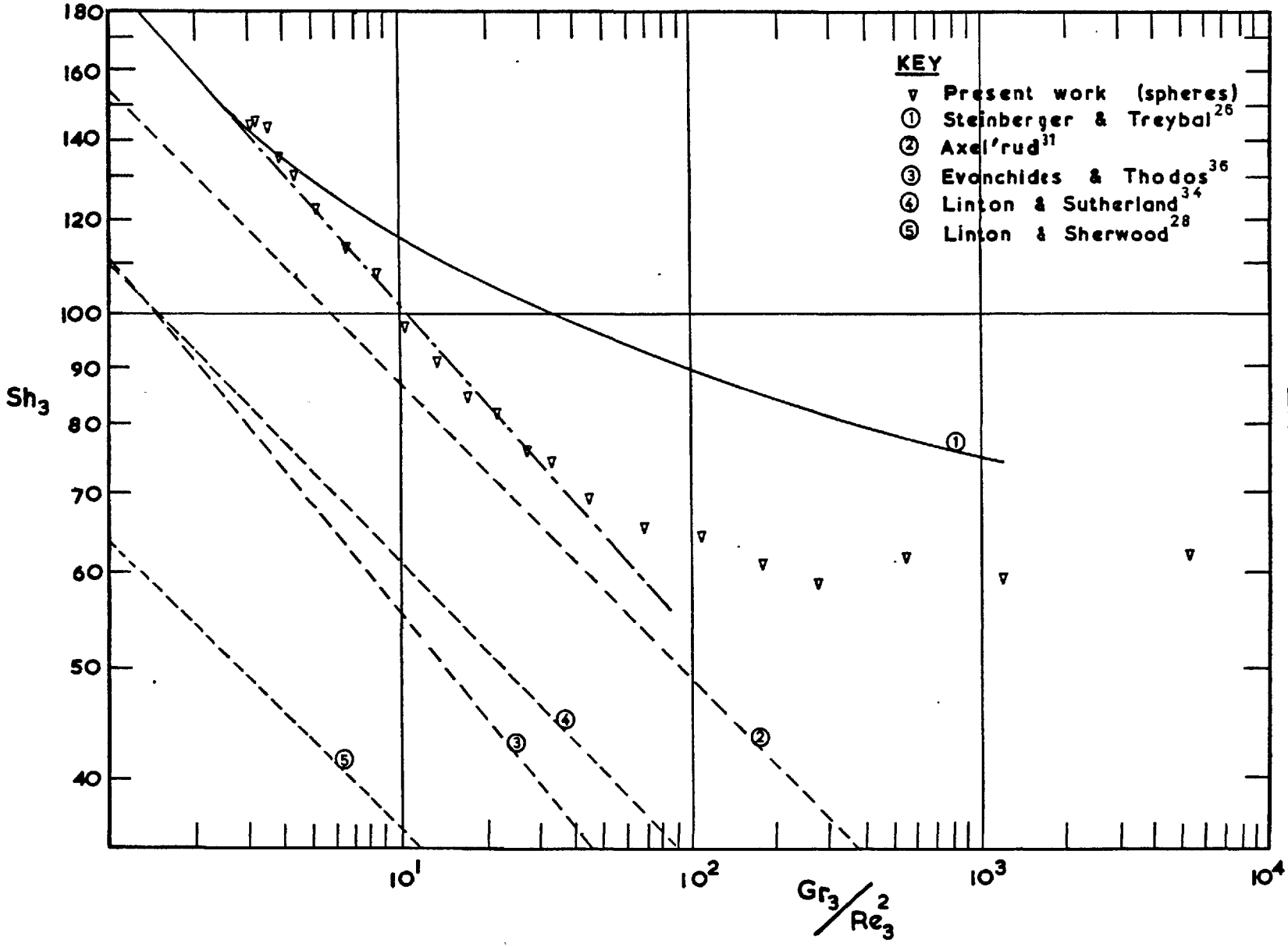
KEY
▽ Present work (spheres)
① Steinberger & Treybal[26]
② Axel'rud[31]
③ Evonchides & Thodos[36]
④ Linton & Sutherland[34]
⑤ Linton & Sherwood[28]
Sh3
Gr3/Re3²
180
160
140
120
100
90
80
70
60
50
40
10¹
10²
10³
10⁴

FIG. 26

This indicates that the effect of free convection was to increase mass transfer rates even at the lowest value of (Gr_3/Re_3^2) employed in the present work. This conclusion is in agreement with the evidence of the schlieren photographs which indicate an effect of free convection upon the flow patterns over the complete range of (Gr_3/Re_3^2) investigated. The slope of the present data is greater than that of several of the extrapolations shown in fig.26. Many of these correlations have been obtained, however, by assuming a value of 0.5 for n when correlating data in the form of equations (5.143) or (5.144). This choice of n determines the slope of these correlations when they are plotted in fig.26.

Also shown in fig.26 is the correlation for interacting free and forced convection proposed by Steinberger and Treybal [26] i.e.

$$Sh = 2 + 0.569\ (Gr.Sc)^{1/4} + 0.347\ Sc^{0.312}\ Re^{0.62} \qquad (5.145)$$

This correlation includes an additive free convection term and therefore appears as a curve in fig.26. At low values of (Gr_3/Re_3^2), however, the effect of the free convection term decreases and the plot of the correlation on fig.26 approximates to a straight line. The data of the present work are seen to be in close

agreement with the correlation of Steinberger and Treybal at the lower end of the range of (Gr_3/Re_3^2) investigated. An extrapolation of the straight line portion of their correlation, shown as a dot-dash line on fig.26, falls through the present data below $(Gr_3/Re_3^2)_{A.B.}$ This does not indicate the absence of free convection, however: even in the portion of the Steinberger-Treybal correlation which is approximated to a straight line in fig.26, the values of the Sherwood number predicted by equation (5.145) are considerably increased by the presence of the free convective term. At $(Gr_3/Re_3^2) = 1$ for example, which for one inch diameter benzoic acid spheres in water at 25.0°C corresponds to a Reynolds number of 344, the Steinberger-Treybal correlation predicts an overall Sherwood number of 166.5 of which 61.5, or 37%, is the contribution of the free convective term.

Sparrow, Eichhorn and Gregg [55] proposed that free convection should be considered as having negligible effect upon mass transfer rates if its contribution to the overall Sherwood number is less than 5%. Using this criterion the Steinberger-Treybal correlation predicts an influence of free convection up to Reynolds numbers of approximately 1.6×10^4. This corresponds to a value of (Gr_3/Re_3^2) of approximately 7×10^{-4} for one

inch diameter benzoic acid spheres in water at 25.0°C. Other workers have assumed the effect of free convection to be negligible at much lower Reynolds numbers than 1.6×10^4. It should be pointed out, however, that the data of Steinberger and Treybal were obtained at Reynolds numbers below 1.7×10^3.

The above considerations indicate that although the present data below $(Gr_3/Re_3^2)_{A.B}$ fall on straight lines, the effect of free convection upon mass transfer rates may not be negligible. Comparison with correlations for purely forced convection show that, even at the highest Reynolds numbers employed in the present work, mass transfer was increased by the effect of free convection. Further work is clearly necessary above $Re_3 = 200$, in order to discover the manner in which the data in this region approach the limiting curves for forced convection.

Although the above comparisons have only been made for spheres, the parallel nature of the curves in fig.25 indicate that the same conclusions regarding the effect of free convection may be made for the other shapes.

In the above discussion the value of (Gr_3/Re_3^2) above which forced convection may be neglected in the prediction of overall mass transfer rates for spheres

has been taken to be $(Gr_3/Re_3^2)_{A.B} = 160$. Inspection of the data in fig.25 shows that little error would be incurred if this value were instead to be taken to be $(Gr_3/Re_3^2)_{TR} = 45$. Use of the criterion $(Gr_3/Re_3^2)_{TR}$ may be extended to the other shapes investigated to obtain a simple and useful method for the prediction of mass transfer rates from oblate spheroidal bodies in the presence of interacting free and forced convection which may be stated as follows. At values of (Gr_3/Re_3^2) less than $(Gr_3/Re_3^2)_{TR}$ mass transfer rates may be predicted by the expression recommended in Section 5.2.1 i.e.

$$Sh_3 = 0.632\ Re_3^{0.59}\ Sc^{1/3} \qquad (5.146)$$

Above $(Gr_3/Re_3^2)_{TR}$ mass transfer rates may be predicted by the expression proposed by Sandoval [11] for free convection i.e.

$$Sh_3 = 0.121\ (Gr.Sc)^{1/3} \qquad (5.147)$$

Use of equation (5.147) results in little error for bodies with eccentricities close to one. The error increases, however, for flatter bodies: the mass transfer rates for an oblate spheroid with eccentricity 4:16 predicted by equation (5.147) are a maximum of approximately 25% lower than those observed in the present work. For the other oblate spheroidal bodies investigated the use

of equation (5.147) results in predicted mass transfer rates approximately 18%, 10% and 2% lower than those observed in the present work for bodies with eccentricities 7:16, 10:16, and 13:16 respectively.

It must be stressed, however, that the above recommendation is based upon data obtained within the limits $0 \leqslant Re_3 \leqslant 195$ and $2.15 \times 10^4 \leqslant Gr_3 \leqslant 11.8 \times 10^4$ with the Schmidt number constant at 1005. Further work over other ranges of the groups Re_3, Gr_3, and Sc is recommended in order to investigate the generality of the above proposal.

5.4. COMPARISON WITH PREVIOUS WORK.

Fig.27 shows the data of the present work, as a plot of Sh_3 vs. Re_3 on logarithmic coordinates, together with all the published correlations for mass transfer from spheres and oblate spheroids at Reynolds numbers below 200.

Rowe, Claxton and Lewis [38] found that their data for solid-gas systems and for solid-liquid systems could not be represented by a single correlation. They proposed a correlation of the form :

$$Sh = 2 + C_{17} Re^{1/2} Sc^{1/3} \qquad (5.148)$$

where C_{17} is 0.69 for mass transfer into air and 0.79 for

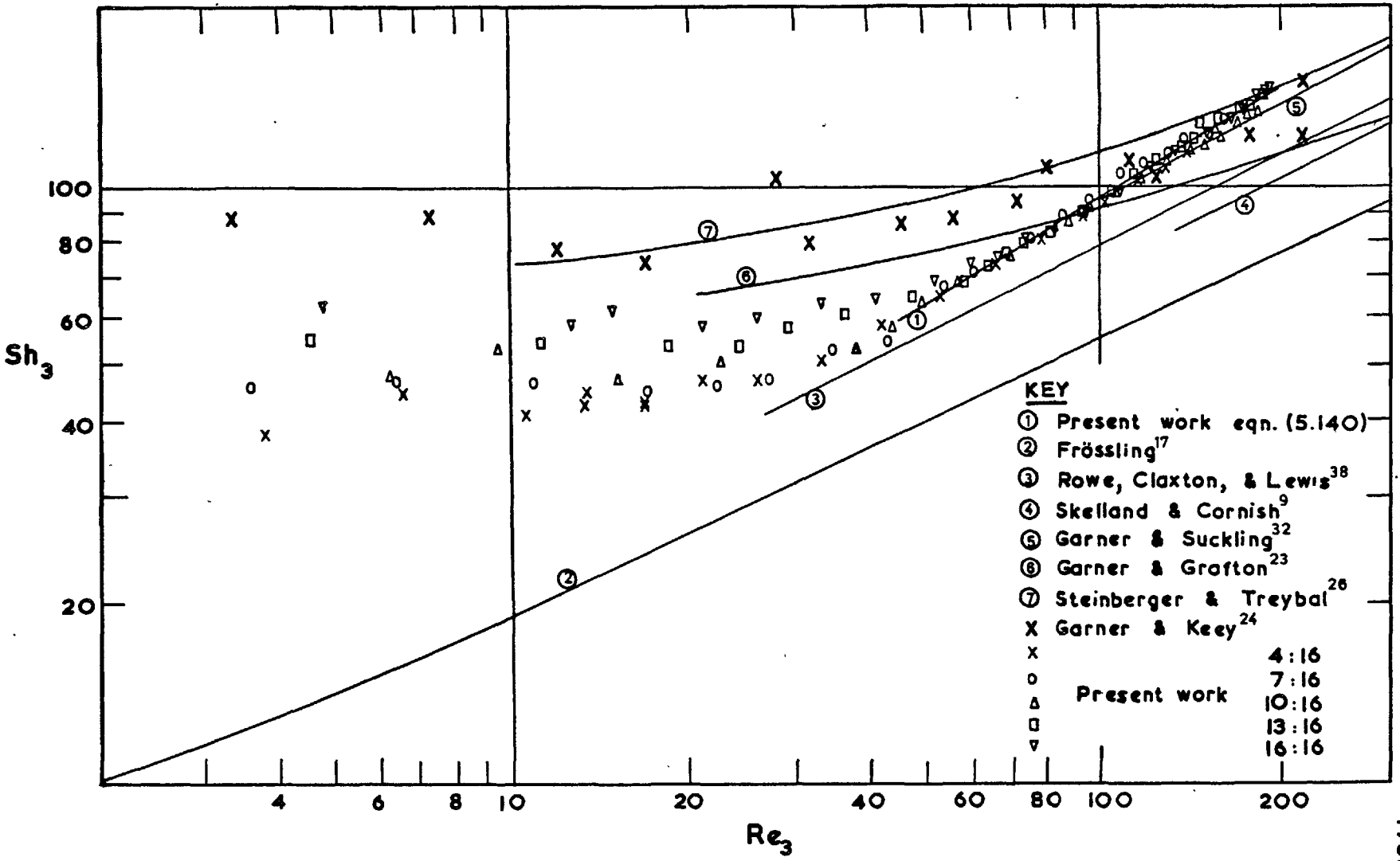
Sh3
Re3
100
80
60
40
20
4
6
8
10
20
40
60
80
100
200
KEY
① Present work eqn. (5.140)
② Frössling[17]
③ Rowe, Claxton, & Lewis[38]
④ Skelland & Cornish[9]
⑤ Garner & Suckling[32]
⑥ Garner & Grafton[23]
⑦ Steinberger & Treybal[26]
X Garner & Keey[24]
Present work
4:16
7:16
10:16
13:16
16:16

FIG. 27

mass transfer into water. The correlation of Rowe, Claxton and Lewis for mass transfer into water is shown in fig.27. The correlation of Steinberger and Treybal [26], which is dependent upon Grashof number, has been plotted using the Grashof number for the spheres of the present work. The data of Garner and Keey [24] for spheres in opposing flow have been taken from the published logarithmic plot and converted from 30.0°C to 25.0°C on the assumption that $Sh \propto Sc^{1/3}$. In the Reynolds number range under consideration the Sherwood number is probably a function of the Grashof number as well as of the Schmidt number. Since the form of this function is not known, however, it is not possible to convert the data of Garner and Keey except by the above crude approximation. Also included in fig.27 are the correlations of Garner and Suckling [32] and Garner and Grafton [23] for mass transfer from spheres in solid-liquid systems and of Frossling [17] for mass transfer from spheres in solid-gas systems. The correlation of Skelland and Cornish [9] for mass transfer from oblate spheroidal bodies into a gas stream is also shown in fig.27.

As found by Rowe, Claxton and Lewis [38], the data for solid-gas and solid-liquid systems cannot be uniquely represented by a correlation of the form of

equation (5.148) even when mass transfer occurs by forced convection alone. At low Reynolds numbers the differences between the two types of system become more marked as the influence of free convection increases; solid-gas systems having Grashof numbers very much less than those of solid-liquid systems. The correlation for solid-gas systems included in fig.27 are not, therefore, expected to be in agreement with those for solid-liquid systems. The Skelland-Cornish correlation is included since it is the only published correlation for oblate spheroids. The Frossling correlation is included for completeness.

The scatter of the data of the present work for a single shape is seen to be much less than that of the data of Garner and Keey which cover approximately the same Reynolds number range. Above Re_{TR} ($Re_3 = 45$), where the data are unified by the use of d_3, the scatter of the combined data is still less than that of Garner and Keey's data for spheres. Garner and Keey claimed that their data indicated a minimum in the mass transfer rate at a Reynolds number of approximately fifty. Fig.27 shows that the scatter of their data is so large that below $Re_3 = 100$ their data may equally well be represented by a horizontal line. In this region the mass transfer rates recorded by Garner and Keey are somewhat greater

than those of the present work. This may have been due to some constant error introduced by the photographic technique employed by Garner and Keey to obtain mass transfer rates, instabilities in the velocity profile in their water tunnel or the stratified nature of the compressed spheres used by these workers. Further, they probably introduced test bodies into the water tunnel by opening a port-hole in the side of the tunnel and forcing the test object into the tunnel against the outward rushing jet of water. Apart from the departure from steady state conditions which would have resulted from this technique, the mass transfer which occurred before the body reached the test position may have been considerable.

The correlation of Rowe, Claxton and Lewis was obtained for a horizontal water flow past benzoic acid spheres. In this situation the forces of free convection and forced convection are not directly opposed and mass transfer rates might be expected to be different from those obtained in the present work. Their correlation indicates, in fact, that mass transfer is slightly less for horizontal flow than for vertical opposing flow.

The correlations of Steinberger and Treybal, Garner and Suckling, and Garner and Grafton, are shown

from the lowest value of Reynolds number investigated by these workers to a Reynolds number of 200. These correlations are all, in fact, predominantly based upon data obtained at Reynolds numbers greater than 200 and are therefore "weighted" by the data obtained outside the range of the present investigation.

The slope of the present data above Re_{TR} appears to be slightly greater than the slopes of some of the other correlations shown in fig.27. It should be emphasized that the correlations of Rowe, Claxton and Lewis, Frossling, and Garner and Suckling were obtained on the assumption that the exponent of the Reynolds number was 0.5. The slope of these correlations on fig.27 are therefore fixed by this assumption. As mentioned in section (5.2.1) the increased slope of the present data is possibly an effect of free convection.

It may be concluded from fig.27 that the data of the present work show reasonable agreement with those correlations of other workers which are based upon data for the benzoic acid - water system.

CHAPTER 6.

CONCLUSIONS.

1. Plots of Sherwood number versus Reynolds number showed that, within the Reynolds number range investigated, i.e. $0 \leqslant Re_3 \leqslant 195$, the mass transfer data fell into two distinct regions; above and below a Reynolds number of 45. For Reynolds numbers greater than 45 the data for oblate spheroidal bodies of eccentricities 4:16, 7:16, 10:16, 13:16, and 16:16, were successfully unified by the use of the characteristic dimensions d_3 (the surface area of the spheroid divided by the perimeter normal to flow) and d_5 (the arithmetic mean of the major and minor axes of the spheroid). For Reynolds numbers less than 45 none of the eight characteristic dimensions employed successfully unified the data.

2. A statistical analysis of the data for Reynolds numbers greater than 45 showed that when these data were correlated by an expression of the form :

$$Sh_3 = C_{1_3} + C_{2_3} \, Re_3^{n_3} \, Sc^{1/3} \qquad (6.1)$$

the minimum estimate of variance occurred when the value of n_3 was 0.78. However, for any value of n_3 in the range 0.2 to 1.4 the estimate of variance fell within

the 90% confidence range of the minimum estimate of variance. Similarly, when the data were correlated by an expression of the form :

$$Sh_5 = C_{1_5} + C_{2_5} Re_5^{n_5} Sc^{1/3} \qquad (6.2)$$

the minimum estimate of variance occurred when the value of n_5 was 0.63; values of n_5 from 0.15 to 1.1 fell within the 90% confidence range of this minimum estimate of variance.

With these large ranges of the exponents of the Reynolds number possible, the choice between d_3 and d_5 cannot be made on a purely statistical basis. It was decided to represent the present data for Reynolds numbers greater than 45 by a correlation based upon the characteristic dimension d_3 in order to preserve continuity with the correlations for oblate spheroids presented by other workers [9,11]. The correlation chosen was that with the minimum estimate of variance, i.e.

$$Sh_3 = 23.7 + 0.196\, Re^{0.78} Sc^{1/3} \qquad 45 \leqslant Re_3 \leqslant 195 \qquad (6.3)$$

The data were almost equally well represented by the somewhat simpler expression :

$$Sh_3 = 0.632\, Re_3^{0.59} Sc^{1/3} \qquad 45 \leqslant Re_3 \leqslant 195 \qquad (6.4)$$

The values of Sh_3 predicted by equations (6.3) and (6.4) are higher than the values predicted at the corresponding Reynolds numbers by the extrapolations of the published correlations for forced convection alone. This suggests the possible influence of free convection upon mass transfer rates even at the highest Reynolds numbers investigated in the present work.

3. A plot of characteristic dimension against eccentricity showed that the two characteristic dimensions which most successfully unified the data for Reynolds numbers greater than 45, i.e. d_3 and d_5, are similarly related to eccentricity. Any characteristic dimension which, when plotted in this manner, is related to eccentricity in a similar way, would also successfully unify mass transfer data for oblate spheroids of various eccentricities.

4. At Reynolds numbers less than 45 none of the characteristic dimensions employed successfully unified the data for all five oblate spheroidal shapes. For spheres the mass transfer rates were independent of the Reynolds number in this region; the mass transfer rate being that predicted for free convection alone. For

the other shapes the relationships between Reynolds number and Sherwood number in this region appeared to be continuous curves, asymptotic to the horizontal lines through the limiting Sherwood numbers for free convection alone. The scatter of the data points in this region was such, however, that analysis could not be usefully pursued beyond this qualitative interpretation.

5. Analysis of the equations of motion and diffusion showed that the dimensionless group (Gr/Re^2) is of importance in the correlation of mass transfer data for interacting free and forced convection. Plots of Sh vs. (Gr/Re^2) based upon d_3 and d_5 resulted in a series of parallel curves for the five oblate spheroidal shapes. When other characteristic dimensions were employed no regular relationship existed between the curves for the individual shapes. This emphasises the importance of the characteristic dimensions d_3 and d_5 in the correlation of mass transfer data for oblate spheroids.

The plot of Sh_3 vs. (Gr_3/Re_3^2) showed that the data for each shape could be represented by straight lines above $(Gr_3/Re_3^2) = 160$ and below $(Gr_3/Re_3^2) = 16$. Above $(Gr_3/Re_3^2) = 160$ the mass transfer rates were independent of the value of (Gr_3/Re_3^2) up to the highest

value of this group used in the present work i.e. approximately 5250. For the sphere this mass transfer rate was that due to free convection alone but for the other shapes this mass transfer rate was greater than that for free convection alone.

Comparison of the correlations of other workers with the straight line through the present data for spheres below $(Gr_3/Re_3^2) = 16$, showed that, even though the data fell on a straight line, the mass transfer rate was considerably increased from the predicted rate for forced convection alone.

The extrapolations of the straight lines through the data above $(Gr_3/Re_3^2) = 160$ and below $(Gr_3/Re_3^2) = 16$ intersected at a value of (Gr_3/Re_3^2) which was approximately equal to 45 for all shapes. For (Gr_3/Re_3^2) less than 45 the data of the present work could be represented by the expression :

$$Sh_3 = 0.632\ Re_3^{0.59}\ Sc^{1/3} \qquad (6.4)$$

In order to represent the data of the present work for (Gr_3/Re_3^2) greater than 45 the correlation for free convection proposed by Sandoval [11] i.e.

$$Sh_3 = 0.121\ (Re_3.Sc)^{1/3} \qquad (6.5)$$

could be employed. Use of equation (6.5) results in little

error for spherical or near spherical bodies. For bodies with eccentricities 4:16, 7:16, 10:16, and 13:16 the mass transfer rates predicted by equation (6.5) are a maximum of 25%, 18%, 10% and 2% respectively, lower than those observed in the present work. It is recommended that further work be carried out, in order to test the above method of representing mass transfer data for oblate spheroids in the presence of interacting free and forced convection, over other ranges of the Reynolds, Grashof, and Schmidt numbers than those employed in the present work i.e. $0 \leqslant Re_3 \leqslant 195$; $2.15 \times 10^4 \leqslant Gr_3 \leqslant 11.8 \times 10^4$; $Sc = 1005$.

6. The schlieren photographs showed the existence of four distinct flow regimes in the Reynolds number range investigated i.e. $0 \leqslant Re_3 \leqslant 195$. The flow patterns in these four regimes may be summarized as :

1. Downflow with steady tail.
2. Downflow with disturbed tail.
3. Both up-and down-flow periodically prediminant.
4. Upflow with a steady separation angle which is dependent upon the Reynolds number.

The first three of these regimes occurred when

values of (Gr_3/Re_3^2) were greater than 160 i.e. in the region where mass transfer rates for the sphere were those predicted for free convection alone. It is concluded that some compensatory effect between local mass transfer rates results in constant overall mass transfer rates. It is recommended that further work, possibly employing a double exposure photographic technique, be carried out in order to investigate the variation of local mass transfer rates.

7. The schlieren photographs showed that free convection influenced the flow patterns around the dissolving bodies at values of (Gr_3/Re_3^2) considerably less than 16, probably even at the lowest value of this group investigated in the present work. This supported the conclusion that mass transfer rates were influenced by free convection even at these low values of (Gr_3/Re_3^2). It is recommended that further work be carried out at values of Re_3 greater than 195 in order to investigate the way in which the data for interacting free and forced convection, plotted as Sh_3 vs. (Gr_3/Re_3^2), approach the limiting data for forced convection alone.

8. The value of the schlieren technique in the interpretation of mass transfer data has been illustrated. The schlieren photographs showed the complex nature of the flow patterns around dissolving bodies when free and forced convection interact. Attempts to solve the diffusion equation by the use of simple assumed velocity distributions are clearly great oversimplifications in this situation.

9. The concept of designing low speed water tunnels on the basis of a packed bed has been tested and found to be successful.

APPENDIX. 1.

TABULATED DATA.

TABLE 13.

CHARACTERISTIC DIMENSIONS, AREAS AND VOLUMES OF OBLATE SPHEROIDS.

		e=4.16	e=7.16	e=10.16	e=13.16	e=16.16
Surface Area	cm^2	11.484	13.301	15.444	17.788	20.268
Volume	Cm^3	2.145	3.754	5.363	6.971	8.580
d_1	cm	1.600	1.928	2.172	2.370	2.540
d_2	cm	0.635	1.111	1.588	2.064	2.540
d_3	cm	1.439	1.667	1.935	2.229	2.540
d_4	cm	1.912	2.058	2.217	2.380	2.540
d_5	cm	1.588	1.826	2.064	2.302	2.540
d_6	cm	1.121	1.693	2.083	2.352	2.540
d_7	cm	2.540	2.540	2.540	2.540	2.540
d_8	cm	1.270	1.680	2.008	2.290	2.540

TABLE 14

PHYSICAL PROPERTIES OF BENZOIC ACID-WATER SYSTEMS AT 25.0°C.

PROPERTY	VALUE	REFERENCE
c_s	3.45 g./litre	87
ρ_s	0.99766 $g./cm^3$	11
ρ_{H_2O}	0.99707 $g./cm^3$	81
μ_{H_2O}	0.8937 centipoise	82
D_v	8.92×10^{-6} $cm^2/sec.$	calculated
Sc	1005	calculated

TABLE 15.

DISSOLUTION DATA (All runs at 25.0°C.)

RUN NO.	ECCENTRICITY	RUN DURATION (hr.)	TOTAL WEIGHT LOSS (mg)	FLOW VELOCITY (cm/sec)	k_c (cm/hr)
1	4.16	1.25	52.4	0.132	1.06
2	4.16	1.25	47.45	0.083	0.958
3	4.16	1.25	50.5	0.041	1.02
4	4.16	1.25	50.05	0.084	1.01
5	4.16	1.25	47.85	0.104	0.967
6	16.16	3.00	174.2	0.147	0.830
7	4.16	1.25	47.2	0.104	0.953
8	16.16	3.00	171.35	0.118	0.817
9	10.16	2.00	90.85	0.141	0.853
10	16.16	3.00	160.55	0.092	0.765
11	4.16	1.25	52.65	0.163	1.06
12	16.16	3.00	185.2	0.184	0.883
13	10.16	2.00	93.7	0.178	0.879
14	16.16	3.00	202.6	0.234	0.966
15	4.16	1.25	63.9	0.263	1.29
16	10.16	2.00	113.2	0.231	1.06
17	4.16	1.25	56.4	0.208	1.14
18	16.16	3.00	218.45	0.263	1.04
19	10.16	2.00	120.3	0.262	1.13
20	10.16	2.00	103.1	0.203	0.968
21	16.16	3.00	198.35	0.212	0.946
22	4.16	1.25	72.45	0.329	1.46
23	10.16	1.75	141.7	0.447	1.52
24	10.16	1.75	123.35	0.363	1.32
25	16.16	2.75	204.9	0.293	1.07
26	10.16	2.00	123.6	0.285	1.16
27	16.16	2.50	238.6	0.425	1.37
28	4.16	1.25	82.1	0.414	1.66
29	10.16	1.75	133.8	0.410	1.44

TABLE 15 (continued)

RUN NO.	ECCENTRICITY	RUN DURATION (hr.)	TOTAL WEIGHT LOSS(mg)	FLOW VELOCITY (cm/sec)	k_c (cm/hr)
30	16.16	2.50	250.35	0.475	1.43
31	16.16	2.75	219.5	0.334	1.14
32	10.16	2.00	133.95	0.327	1.26
33	16.16	2.75	235.8	0.378	1.23
34	4.16	1.25	89.9	0.489	1.82
35	16.16	2.50	270.45	0.541	1.55
36	10.16	1.75	155.15	0.540	1.66
37	10.16	1.75	150.6	0.494	1.62
38	4.16	1.00	81.9	0.631	2.07
39	16.16	2.75	329.15	0.617	1.71
40	10.16	1.75	169.25	0.604	1.82
41	4.16	1.00	78.45	0.574	1.98
42	16.16	2.25	289.7	0.687	1.84
43	4.16	0.83	79.3	0.802	2.40
44	10.16	1.75	175.25	0.661	1.88
45	16.16	3.00	386.8	0.679	1.84
46	4.16	1.00	99.05	0.875	2.50
47	10.16	1.75	192.5	0.727	2.07
48	16.16	3.00	158.95	0	0.758
49	10.16	1.50	174.95	0.852	2.19
50	4.16	1.00	88.6	0.721	2.24
51	4.16	1.50	47.05	0	0.792
52	10.16	2.75	112.65	0	0.769
53	10.16	2.25	100.1	0.089	0.835
54	4.16	1.25	45.15	0.065	0.912
55	10.16	2.00	90.2	0.106	0.846
56	7.16	1.75	74.1	0.146	0.923
57	7.16	1.75	70.75	0.092	0.881
58	16.16	3.17	164.35	0.075	0.742
59	10.16	2.00	84.65	0.071	0.794
60	13.16	2.50	120.15	0.074	0.783

TABLE 15 (continued)

RUN NO.	ECCENTRICITY	RUN DURATION (hr.)	TOTAL WEIGHT LOSS(mg)	FLOW VELOCITY (cm/sec)	k_c (cm/hr)
61	7.16	1.75	73.25	0.059	0.912
62	16.16	3.00	156.9	0.035	0.748
63	13.16	2.50	134.35	0.146	0.876
64	13.16	2.50	121.55	0.045	0.792
65	13.16	2.50	128.35	0.117	0.837
66	7.16	1.75	72.7	0.035	0.905
67	10.16	2.00	95.4	0.044	0.895
68	7.16	1.75	72.2	0.120	0.899
69	13.16	2.50	120.25	0.098	0.784
70	16.16	3.00	164.35	0.053	0.783
71	7.16	1.75	84.7	0.232	1.06
72	13.16	2.50	152.15	0.236	0.992
73	7.16	1.75	82.5	0.187	1.03
74	13.16	2.50	143.75	0.192	0.937
75	7.16	1.50	119.1	0.459	1.73
76	13.16	2.25	204.7	0.455	1.48
77	7.16	1.75	105.55	0.292	1.31
78	13.16	2.75	217.85	0.370	1.29
79	7.16	1.75	118.9	0.367	1.48
80	13.16	2.50	176.95	0.296	1.15
81	13.16	2.50	161.7	0.258	1.05
82	13.16	2.25	219.2	0.498	1.59
83	13.16	2.50	185.6	0.326	1.21
84	7.16	1.75	110.1	0.327	1.37
85	13.16	2.50	213.45	0.417	1.39
86	7.16	1.75	128.2	0.407	1.60
87	7.16	1.75	147.7	0.512	1.84
88	13.16	2.50	257.15	0.552	1.68
89	13.16	2.50	302.4	0.728	1.97
90	7.16	1.75	186.5	0.754	2.32
91	13.16	2.50	287.15	0.635	1.87

TABLE 15 (continued)

RUN NO.	ECCENTRICITY	RUN DURATION (hr.)	TOTAL WEIGHT LOSS(mg)	FLOW VELOCITY (cm/sec)	k_c (cm/hr)
92	7.16	1.75	163.65	0.578	2.04
93	7.16	1.75	170.15	0.633	2.12
94	13.16	2.50	300.65	0.684	1.96
95	7.16	1.75	175.95	0.696	2.20
96	13.16	2.25	284.4	0.768	2.06
97	13.16	2.50	265.95	0.576	1.73
98	7.16	1.50	171.5	0.871	2.49
99	10.16	1.75	193.45	0.799	2.08
100	16.16	2.50	290.15	0.587	1.66
101	16.16	2.25	286.35	0.650	1.82
102	7.16	1.50	161.75	0.816	2.35
103	10.16	1.75	177.7	0.702	1.91
104	10.16	1.75	184.65	0.748	1.98
105	13.16	2.50	283.6	0.595	1.85
106	10.16	1.75	202.35	0.868	2.17
107	4.16	1.25	42.8	0.024	0.864
108	7.16	1.75	72.0	0.019	0.896
109	7.16	1.75	64.55	0	0.804
110	16.16	3.00	165.45	0.017	0.789
111	13.16	2.75	131.4	0	0.779
112	13.16	2.50	122.25	0.018	0.797
113	10.16	2.00	84.8	0.029	0.796
114	13.16	4.50	203.85	0	0.738
115	10.16	3.50	145.35	0	0.779
116	4.16	2.00	63.9	0	0.806
117	7.16	3.00	107.3	0	0.779

TABLE 16.

REYNOLDS NUMBERS.

RUN NO.	Re_1	Re_2	Re_3	Re_4	Re_5	Re_6	Re_7	Re_8
1	23.6	9.4	21.2	28.2	23.4	16.5	37.4	18.7
2	14.8	5.9	13.3	17.7	14.7	10.4	23.5	11.8
3	7.3	2.9	6.5	8.7	7.2	5.1	11.6	5.8
4	14.9	5.9	13.4	17.8	14.8	10.5	23.7	11.9
5	18.6	7.4	16.8	22.3	18.5	13.1	29.6	14.8
6	41.6	41.6	41.6	41.6	41.6	41.6	41.6	41.6
7	18.6	7.4	16.7	22.2	18.4	13.0	29.5	14.8
8	33.3	33.3	33.3	33.3	33.3	33.3	33.3	33.3
9	34.1	25.0	30.4	34.9	32.4	32.8	39.9	31.6
10	26.2	26.2	26.2	26.2	26.2	26.2	26.2	26.2
11	29.0	11.5	26.1	34.7	28.8	20.3	46.1	23.0
12	52.0	52.0	52.0	52.0	52.0	52.0	52.0	52.0
13	43.2	31.6	38.5	44.1	41.1	41.5	50.6	40.0
14	66.2	66.2	66.2	66.2	66.2	66.2	66.2	66.2
15	47.0	18.6	42.2	56.1	46.6	32.9	74.5	37.3
16	55.9	40.8	49.8	57.0	53.1	53.6	65.3	51.7
17	37.2	14.8	33.4	44.4	36.9	26.0	59.0	29.5
18	74.4	74.4	74.4	74.4	74.4	74.4	74.4	74.4
19	63.5	46.4	56.6	64.8	60.3	60.9	74.3	58.7
20	49.1	35.9	43.7	50.1	46.6	47.1	57.4	45.4
21	60.2	60.2	60.2	60.2	60.2	60.2	60.2	60.2
22	58.7	23.3	52.8	70.1	58.2	41.1	93.2	46.6
23	108	79.1	96.4	110	103	104	127	100
24	87.8	64.2	78.3	89.7	83.5	84.3	103	81.2
25	83.1	83.1	83.1	83.1	83.1	83.1	83.1	83.1
26	68.9	50.4	61.4	70.4	65.5	66.1	80.6	63.7
27	120	120	120	120	120	120	120	120
28	73.9	29.3	66.4	88.3	73.3	51.7	117	58.6
29	99.4	72.7	88.6	101	94.5	95.4	116	91.9

TABLE 16 (continued)

RUN NO.	Re_1	Re_2	Re_3	Re_4	Re_5	Re_6	Re_7	Re_8
30	135	135	135	135	135	135	135	135
31	94.7	94.7	94.7	94.7	94.7	94.7	94.7	94.7
32	79.2	57.9	70.5	80.8	75.2	75.9	92.6	73.2
33	107	107	107	107	107	107	107	107
34	87.2	34.6	78.5	104	86.5	61.1	138	69.2
35	153	153	153	153	153	153	153	153
36	131	95.7	117	134	124	126	153	121
37	120	87.5	107	122	114	115	140	111
38	113	44.7	101	134	112	78.8	179	89.3
39	175	175	175	175	175	175	175	175
40	146	107	130	149	139	140	171	135
41	102	40.6	92.1	122	102	71.7	163	81.3
42	195	195	195	195	195	195	195	195
43	143	56.8	129	171	142	100	227	114
44	160	117	143	164	152	154	187	148
45	192	192	192	192	192	192	192	192
46	156	62.0	141	187	155	109	248	124
47	176	129	157	180	167	169	206	163
48	0	0	0	0	0	0	0	0
49	201	147	180	206	191	193	236	186
50	129	51.1	116	154	128	90.2	204	102
51	0	0	0	0	0	0	0	0
52	0	0	0	0	0	0	0	0
53	21.6	15.8	19.3	22.1	20.5	20.7	25.3	20.0
54	11.6	4.6	10.5	13.9	11.6	8.2	18.5	9.2
55	25.6	18.7	22.8	26.2	24.4	24.6	30.0	23.7
56	31.4	18.1	27.1	33.5	29.7	27.5	41.3	27.3
57	19.7	11.4	17.0	21.0	18.7	17.3	26.0	17.2
58	21.2	21.2	21.2	21.2	21.2	21.2	21.2	21.2
59	17.1	12.5	15.3	17.5	16.3	16.4	20.0	15.8
60	19.6	17.1	18.5	19.7	19.1	19.5	21.1	19.0
61	12.6	7.3	10.9	13.5	11.9	11.1	16.6	11.0

TABLE 16 (continued)

RUN NO.	Re_1	Re_2	Re_3	Re_4	Re_5	Re_6	Re_7	Re_8
62	10.0	10.0	10.0	10.0	10.0	10.0	10.0	10.0
63	38.7	33.7	36.1	38.9	37.6	38.4	41.5	37.4
64	11.9	10.4	11.2	12.0	11.6	11.8	12.8	11.5
65	31.0	27.0	29.2	31.1	30.1	30.8	33.2	30.0
66	7.4	4.3	6.4	7.9	7.1	6.5	9.8	6.5
67	10.7	7.8	9.6	11.0	10.2	10.3	12.5	9.9
68	25.8	14.9	22.3	27.5	24.4	22.6	34.0	22.5
69	25.9	22.5	24.3	26.0	25.1	25.7	27.7	25.0
70	14.9	14.9	14.9	14.9	14.9	14.9	14.9	14.9
71	49.9	28.8	43.1	53.3	47.3	43.8	65.8	43.5
72	62.4	54.3	58.7	62.6	60.6	61.9	66.8	60.3
73	40.3	23.2	34.9	43.0	38.2	35.4	53.1	35.1
74	50.8	44.2	47.8	51.0	49.3	50.4	54.4	49.1
75	98.7	56.9	85.3	105	93.4	86.6	130	86.0
76	120	105	113	121	117	119	129	116
77	62.8	36.2	54.3	67.0	59.4	55.1	82.7	54.7
78	97.8	85.1	92.0	98.2	95.0	97.0	105	94.5
79	78.9	45.5	68.2	84.2	74.7	69.3	104	68.7
80	78.2	68.1	73.5	78.5	75.9	77.5	83.8	75.5
81	68.1	59.3	64.1	68.4	66.2	67.6	73.0	65.8
82	132	115	124	132	128	131	141	127
83	86.3	75.2	81.2	86.7	83.8	85.6	92.5	83.4
84	70.3	40.5	60.8	75.1	66.6	61.8	92.7	61.3
85	110	96.0	104	111	107	109	118	106
86	87.6	50.5	75.8	93.5	83.0	77.0	115	76.4
87	110	63.4	95.2	117	104	96.7	145	95.9
88	146	127	137	47	142	145	157	141
89	193	168	181	193	187	191	206	186
90	162	93.5	140	173	154	142	214	141
91	168	146	158	169	163	167	180	162
92	124	71.7	107	133	118	109	164	108
93	136	78.4	118	145	129	120	179	119

TABLE 16 (continued)

RUN NO.	Re_1	Re_2	Re_3	Re_4	Re_5	Re_6	Re_7	Re_8
94	181	157	170	182	176	179	194	175
95	150	86.3	129	160	142	131	197	130
96	203	177	191	204	197	201	218	196
97	152	133	143	153	148	151	163	147
98	187	108	162	200	177	165	247	163
99	194	141	172	198	184	186	226	179
100	166	166	166	166	166	166	166	166
101	184	184	184	184	184	184	184	184
102	176	101	152	187	166	154	231	153
103	170	124	152	174	162	163	199	157
104	181	133	162	185	172	174	212	168
105	157	137	148	158	153	156	169	152
106	210	154	187	215	200	202	246	194
107	4.3	1.7	3.8	5.1	4.2	3.0	6.8	3.4
108	4.2	2.4	3.6	4.4	3.9	3.7	5.5	3.6
109	0	0	0	0	0	0	0	0
110	4.8	4.8	4.8	4.8	4.8	4.8	4.8	4.8
111	0	0	0	0	0	0	0	0
112	4.7	4.1	4.5	4.8	4.6	4.7	5.1	4.6
113	7.1	5.2	6.3	7.2	6.7	6.8	8.3	6.5
114	0	0	0	0	0	0	0	0
115	0	0	0	0	0	0	0	0
116	0	0	0	0	0	0	0	0
117	0	0	0	0	0	0	0	0

TABLE 17.

SHERWOOD NUMBERS.

RUN NO.	Sh_1	Sh_2	Sh_3	Sh_4	Sh_5	Sh_6	Sh_7	Sh_8
1	52.7	20.9	47.4	63.0	52.3	36.9	83.7	41.9
2	47.8	19.0	43.0	57.1	47.4	33.5	75.8	37.9
3	50.8	20.2	45.7	60.7	50.4	35.6	80.7	40.3
4	50.4	20.0	45.3	60.2	50.0	35.3	80.0	40.0
5	48.2	19.1	43.3	57.5	47.8	33.7	76.5	38.2
6	65.7	65.7	65.7	65.7	65.7	65.7	65.7	65.7
7	47.5	18.9	42.7	56.8	47.1	33.3	75.4	37.7
8	64.6	64.6	64.6	64.6	64.6	64.6	64.6	64.6
9	57.7	42.2	51.4	58.9	54.8	55.3	67.5	53.3
10	60.6	60.6	60.6	60.6	60.6	60.6	60.6	60.6
11	53.0	21.0	47.7	63.3	52.6	37.1	84.1	42.1
12	69.9	69.9	69.9	69.9	69.9	69.9	69.9	69.9
13	59.5	43.5	53.0	60.7	56.5	57.1	69.6	55.0
14	76.4	76.4	76.4	76.4	76.4	76.4	76.4	76.4
15	64.3	25.5	57.8	76.9	63.8	45.0	102	51.0
16	71.9	52.5	64.1	73.4	68.3	69.0	84.1	66.5
17	56.8	22.5	51.1	67.8	56.3	39.8	90.1	45.1
18	82.4	82.4	82.4	82.4	82.4	82.4	82.4	82.4
19	76.4	55.8	68.1	78.0	72.6	73.3	89.3	70.6
20	65.5	47.8	58.3	66.8	62.2	62.8	76.6	60.5
21	74.8	74.8	74.8	74.8	74.8	74.8	74.8	74.8
22	72.9	28.9	65.6	87.1	72.4	51.1	116	57.9
23	103	75.2	91.6	105	97.7	98.6	120	95.1
24	89.5	65.4	79.8	91.4	85.1	85.9	105	82.8
25	84.3	84.3	84.3	84.3	84.3	84.3	84.3	84.3
26	78.5	57.4	69.9	80.1	74.6	75.3	91.8	72.6
27	108	108	108	108	108	108	108	108
28	82.6	32.8	74.3	98.7	82.0	57.9	131	65.6
29	97.1	71.0	86.5	99.1	92.3	93.1	114	89.8
30	113	113	113	113	113	113	113	113

TABLE 17 (continued)

RUN NO.	Sh_1	Sh_2	Sh_3	Sh_4	Sh_5	Sh_6	Sh_7	Sh_8
31	90.3	90.3	90.3	90.3	90.3	90.3	90.3	90.3
32	85.0	62.2	75.8	86.8	80.8	81.6	99.5	78.6
33	97.0	97.0	97.0	97.0	97.0	97.0	97.0	97.0
34	90.5	35.9	81.4	108	89.8	63.4	144	71.8
35	122	122	122	122	122	122	122	122
36	113	82.3	100	115	107	108	132	104
37	109	79.9	97.4	112	104	105	128	101
38	103	40.9	92.7	123	102	72.2	164	81.8
39	135	135	135	135	135	135	135	135
40	123	89.8	109	125	117	118	144	114
41	98.7	39.2	88.8	118	97.9	69.1	157	78.3
42	146	146	146	146	146	146	146	146
43	120	47.5	108	143	119	83.9	190	95.0
44	127	93.0	113	130	121	122	149	118
45	146	146	146	146	146	146	146	146
46	125	49.5	112	149	124	87.3	198	98.9
47	140	102	124	143	133	134	163	129
48	60.0	60.0	60.0	60.0	60.0	60.0	60.0	60.0
49	148	108	132	151	141	142	173	137
50	111	44.2	100	133	111	78.1	177	88.5
51	39.5	15.7	35.5	47.2	39.2	27.6	62.6	31.3
52	52.0	38.0	46.4	53.1	49.4	49.9	60.8	48.1
53	56.5	41.3	50.3	57.7	53.7	54.2	66.1	52.2
54	45.4	18.0	40.9	54.3	45.1	31.8	72.1	36.1
55	57.3	41.9	51.0	58.5	54.4	54.9	67.0	53.0
56	55.4	31.9	47.9	59.1	52.5	48.7	73.0	48.3
57	52.9	30.5	45.8	56.5	50.1	46.5	69.7	46.1
58	58.7	58.7	58.7	58.7	58.7	58.7	58.7	58.7
59	53.7	39.3	47.9	54.9	51.1	51.6	62.9	49.7
60	57.8	50.4	54.4	58.1	56.2	57.4	62.0	55.9
61	54.8	31.6	47.4	58.5	51.9	48.1	72.2	47.7

TABLE 17 (continued)

RUN NO.	Sh_1	Sh_2	Sh_3	Sh_4	Sh_5	Sh_6	Sh_7	Sh_8
62	59.2	59.2	59.2	59.2	59.2	59.2	59.2	59.2
63	64.7	56.3	60.8	64.9	62.8	64.2	69.3	62.5
64	58.5	50.9	55.0	58.7	56.8	58.0	62.7	56.5
65	61.8	53.8	58.1	62.0	60.0	61.3	66.2	59.7
66	54.4	31.3	47.0	58.0	51.5	47.8	71.6	47.4
67	60.6	44.3	54.0	61.8	57.6	58.1	70.8	56.0
68	54.0	31.1	46.7	57.6	51.1	47.4	71.1	47.1
69	57.9	50.4	54.4	58.1	56.2	57.4	62.0	55.9
70	62.0	62.0	62.0	62.0	62.0	62.0	62.0	62.0
71	63.4	36.5	54.8	67.6	60.0	55.6	83.5	55.2
72	73.2	63.8	66.9	73.5	71.1	72.7	78.5	70.7
73	61.7	35.6	53.3	65.9	58.4	54.2	81.3	53.8
74	69.2	60.2	65.1	69.5	67.2	68.6	74.1	66.8
75	104	59.9	89.9	111	98.4	91.3	137	90.6
76	109	95.3	103	110	106	109	117	106
77	79.0	45.5	68.3	84.3	74.8	69.3	104	68.8
78	95.3	83.0	89.6	95.7	92.6	94.6	102	92.1
79	88.9	51.3	76.9	94.9	84.2	78.1	117	77.5
80	85.2	74.2	80.1	85.5	82.7	84.5	91.3	82.3
81	77.8	67.8	73.2	78.1	75.6	77.2	83.4	75.2
82	117	102	110	118	114	116	126	113
83	89.3	77.8	84.0	89.7	86.8	88.7	95.7	86.3
84	82.4	47.5	71.2	87.9	78.0	72.3	108	71.8
85	103	89.4	96.6	103	99.8	102	110	99.2
86	95.9	55.3	82.9	102	90.8	84.2	126	83.5
87	110	63.7	95.5	118	105	97.0	146	96.3
88	124	108	116	124	120	123	133	120
89	146	127	137	146	141	144	156	141
90	140	80.4	121	149	132	123	184	122
91	138	120	130	139	134	137	143	133
92	122	70.5	106	131	116	108	161	107
93	127	73.4	110	136	121	112	168	111
94	145	126	136	145	141	144	155	140

TABLE 17 (continued)

RUN NO.	Sh_1	Sh_2	Sh_3	Sh_4	Sh_5	Sh_6	Sh_7	Sh_8
95	132	76.3	114	141	125	116	174	115
96	152	132	143	153	148	151	163	147
97	128	111	120	129	124	127	137	124
98	150	86.3	129	160	142	131	197	130
99	140	103	125	143	133	135	164	130
100	131	131	131	131	131	131	131	131
101	144	144	144	144	144	144	144	144
102	141	81.4	122	151	134	124	186	123
103	129	94.3	115	132	123	124	151	119
104	134	97.9	119	137	127	129	157	124
105	136	119	128	137	133	135	146	132
106	147	107	131	150	140	141	172	136
107	43.1	17.1	38.7	51.5	42.7	30.2	68.4	34.2
108	53.9	31.0	46.6	57.5	51.0	47.3	70.9	46.9
109	48.3	27.8	41.7	51.5	45.7	42.4	63.6	42.1
110	62.4	62.4	62.4	62.4	62.4	62.4	62.4	62.4
111	57.5	50.1	54.1	57.7	55.8	57.0	61.6	55.5
112	58.8	51.2	55.3	59.1	57.1	58.4	63.1	56.8
113	53.8	39.4	48.0	55.0	51.2	51.7	63.0	49.8
114	54.5	47.5	51.3	54.7	52.9	54.1	58.4	52.7
115	52.7	38.5	47.0	53.8	50.1	50.6	61.7	48.8
116	40.2	16.0	36.2	48.0	39.9	28.2	63.8	31.9
117	46.8	27.0	40.5	50.0	44.3	41.1	61.7	40.8

TABLE 18.

SHERWOOD NUMBERS BASED ON SURFACE AREA OF SPHERE OF SAME VOLUME.

RUN NO.	Sh_{1f}	RUN NO.	Sh_{1f}	RUN NO.	Sh_{1f}	RUN NO.	Sh_{1f}
1	75.3	31	90.3	61	62.4	91	139
2	68.2	32	88.6	62	59.2	92	139
3	72.6	33	97.0	63	65.2	93	145
4	71.9	34	129	64	59.0	94	146
5	68.8	35	122	65	62.3	95	151
6	65.7	36	117	66	61.9	96	153
7	67.8	37	114	67	63.1	97	129
8	64.6	38	147	68	61.5	98	170
9	60.1	39	135	69	58.3	99	146
10	60.6	40	128	70	62.0	100	131
11	75.7	41	141	71	72.1	101	144
12	69.9	42	146	72	73.8	102	161
13	62.0	43	171	73	70.3	103	134
14	76.4	44	133	74	69.7	104	140
15	91.8	45	146	75	118	105	138
16	74.9	46	178	76	110	106	153
17	81.1	47	146	77	89.9	107	61.5
18	82.4	48	60.0	78	96.1	108	61.3
19	79.6	49	154	79	101	109	55.0
20	68.2	50	159	80	85.8	110	62.4
21	74.8	51	56.3	81	78.4	111	57.9
22	104	52	54.2	82	118	112	59.3
23	107	53	58.9	83	90.0	113	56.1
24	93.3	54	64.9	84	93.8	114	54.9
25	84.3	55	59.7	85	104	115	55.0
26	81.8	56	63.1	86	109	116	57.4
27	108	57	60.3	87	126	117	53.3
28	118	58	58.7	88	125		
29	101	59	56.0	89	147		
30	113	60	58.3	90	159		

TABLE 19.

GRASHOF NUMBERS (25.0°C.)

	e=4.16	e=7.16	e=10.16	e=13.16	e=16.16
$Gr_1 \times 10^{-4}$	2.96	5.18	7.40	9.62	11.8
$Gr_2 \times 10^{-4}$	0.185	0.991	2.89	6.35	11.8
$Gr_3 \times 10^{-4}$	2.15	3.35	5.24	8.00	11.8
$Gr_4 \times 10^{-4}$	5.05	6.29	7.87	9.73	11.8
$Gr_5 \times 10^{-4}$	2.89	4.39	6.35	8.81	11.8
$Gr_6 \times 10^{-4}$	1.02	3.51	6.53	9.39	11.8
$Gr_7 \times 10^{-4}$	11.8	11.8	11.8	11.8	11.8
$Gr_8 \times 10^{-4}$	1.48	3.43	5.85	8.67	11.8

TABLE 20.

PRODUCT OF GRASHOF AND SCHMIDT NUMBERS (25.0°C.)

	e=4.16	e=7.16	e=10.16	e=13.16	e=16.16
$Gr_1 x Sc x 10^{-7}$	2.97	5.21	7.44	9.67	11.9
$Gr_2 x Sc x 10^{-7}$	0.186	0.996	2.90	6.38	11.9
$Gr_3 x Sc x 10^{-7}$	2.16	3.36	5.26	8.04	11.9
$Gr_4 x Sc x 10^{-7}$	5.07	6.33	7.91	9.78	11.9
$Gr_5 x Sc x 10^{-7}$	2.90	4.42	6.38	8.86	11.9
$Gr_6 x Sc x 10^{-7}$	1.02	3.53	6.57	9.44	11.9
$Gr_7 x Sc x 10^{-7}$	11.9	11.9	11.9	11.9	11.9
$Gr_8 x Sc x 10^{-7}$	1.49	3.44	5.88	8.71	11.9

TABLE 21.

GRASHOF NUMBERS DIVIDED BY REYNOLDS NUMBERS SQUARED.

RUN NO.	$\frac{Gr_1}{Re_1^2}$	$\frac{Gr_2}{Re_2^2}$	$\frac{Gr_3}{Re_3^2}$	$\frac{Gr_4}{Re_4^2}$	$\frac{Gr_5}{Re_5^2}$	$\frac{Gr_6}{Re_6^2}$	$\frac{Gr_7}{Re_7^2}$	$\frac{Gr_8}{Re_8^2}$
1	53.2	21.1	47.8	63.5	52.7	37.2	84.4	42.2
2	134	53.4	121	161	133	94.2	213	107
3	559	222	502	668	554	391	887	443
4	133	52.7	119	159	132	92.9	211	105
5	85.2	33.8	76.6	102	84.5	59.7	135	67.6
6	68.3	68.3	68.3	68.3	68.3	68.3	68.3	68.3
7	85.6	34.0	77.0	102	85.0	60.0	134	68.0
8	107	107	107	107	107	107	107	107
9	63.5	46.4	56.6	64.8	60.3	60.9	74.2	58.7
10	173	173	173	173	173	173	173	173
11	35.1	13.9	31.6	42.0	34.9	24.6	55.8	27.9
12	43.7	43.7	43.7	43.7	43.7	43.7	43.7	43.7
13	39.6	28.9	35.3	40.4	37.6	38.0	46.3	36.6
14	27.0	27.0	27.0	27.0	27.0	27.0	27.0	27.0
15	13.4	5.33	12.1	16.0	13.3	9.40	21.3	10.7
16	23.7	17.3	21.1	24.2	22.5	22.7	27.7	21.9
17	21.4	8.50	19.3	25.6	21.2	15.0	34.0	17.0
18	21.4	21.4	21.4	21.4	21.4	21.4	21.4	21.4
19	18.3	13.4	16.3	18.7	17.4	17.6	21.5	17.0
20	30.7	22.4	27.4	21.3	29.2	29.5	35.9	28.4
21	32.7	32.7	32.7	32.7	32.7	32.7	32.7	32.7
22	8.59	3.41	7.72	10.3	8.52	6.01	13.6	6.82
23	6.32	4.62	5.63	6.45	6.00	6.06	7.39	5.84
24	9.59	7.01	8.54	9.79	9.11	9.20	11.2	8.87
25	17.1	17.1	17.1	17.1	17.1	17.1	17.1	17.1
26	15.6	11.4	13.9	15.9	14.8	14.9	18.2	14.4
27	8.18	8.18	8.18	8.18	8.18	8.18	8.18	8.18
28	5.42	2.15	4.88	6.48	5.38	3.80	8.61	4.30
29	7.49	5.47	6.67	7.64	7.11	7.18	8.76	6.92
30	6.53	6.53	6.53	6.53	6.53	6.53	6.53	6.53

TABLE 21 (continued)

RUN NO.	$\frac{Gr_1}{Re_1^2}$	$\frac{Gr_2}{Re_2^2}$	$\frac{Gr_3}{Re_3^2}$	$\frac{Gr_4}{Re_4^2}$	$\frac{Gr_5}{Re_5^2}$	$\frac{Gr_6}{Re_6^2}$	$\frac{Gr_7}{Re_7^2}$	$\frac{Gr_8}{Re_8^2}$
31	13.2	13.2	13.2	13.2	13.2	13.2	13.2	13.2
32	11.8	8.63	10.5	12.1	11.2	11.3	13.8	10.9
33	10.3	10.3	10.3	10.3	10.3	10.3	10.3	10.3
34	3.89	1.54	3.50	4.65	3.86	2.72	6.17	3.09
35	5.03	5.03	5.03	5.03	5.03	5.03	5.03	5.03
36	4.32	3.16	3.85	4.41	4.10	4.14	5.05	3.99
37	5.17	3.78	4.60	5.27	4.91	4.96	6.04	4.78
38	2.34	0.927	2.10	2.79	2.32	1.64	3.71	1.85
39	3.87	3.87	3.87	3.87	3.87	3.87	3.87	3.87
40	3.46	2.53	3.08	3.53	3.29	3.32	4.04	3.20
41	2.82	1.12	2.54	3.37	2.80	1.98	4.48	2.24
42	3.13	3.13	3.13	3.13	3.13	3.13	3.13	3.13
43	1.44	0.573	1.30	1.72	1.43	1.01	2.29	1.15
44	2.88	2.11	2.57	2.94	2.74	2.77	3.37	2.67
45	3.20	3.20	3.20	3.20	3.20	3.20	3.20	3.20
46	1.21	0.481	1.09	1.45	1.20	0.849	1.92	0.96
47	2.39	1.74	2.13	2.44	2.27	2.29	2.79	2.21
48	*	*	*	*	*	*	*	*
49	1.82	1.33	1.62	1.86	1.73	1.75	2.13	1.68
50	1.79	0.709	1.61	2.13	1.77	1.25	2.83	1.42
51	*	*	*	*	*	*	*	*
52	*	*	*	*	*	*	*	*
53	158	116	141	162	151	152	185	146
54	218	86.5	196	261	216	153	346	173
55	113	82.3	100	115	107	108	132	104
56	52.7	30.4	45.5	56.2	49.9	46.3	69.4	45.9
57	133	76.8	115	142	126	117	176	116
58	263	263	263	263	263	263	263	263
59	252	184	225	258	240	242	295	233
60	249	217	234	250	242	247	267	241
61	326	188	281	347	308	286	429	284
62	1180	1180	1180	1180	1180	1180	1180	1180

TABLE 21 (continued)

RUN NO.	$\frac{Gr_1}{Re_1^2}$	$\frac{Gr_2}{Re_2^2}$	$\frac{Gr_3}{Re_3^2}$	$\frac{Gr_4}{Re_4^2}$	$\frac{Gr_5}{Re_5^2}$	$\frac{Gr_6}{Re_6^2}$	$\frac{Gr_7}{Re_7^2}$	$\frac{Gr_8}{Re_8^2}$
63	64.1	55.8	60.3	64.4	62.3	63.6	68.7	61.9
64	678	590	638	681	658	673	726	655
65	100	87.1	94.1	100	97.2	99.3	107	96.6
66	933	538	807	996	884	820	1230	813
67	643	470	573	656	611	616	752	594
68	77.9	44.9	67.3	83.7	73.7	68.4	103	67.8
69	144	125	135	144	140	143	154	139
70	534	534	534	534	534	534	534	534
71	20.8	12.0	18.0	22.2	19.7	18.3	27.4	18.1
72	24.7	21.5	23.2	24.8	24.0	24.5	26.5	23.9
73	31.8	18.4	27.5	34.0	30.1	28.0	41.9	27.7
74	37.3	32.4	35.0	37.4	36.2	37.0	39.9	36.0
75	5.32	3.07	4.60	5.68	5.04	4.67	7.01	4.64
76	6.65	5.79	6.25	6.67	6.46	6.59	7.12	6.42
77	13.1	7.58	11.4	14.0	12.4	11.5	17.3	11.5
78	10.1	8.76	9.46	10.1	9.77	9.98	10.8	9.71
79	8.32	4.79	7.19	8.88	7.87	7.30	11.0	7.25
80	15.7	13.7	14.8	15.8	15.3	15.6	16.9	15.2
81	20.7	18.0	19.5	20.8	20.1	20.5	22.2	20.0
82	5.54	4.82	5.21	5.56	5.38	5.50	5.94	5.35
83	12.9	11.2	12.1	13.0	12.5	12.8	13.8	12.5
84	10.5	6.03	9.05	11.2	9.91	9.19	13.8	9.12
85	7.91	6.89	7.44	7.95	7.69	7.85	8.48	7.64
86	6.74	3.89	5.83	7.20	6.38	5.92	8.88	5.88
87	4.27	2.46	3.69	4.56	4.04	3.75	5.63	3.72
88	4.51	3.92	4.24	4.52	4.38	4.47	4.83	4.35
89	2.59	2.26	2.44	2.60	2.52	2.57	2.78	2.51
90	1.97	1.13	1.70	2.10	1.86	1.73	2.59	1.71
91	3.41	2.97	3.20	3.42	3.31	3.38	3.65	3.29
92	3.35	1.93	2.90	3.57	3.17	2.94	4.41	2.92
93	2.80	1.61	2.42	2.98	2.65	2.45	3.68	2.44

TABLE 21 (continued)

RUN NO.	$\frac{Gr_1}{Re_1^2}$	$\frac{Gr_2}{Re_2^2}$	$\frac{Gr_3}{Re_3^2}$	$\frac{Gr_4}{Re_4^2}$	$\frac{Gr_5}{Re_5^2}$	$\frac{Gr_6}{Re_6^2}$	$\frac{Gr_7}{Re_7^2}$	$\frac{Gr_8}{Re_8^2}$
94	2.94	2.56	2.77	2.95	2.86	2.92	3.15	2.84
95	2.31	1.33	2.00	2.47	2.19	2.03	3.04	2.01
96	2.33	2.03	2.20	2.34	2.27	2.32	2.50	2.25
97	4.15	3.61	3.90	4.17	4.03	4.12	4.45	4.01
98	1.47	0.849	1.27	1.57	1.40	1.29	1.94	1.28
99	1.97	1.44	1.76	2.02	1.88	1.89	2.31	1.83
100	4.28	4.28	4.28	4.28	4.28	4.28	4.28	4.28
101	3.49	3.49	3.49	3.49	3.49	3.49	3.49	3.49
102	1.68	0.968	1.45	1.79	1.59	1.47	2.21	1.46
103	2.56	1.87	2.28	2.61	2.43	2.45	2.99	2.37
104	2.25	1.64	2.01	2.30	2.14	2.16	2.63	2.08
105	3.88	3.38	3.65	3.90	3.77	3.85	4.16	3.75
106	1.67	1.22	1.49	1.71	1.59	1.61	1.96	1.55
107	1630	646	1460	1940	1610	1140	2580	1290
108	2990	1720	2590	3190	2830	2630	3940	2610
109	*	*	*	*	*	*	*	*
110	5240	5240	5240	5240	5240	5240	5240	5240
111	*	*	*	*	*	*	*	*
112	4290	3740	4040	4310	4170	4260	4600	4150
113	1470	1080	1310	1500	1400	1410	1720	1360
114	*	*	*	*	*	*	*	*
115	*	*	*	*	*	*	*	*
116	*	*	*	*	*	*	*	*
117	*	*	*	*	*	*	*	*

* = infinity (free convection runs)

APPENDIX 2.

ORIFICE PLATE CALIBRATION CONSTANTS.

TABLE 22

Orifice Diameter inches	CALIBRATION CONSTANTS			
	C_7	C_8	C_9	C_{10}
0.15	-0.001	-0.015	0.393	-0.013
0.33	-0.000	-0.006	2.052	-0.033
0.44	-0.007	0.139	2.796	1.598
0.60	-0.005	0.058	6.987	0.141
0.75	-0.024	0.327	11.366	3.112

BIBLIOGRAPHY.

1. Hughes, R.R., and Gilliland, E.R., Chem.Eng. Prog., V48, 497, (1952).

2. Klee, A.J., and Treybal, R.E. A.I.Ch.E.Journal, V2, 444, (1956).

3. Lewis, J.B., Jones, I., and Pratt, H.R.C. Trans.Inst.Chem.Engrs., V29, 126, (1951)

4. Weaver, R.E.C., Lapidus, L., and Elgin, J.C. A.I.Ch.E.Journal, V5, 533, (1959).

5. Hu, S., and Kintner, R.C. A.I.Ch.E.Journal, V1, 42, (1955).

6. Licht, W., and Narasimhamarty, G.S.R. A.I.Ch.E.Journal, V1, 366, (1955).

7. Keith, F.W.Jr., and Hixson, A.N. Ind.Eng.Chem., V47, 258, (1955).

8. Elzinga, E.R.Jr., and Banchero, J.T. A.I.Ch.E.Journal, V7, 394, (1961).

9. Skelland, A.H.P., and Cornish, A.R.H. A.I.Ch.E.Journal, V9, 73, (1963).

10. Beg, S.A. Ph.D.Thesis, Imperial College, London (1966)

11. Sandoval, A.H. M.Sc.Thesis, Imperial College, London (1965).

12. Lewis, W.K. Ind.Eng.Chem., V8, 825, (1916).

13. Lewis, W.K., and Whitman, W.G. Ind.Eng.Chem., V16, 1215, (1924).

14. Higbie, R. Trans.Amer.Inst.Chem.Engrs., V.31, 365, (1935).

15. Dankwerts, P.V. Ind.Eng.Chem., V43, 1460, (1951).

16. Toor, H.L., and Marchello, J.M.
A.I.Ch.E.Journal, V4, 97, (1958).

17. Frossling, N. Gerlands.Beitr.Geophys., V52, 170, (1938).

18. Langmuir, I. Phys.Rev., V12(2), 368, (1918).

19. Pohlhausen, E. Z.angew.Math.Mech., V1, 115, (1921).

20. Kroujiline, G. Tech.Phys.(U.S.S.R.), V8, 123, (1938).

21. Frossling, N. Lunds Asskr.N.F., V36, No.4, (1940).

22. Boltze, E. Thesis, Gottingen, (1908).

23. Garner, F.H., and Grafton, R.W.
Proc.Roy.Soc., A224, 64, (1954).

24. Garner, F.H., and Keey, R.B.
Chem.Eng.Science, V9, 119, (1958).

25. Krischer, O., and Loos, G. Chem.Ing.Tech., V30, 31, 69, (1958).

26. Steinberger, R.L., and Treybal, R.E.
A.I.Ch.E.Journal, V6, 227, (1960).

27. Vyrubov, D.N. J.Tech.Phys. Moscow, V9, 1923, (1939).
Canadian Defence Research Board Translation Sept. (1949).

28. Linton, W.H.Jr., and Sherwood, T.K.
Chem.Eng.Prog., V46, 258, (1950).

29. Maisel, D.S., and Sherwood, T.K.
Chem.Eng.Prog., V46, 172, (1950).

30. Ranz, W.E., and Marshall, W.R.
Chem.Eng.Prog., V48, 141, 173, (1952).

31. Axel'rud, G.A. Zh.Prkl.Khim.Leningrad, V27, 1446, (1953).

32. Garner, F.H., and Suckling, R.D.
A.I.Ch.E.Journal, V4, 114, (1958).

33. Steele, L.R., and Geankoplis, C.J.
A.I.Ch.E.Journal, V5, 178, (1959).

34. Linton, M., and Sutherland, K.L.
Chem.Eng.Science, V12, 214, (1960).

35. Pasternak, I.S., and Gauvin, W.H.
A.I.Ch.E.Journal, V7, 254, (1961).

36. Evonchides, S., and Thodos, G.
A.I.Ch.E.Journal, V7, 78, (1961).

37. Yen, Y.C., and Thodos, G.
A.I.Ch.E.Journal, V8, 34, (1962).

38. Rowe, P.N., Claxton, K.T., and Lewis, J.B.
Trans.Inst.Chem.Engrs, V43, 14,(1965).

39. Friedlander, S.K. A.I.Ch.E.Journal, V3, 43, (1957).

40. Tomotika, S., and Aoi, T.
Quart.J.Mech.Appl.Math., V3, 140, (1950).

41. Friedlander, S.K. A.I.Ch.E.Journal, V7, 347, (1961).

42. Yuge, T. Rep.Inst.High Speed Mech., Tohoku Univ., V6, 143, (1956).

43. Mathers, W.G., Madden, A.J., and Piret, E.
Ind.Eng.Chem., V49, 961, (1957).

44. Garner, F.H., and Keey, R.B.
Chem.Eng.Science, V9, 218, (1958).

45. King, W.J. Mech.Eng., V54, 347, (1932).

46. Saunders, O.A. Proc.Roy.Soc., A172, 55, (1939).

47. Garner, F.H., and Hoffman , J.M.
A.I.Ch.E.Journal, V7, 48, (1961).

48. Wagner, C. Journal Phys.Colloid Chem., V53, 1030, (1949).

49. Krischer, O. Die wissenschaftlichen Grundlagen der Trocknungstechnik
Springer-Verlag, Berlin (1956) p.130.

50. Kramers, H.A. Physica, V12, 61, (1946).

51. Houghton, H.G. Physics, V4, 419, (1933).

52. Powell, R.W. Trans.Inst.Chem.Engrs., V18, 36, (1940)

53. Acrivos, A. A.I.Ch.E.Journal, V4, 285, (1958).

54. Sparrow, E.M., and Gregg, E.L.
Journal App.Mech., V26, 133, (1959).

55. Sparrow, E.M., Eichhorn, R., and Gregg, E.L.
Phys.Fluids, V2, 319, (1959).

56. Van der Hegge Zijnen, B.G.
App.Sci.Res., A6, 129, (1956).

57. Yuge, T. Trans.Am.Soc.Mech.Engrs., C82, 214, (1960).

58. Allander, C.G. Kungel, Techniska Hogskalans Handlinger, Nr.70, (1953).

59. Yamagata, K. Trans.Soc.Mech.Engrs., (Japan), V9; No.37, 132, (1943).

60. Pei, D.C.T., A.I.Ch.E.Symp.Series 59, V61, 57,(1965)

61. Happel, J., and Brenner, H.,
"Low Reynolds Number Hydrodynamics",
Prentice-Hall, N.J. (1965).

62. Bird, R., Stewart, W., and Lightfoot, E.
"Notes on Transport Phenomena" Chapman & Hall, London, (1958).

63. Warshay, M., Bogusz, E., Johnson, M., and Kintner, R.C.
Can.Journ.Chem.Eng., V37, 29, (1959).

64. Pasternak, I.S., and Gauvin, W.H.
Can.Journ.Chem.Eng., V38, 35, (1960).

65. Tsoubouchi, T., and Sato, S.
Chem.Eng.Prog.Symp.Series No.30, V56, 269, (1960).

66. Williams, G.C. Sc.D. Thesis, M.I.T. (1942).

67. Brown, G.G., and asscoiates.
"Unit Operations" Wiley & Sons Inc. New York (1950).

68. Uno, S., and Kintner, R.C.
A.I.Ch.E.Journal, V2, 420, (1956).

69. Strom, J.R., and Kintner, R.C.
A.I.Ch.E.Journal, V4, 153, (1958).

70. Newton, I. "Mathematica Principa", Univ.California Press, 1934, p.348.

71. Fagan, A.M., and Happel, J.
A.I.Ch.E.Journal, V6, 55, (1960).

72. Arthur, J.A., Linnett, J.W., Rayner, Mrs.E.J., and Sington, E.P.C. Trans.Faraday Soc., V46, 270, (1950).

73. Muskat, M. "Flow of Homogeneous Fluids Through Porous Media" McGraw-Hill, New York, (1937), p.14.

74. Lemich, R., and Levy, M.R.
A.I.Ch.E.Journal, V7, 240, (1961).

75. "Handbook of Chemistry and Physics" 39th Ed.
Chemical Rubber Publishing Co. London (1957),p.791

76. Holder, D.W., and North, L.J.
Notes on Applied Science No.31 (Schlieren Methods) H.M.S.O. (1963).

77. Stanton, T.E. Proc.Roy.Soc., A85, 366, (1911).

78. Stanton, T.E. Proc.Roy.Soc., A97, 413, (1920).

79. Barker, M. Proc.Roy.Soc., A101, 435, (1922).

80. Schlichting, H., "Boundary Layer Theory", 4th Edition, McGraw-Hill, New York, (1962),p.168.

81. Perry, J.H., ed., "Chemical Engineers Handbook", 3rd Edition, McGraw-Hill, New York, (1950), p.175 & p.538.

82. Lange, N.A., "Handbook of Chemistry", 10th Edition, McGraw-Hill, New York, (1961), p.1668 & p.326.

83. Othmer, D.F., and Thaker, M.S. Ind.Eng.Chem., V45, 589, (1953).

84. Wilke, C.R., and Pin Chang, A.I.Ch.E.Journal, V1, 264, (1955).

85. Hixson, A., and Wilkens, H. Ind.Eng.Chem., V25, 1196, (1933).

86. Vasudev, A. Dissertation Abstracts, V25, 1079,(1964)

87. Bourgoin, R. Ann.Chim.Phys., V15, 161, (1878).

88. Skelland, A.P.H., and Wellek, R.M. A.I.Ch.E.Journal, V10, 491, (1964).

89. Volk, W. "Applied Statistics for Engineers", McGraw-Hill, New York, (1958), p.152.